

THE NATURE OF THE INTRAMOLECULAR
HYDROGEN BOND IN THE ENOL TAUTOMER
OF 2, 4-PENTANEDIONE

Thesis by

Phoebe Kin-Kin Dea

In Partial Fulfillment of the Requirements

For the Degree of
Doctor of Philosophy

California Institute of Technology
Pasadena, California

1972

(Submitted December 6, 1971)

To my parents and my family.

ACKNOWLEDGMENTS

It is a pleasure to acknowledge my research advisor, Professor Sunney I. Chan, for his continued guidance and encouragement during the course of my studies at Caltech.

Many helpful and interesting discussions with members of the Chan group are deeply appreciated. Special thanks are due to Dr. Dale R. Clutter, who collaborated with me during the first of my Caltech years.

I would also like to thank Mrs. Karen Gleason for the expert typing of this thesis.

Financial assistance from the California Institute of Technology throughout my graduate work is gratefully acknowledged.

I am indebted to my family. My parents, though far away, have given me every moral support. I am especially grateful to my husband Frank for the love, understanding and frequently stimulating discussions which we have shared. I also wish to thank my in-laws for taking such good care of our daughter while I am in school. Last, but not least, I must mention Denise, who is always a joy to hold.

ABSTRACT

The nature of the intramolecular hydrogen bond in the enol tautomer of 2, 4-pentanedione has been studied in detail using high resolution proton, deuterium and ^{13}C magnetic resonance spectroscopy. An unusually large deuterium isotope effect on the chemical shift of the bridge hydrogen has been observed. This unexpected result, together with the observation of a pronounced temperature dependence for both the bridge proton and deuterium resonances, as well as a temperature dependence of the carbonyl resonances, suggest that two states with different chemical shifts for the bridge hydrogen are involved in rapid equilibrium and that the anomalous deuterium isotope effect has its origin in the effect of deuterium substitution on the energy separation between these states. The results of a least-squares analysis of the OH and the OD temperature data in terms of a two-state model indicate that the energy separation for the proton and deuterated systems in the two states are 405 cm^{-1} and 215 cm^{-1} ; but essentially identical chemical shifts were obtained for the OH proton as for the OD deuterium in each state (-14.15 and -10.10 ppm from the enol methyl group respectively).

It is proposed that these states correspond to the symmetric and asymmetric structures of the intramolecular hydrogen bond. Results of our CNDO/2 calculations on the enol tautomer have indicated that these two structures have quite similar energies. In particular, it is suggested that the potential function associated with the vibrational motion of the bridge hydrogen is symmetric double minimum

in nature when the donor-acceptor vibration (symmetric stretch) is in its zeroth vibrational state and the potential function becomes asymmetric when the symmetric stretch is excited by one or more vibrational quanta. By exciting the symmetric O···O stretch, we expect a charge shift in the π system which can alter the effective potential function for the bridge hydrogen. The $0 \rightarrow 1$ transition of the symmetric stretch is observed at 418 cm^{-1} in the Raman spectrum of the normal compound and 230 cm^{-1} in the deuterated molecule. This difference of 188 cm^{-1} in the energy separation of the ground and first excited vibrational states of the symmetric stretch would be expected to give rise to the large deuterium isotope effect observed in our magnetic resonance experiments.

TABLE OF CONTENTS

<u>Part</u>	<u>Title</u>	<u>Page</u>
I	GENERAL INTRODUCTION	1
II	EXPERIMENTAL	4
	1. Materials	4
	2. Synthesis	5
	3. Sample Preparation	6
	4. NMR Measurements	8
III	RESULTS	14
	1. Deuterium Isotope Effect	14
	2. Temperature Studies	21
	3. Effect of Substitution	25
	4. Solvent Effects	25
IV	DISCUSSION	34
	1. Deuterium Isotope Effect	34
	2. Temperature Studies	41
	3. Model	49
	4. Molecular Orbital Calculations	56
	5. The Nature of the Two States	71
	6. Analysis of the NMR Data in Terms of the Two-State Model	74
	7. Potential Function	79
	8. Effect of Substitution	90
	9. Solvent Effect	93

<u>Part</u>	<u>Title</u>	<u>Page</u>
V	CARBON-13 NMR STUDIES	109
VI	CONCLUSION	124
	REFERENCES	125
	APPENDIX	128
	PROPOSITION I	135
	PROPOSITION II	150
	PROPOSITION III	159
	PROPOSITION IV	164
	PROPOSITION V	169

acid. Thus, the enol tautomer exists primarily as the intramolecularly hydrogen-bonded monomer.

The objective of this research is to obtain some information about the potential function associated with the vibrational motion of the bridge hydrogen in the strong intramolecular hydrogen bond in acetylacetone. The question at hand is whether the hydrogen bond in the enol structure is best described as a vinyl alcohol group hydrogen-bonded to a carbonyl oxygen, in which case the molecule would have C_s symmetry; or whether the potential function for the vibration of the bridge hydrogen is symmetrically double minimum in nature, so that the molecule would have C_{2v} symmetry. Needless to say, in the latter case, if the barrier height separating the two potential energy minima is sufficiently high so that the tunnelling of the proton is slow compared with the time scale of observation, then it may not be possible to distinguish between the two alternatives. For example, the time scale of observation is fast in infrared spectroscopy, and the tunnelling frequency might be slow compared with the time scale of observation so that the infrared spectrum is effectively determined by C_s selection rules.

In principle, the best approach to elucidate the nature of the potential function of the intramolecular hydrogen bond is to examine the transitions between the energy levels of the O-H...O stretching vibration in the near infrared. The IR spectrum of acetylacetone has previously been reported by Rasmussen et al.,⁽¹²⁾ Smith,⁽¹³⁾ Bellamy and Beecher,⁽¹⁴⁾ and Bratoz et al.⁽¹⁵⁾ in organic solvents, and by Mecke and Funck⁽¹⁰⁾ in organic solvents as well as in the gaseous phase. Recently, Ernstbrunner⁽¹⁶⁾ studied the vibrational spectra of

acetylacetone and deuterated acetylacetone and its anion with the help of Raman spectroscopy. Unfortunately, the region in the O-H...O stretching vibration was quite complicated and revealed little detail. Shigorin *et al.* ⁽¹⁷⁾ have examined the IR spectra of acetylacetone in the solid state. Here, the crystal revealed a broad O-H...O stretch which was split into two bands about 53 cm^{-1} apart at -150°C . This splitting was attributed to the possibility of quantum mechanical tunnelling in the first excited state degenerate levels of the bridge hydrogen between the two equivalent wells in the double minimum potential. In the frozen glass, however, these investigators reported an appreciable drop in the band at 2700 cm^{-1} but reported the concomitant appearance of a new band at 3200 cm^{-1} . These results would seem to suggest that the potential function is double minimum in nature except in the case of frozen glass, where intermolecular effects can result in a reduction of the symmetry of the potential function for some of the enol molecules. In solution, however, the IR spectrum has been interpreted in terms of C_s symmetry and, in fact, Ogoshi and Nakamoto ⁽¹⁸⁾ have performed a normal coordinate analysis of this molecule assuming C_s symmetry. Thus, there seems to be some ambiguity regarding the symmetry of the potential function of the hydrogen bond.

This paper summarizes an attempt to shed some light on this problem using magnetic resonance spectroscopy. As is well known, the nmr time scale is long and the quantum mechanical tunnelling of the bridge hydrogen in a symmetric double minimum potential is expected to be fast with respect to the nmr time scale. However, the chemical shift of the bridge hydrogen is a sensitive probe of the

average electron density at the proton. The chemical shift of the bridge hydrogen in the enol tautomer of 2,4-pentanedione is known to be temperature dependent from previous work.⁽⁸⁾ This temperature dependence of the chemical shift suggests that two or more states with different chemical shifts for the bridge hydrogen are involved in rapid equilibrium. These states have been assigned to the intramolecular hydrogen-bonded and the "open" form, but irrespective of the nature of these states, it is possible to ascertain the nature of the potential function from the effect of deuterium isotope substitution on the vibrational energy levels. The energy levels associated with the vibrational motion of the bridge hydrogen should be extremely sensitive to the anharmonicity of the potential well. Any unusual changes on the energy levels of the states as a result of deuterium isotopic substitution should be reflected in the average chemical shift of the bridge hydrogen and the bridge deuterium. In this study, we shall show how this can be used to provide some information about the nature of the potential function for the intramolecular hydrogen bond.

II. EXPERIMENTAL

1. Materials. Acetylacetone, ethyl acetoacetate, 1,3-diphenyl-1,3-propanedione, cyclohexane, carbon tetrachloride, chloroform and n-butyl ether were obtained from Matheson, Coleman & Bell; 1-phenyl-1,3-butanedione and 3-methyl-2,4-pentanedione from K and K Laboratories; deuterated water from Columbia Organic Chemical Company; methanol-d₁ from Diaprep Inc.; cyclohexane-d_{1,2}, ethylene

glycol-d₆, acetic acid-d₃ and methyl-d₃ alcohol from Merck Sharp and Dohme of Canada.

2. Synthesis. The partially deuterated acetylacetone was prepared by adding deuterated water to acetylacetone in the ratio of 2:1 by volume and the mixture was warmed until it became homogeneous at about 80°C. The solution was refluxed at this temperature for twenty-four hours to allow for sufficient exchange. The partially deuterated acetylacetone was then separated from water by fractional distillation. Upon comparison of the intensity of the pmr spectrum of the partially deuterated compound with that of the normal compound, it was ascertained that about 90% deuteration was achieved in the OH and α -CH positions. The methyl groups were also found to be deuterated to the extent of 10%. No further increase in the extent of deuteration was observed by further prolonged refluxing. Partially deuterated 3-methyl-2, 4-pentanedione and partially deuterated ethyl acetoacetate were prepared in a similar manner.

Partially deuterated 1, 3-diphenyl-1, 3-propanedione and 1-phenyl-1, 3-butanedione were prepared by refluxing the normal compounds in deuterated water at 80°C for twenty-four hours, in the process of which the solid melted into oil globules and an emulsion was formed. Several drops of diethylamine were added to the refluxing mixtures to increase the amount of enol present and to enhance the keto-enol conversion rate; diethylamine has been shown to form a hydrogen-bonded complex between the enolic OH group and the nitrogen lone pair. ⁽³⁾ Chloroform extraction was used to recover the partially deuterated

β -diketone from the refluxed mixture. The solvent was then distilled, and the partially deuterated compounds obtained were dried in a vacuum dessicator. PMR analysis indicated that the OH and α -CH positions were deuterated to the extent of 50% with no apparent exchange in the phenyl rings.

3. Sample Preparation. It was found in the course of this work that the presence of a trace amount of water in acetylacetone as well as other β -diketones broadens the linewidth of the OH resonance considerably. If a pure acetylacetone sample sealed under vacuum was compared with one containing 0.1 M water, the linewidth was found to broaden from 2.2 Hz to 41.2 Hz. A summary of the effect of water on the OH resonance of acetylacetone is depicted in Table I. As expected, the chemical shift of the bridge hydrogen also moves upfield as the concentration of water increases. At a water concentration of 0.1 M, an upfield shift of 0.45 ppm from its corresponding position in anhydrous acetylacetone was observed. Hence, all possible precautions were taken to dry the samples prior to nmr measurements.

A high vacuum line was assembled for this purpose. The line was initially washed with carbon tetrachloride followed by hot hydrofluoric acid solution, and was rinsed thoroughly with distilled water. It was then rinsed with acetone, pumped overnight, and flamed out many times before use. All manipulations pertaining to the preparation of samples were undertaken in the vacuum system.

Acetylacetone was degassed and vacuum distilled twice over phosphorus pentoxide. It was then stored over phosphorus pentoxide

TABLE I. Effect of Water on the OH Resonance in Acetylacetone.
The Chemical Shifts are measured relative to Enol
Methyl Groups.

<u>SAMPLE</u>	<u>LINE WIDTH (Hz)</u>	<u>CHEMICAL SHIFT (ppm)</u>
Pure acetylacetone sealed under vacuum	2.20	-13.630
Pure acetylacetone sealed after 3 minutes exposure to air	5.89	-13.627
Pure acetylacetone with 0.01 <u>M</u> water added	9.40	-13.542
Pure acetylacetone with 0.1 <u>M</u> water added	41.20	-13.181

under vacuum. The solvents n-butyl ether and cyclohexane were degassed and vacuum distilled twice over calcium hydride. The ether was then stored under the vacuum line over sodium and the cyclohexane over calcium hydride. All solutions of acetylacetone and deuterated acetylacetone were made up by volume by vacuum distillation into nmr sample tubes. All samples were subsequently sealed under vacuum.

The linewidth of the OH resonance in the acetylacetone solutions prepared was used as an indication of the dryness of the samples. The linewidths observed in all the samples used were of the order of 2 Hz except those diluted in n-butyl ether, which were consistently broader. In the latter samples, the linewidth measurements were reproducible for different samples of the same concentration, suggesting an alternate explanation of the observed line broadening in this case.

4. NMR Measurements. Several high resolution Varian spectrometers were used in this work: Varian HR-220 and HA-100 spectrometers were used for the proton studies; a Varian DP 60 spectrometer operating at 6.5 MHz and a Varian HA-100 spectrometer equipped with a V4311 RF unit and V4333A probe operating at 15 MHz were employed for the deuterium studies; while a Varian HR-220 spectrometer equipped with a V4334 probe operating at 15.3 MHz was used for the carbon-13 studies. The sensitivity is greatly improved where necessary by a Fourier transform accessory interfaced to a Varian 620i computer. All the spectrometers were fitted with standard variable temperature probes except the one operating at 6.5 MHz, which was only capable of room temperature measurements. Ethylene glycol-d₆ and a 1:1 mixture of

methanol- d_1 and methyl- d_3 alcohol were used to determine the probe temperatures in the deuterium variable temperature studies; the standard ethylene glycol and methanol samples supplied by Varian were used in the variable temperature proton studies on the HR-220 and HA-100 spectrometers.

In the course of these studies, it was found that the temperature indicated by the ethylene glycol splitting as given by the temperature chart in the HA-100 technical manual was approximately 2°C lower than that given in the HR-220 manual throughout the temperature range from 10°C to 190°C . The temperature calibrations were therefore checked using a copper-constantan thermocouple; the results were subsequently shown to be identical with those given in the HR-220 manual. At low temperatures where the methanol standard is used, the thermocouple and methanol calibrations were identical from -40°C to 0°C but discrepancies occur at higher temperatures. The temperature given by the methanol shift as indicated by the temperature chart in the HA-100 manual for example was about 5°C higher than the thermocouple calibration at 60°C . Thus, for the same probe temperature, two different temperatures would be obtained depending on whether the methanol or ethylene glycol splitting was used for the calibration. To correct for this inconsistency, appropriate adjustments were made using the thermocouple measurements. The temperature calibration charts for the ethylene glycol and methanol samples are shown in Figs. 1 and 2 respectively.

FIGURE 1

A temperature calibration chart for ethylene glycol. The chemical shift shown refers to the chemical shift difference between the $-\text{CH}_2-$ group and the $-\text{OH}$ group. The dotted line refers to the calibration given by the HA-100 technical manual. The solid line is the corrected temperature measurement using the thermocouple calibration.

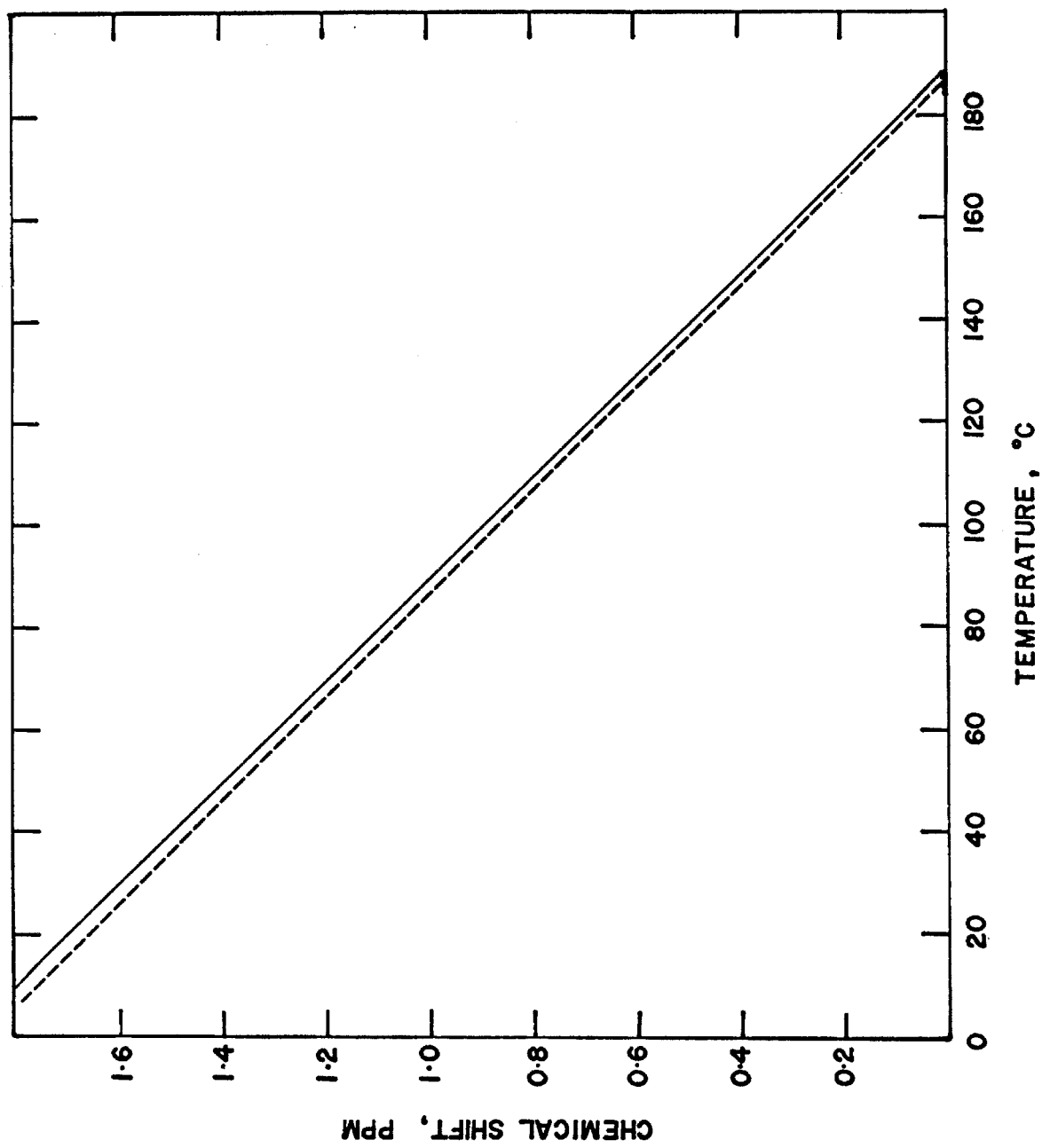
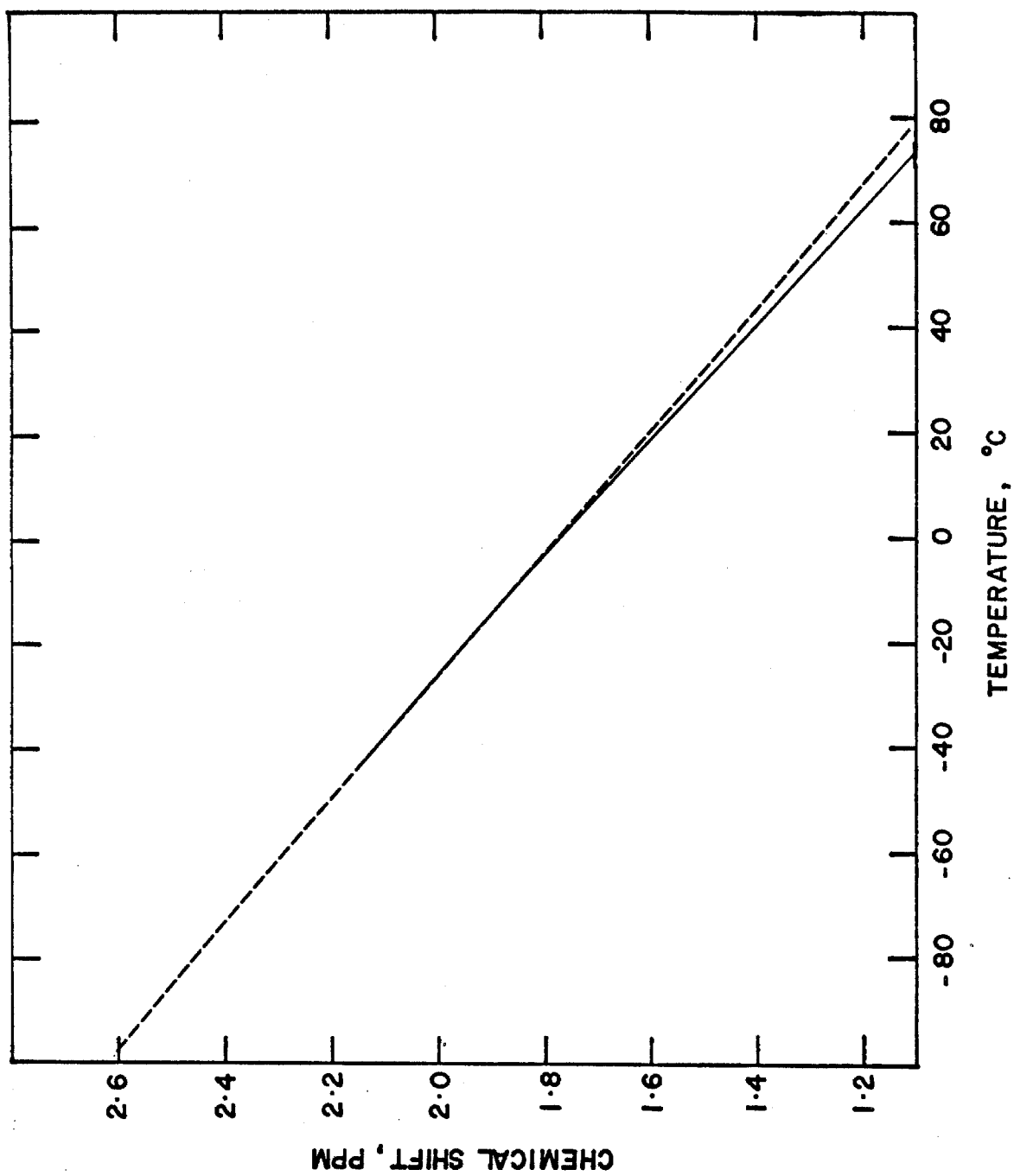


FIGURE 2

A temperature calibration chart for methanol. The chemical shift shown refers to the chemical shift difference between the $-CH_3$ group and the $-OH$ group. The dotted line refers to the calibration given by the HA-100 technical manual. The solid line is the corrected temperature measurement using the thermocouple calibration.



III. RESULTS

1. Deuterium Isotope Effect

A typical proton and deuterium spectrum of dilute acetylacetone in cyclohexane at 30°C is shown in Figs. 3 and 4. Separate resonance signals were observed for the various protons in the keto and enol tautomers. The assignment of the proton spectrum indicated is identical to that previously given by Reeves.⁽³⁾ A comparison of the proton and deuterium spectra indicates that the deuterium isotope effects are negligible except for the bridge hydrogen of the enol tautomer.

In Table II, we have summarized the effect of deuterium substitution on the chemical shift between the bridge hydrogen and the methyl hydrogens of the enol tautomer in the pure liquid and upon dilution in cyclohexane and n-butyl ether. Insofar as it was possible to ascertain, the pronounced isotope effect is independent of concentration and the solvent system. For comparison, we have also summarized the deuterium isotope effect on the α -CH in these systems in Table III. Whereas the isotope effect on the magnetic shielding of hydrogen bonded to carbon and oxygen are generally thought to be small⁽¹⁹⁾ (certainly less than 0.1 ppm), and are usually interpreted in terms of modifications in zero-point vibrational amplitudes upon isotopic substitution,⁽²⁰⁾ the effect observed in the case of the bridge hydrogen in acetylacetone is an order of magnitude larger. Thus, the pronounced isotope effect observed cannot be attributed primarily to the effect of deuterium substitution on the average magnetic shielding of the bridge hydrogen.

FIGURE 3

A 100 MHz proton spectrum of acetyl-
acetone at 30°C.

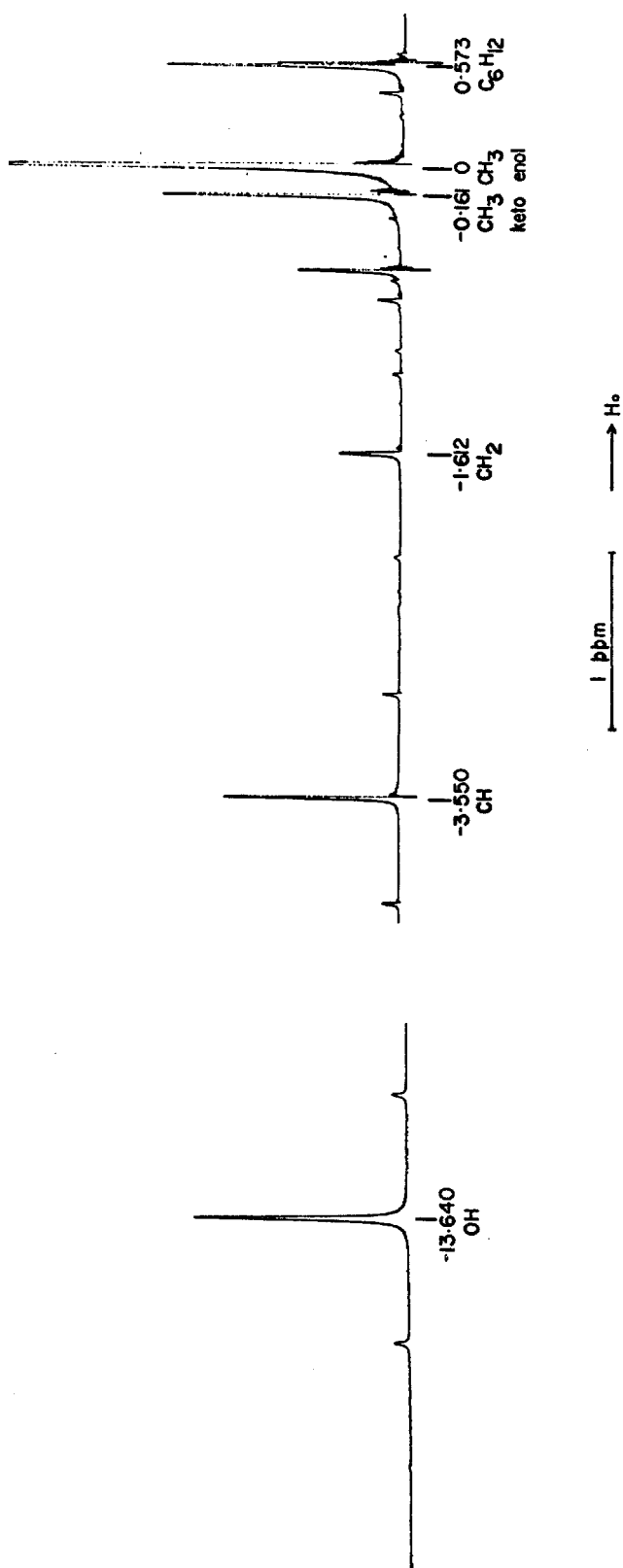


FIGURE 4

A 15 MHz deuteron spectrum of partially deuterated acetylacetone at 30°C.

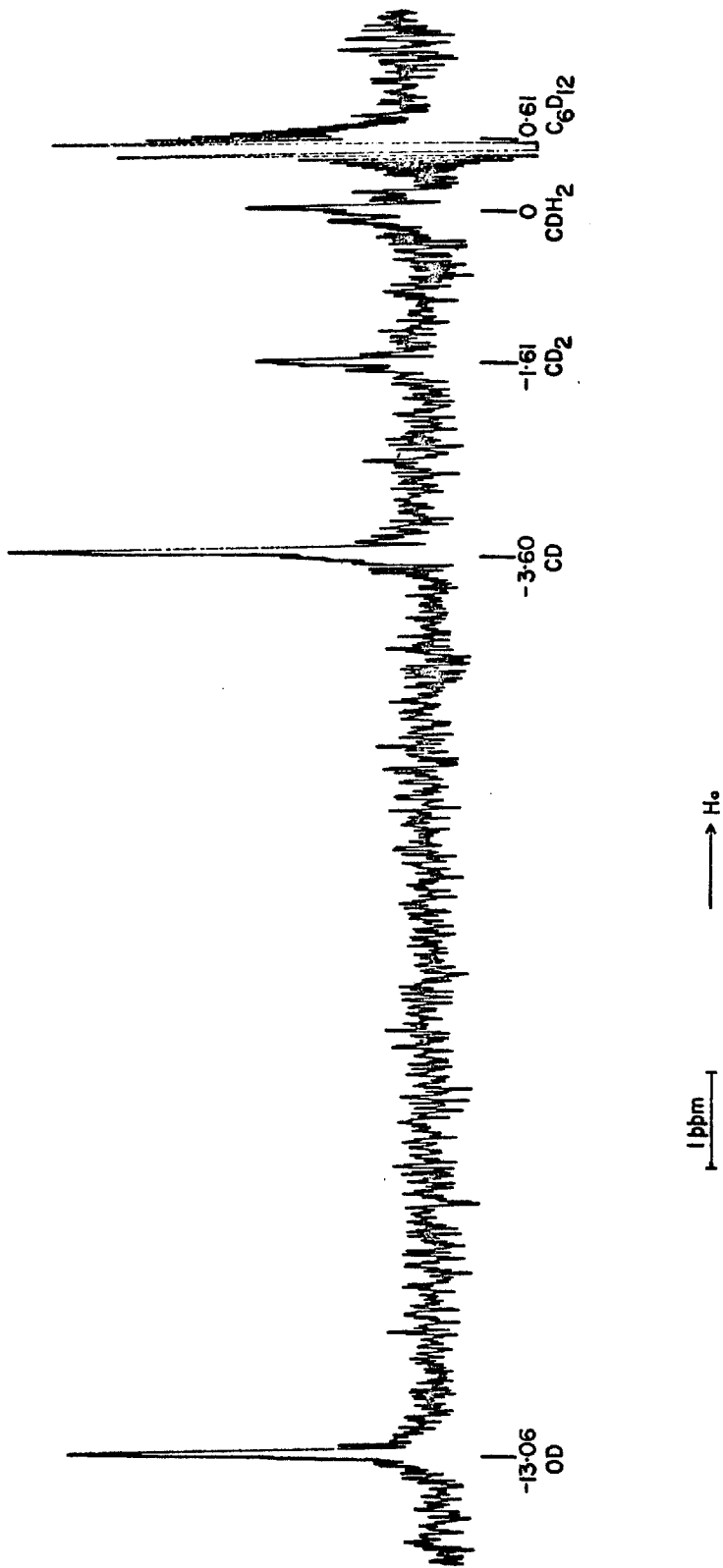


TABLE II. Observed proton and deuteron chemical shifts of hydroxyl groups in several hydrogen-bonded systems at 27°C.

<u>System</u>	<u>δ_{OH},^a ppm</u>	<u>δ_{OD}, ppm</u>	<u>$\delta_{\text{OD}} - \delta_{\text{OH}}$ ppm</u>
Acetylacetone ^d			
pure (anhydrous)	-13.640	-13.06 ^b	+ 0.58
0.16 mole fraction in cyclohexane	-13.641	-13.09 ^b	+ 0.55
0.12 mole fraction in n-butyl ether	-13.585	-13.01 ^b	+ 0.58
3-Methyl-2, 4-pentanedione ^e			
0.5 mole fraction in cyclohexane	-15.020	-14.57 ^c	+ 0.45
1, 3-Diphenyl-1, 3-propanedione ^e			
0.15 mole fraction in carbon tetra- chloride	-15.524	-15.07 ^c	+ 0.45
1-Phenyl-1, 3-butanedione ^e			
0.3 mole fraction in carbon tetra- chloride	-14.812	-14.39 ^c	+ 0.42
Ethyl acetoacetate ^e			
0.2 mole fraction in carbon tetra- chloride	-10.639	-10.66 ^c	- 0.02

^a Measured at 100 MHz; experimental error \pm 0.005 ppm.

^b Measured at 15 MHz; experimental error \pm 0.03 ppm.

^c Measured at 6.5 MHz; experimental error \pm 0.1 ppm.

^d δ_{OH} and δ_{OD} are measured relative to the chemical shifts of the methyl group(s) (-CH₃ and -CD₃ respectively) in the same molecule.

^e Chemical shifts are measured relative to cyclohexane.

TABLE III. Observed proton and deuteron chemical shifts of α -CH and α -CD groups in several hydrogen-bonded systems at 27°C.

<u>System</u>	δ_{CH} ^a ppm	δ_{CD} ppm	$\delta_{\text{CD}} - \delta_{\text{CH}}$ ppm
Acetylacetone ^d			
pure (anhydrous)	-3.552	-3.60 ^b	-0.05
0.16 mole fraction in cyclohexane	-3.446	-3.50 ^b	-0.05
0.12 mole fraction in n-butyl ether	-3.470	-3.53 ^b	-0.06
3-Methyl-2,4-pentanedione ^e			
0.5 mole fraction in cyclohexane	-3.410	-3.55 ^c	-0.09
1,3-Diphenyl-1,3-propanedione ^e			
0.15 mole fraction in carbon tetra- chloride	-5.286	-5.51 ^c	-0.22
1-Phenyl-1,3-butanedione ^e			
0.3 mole fraction in carbon tetra- chloride	-4.632	-4.81 ^c	-0.18
Ethyl acetoacetate ^e			
0.2 mole fraction in carbon tetra- chloride	-3.644	-3.69 ^c	-0.04

^a Measured at 100 MHz; experimental error ± 0.005 ppm.

^b Measured at 15 MHz; experimental error ± 0.03 ppm.

^c Measured at 6.5 MHz; experimental error ± 0.1 ppm.

^d δ_{OH} and δ_{OD} are measured relative to the chemical shifts of the methyl group(s) ($-\text{CH}_3$ and $-\text{CD}_3$ respectively) in the same molecule.

^e Chemical shifts are measured relative to cyclohexane.

The deuterium isotope effect may also have its origin in apparent isotope effects if the kinetics of exchange between different states fall in between the two time scales of measurement of the proton and deuteron magnetic resonance experiments. We have eliminated this possibility by a detailed investigation of the frequency dependence of both the proton and deuteron chemical shifts. These results are summarized in Table IV. The proton magnetic resonance measurements were undertaken at 60, 100 and 220 MHz and the deuteron magnetic resonance studies were taken at 6.5 and 15 MHz. The chemical shifts observed at various frequencies were identical within experimental error.

2. Temperature Studies

It is known from previous work⁽⁸⁾ that the chemical shift of the bridge hydrogen in acetylacetone is temperature dependent. We have repeated these measurements using anhydrous material, and in addition, have examined the temperature dependence of the deuteron chemical shift. The results for acetylacetone in cyclohexane are shown in Fig. 5. An upfield shift of 0.025 ppm was observed for each 10°C rise in temperature over a range of 0 to 100°C. The linewidth of the OH resonance was of the order of 2 Hz throughout this temperature range and was found to be independent of the strength of the magnetic field. This temperature dependence is essentially identical for the proton and deuteron chemical shifts.

FIGURE 5

Temperature dependence of the proton and deuteron chemical shifts observed for the bridge hydrogen in the enol tautomer of acetylacetone in cyclohexane.

δ_{OH} and δ_{OD} are measured relative to chemical shifts of enol methyl groups ($-\text{CH}_3$ and $-\text{CD}_3$ respectively).

Concentration of acetylacetone is 0.086 mole fraction in proton magnetic resonance experiments and 0.16 mole fraction in deuteron magnetic resonance experiments.

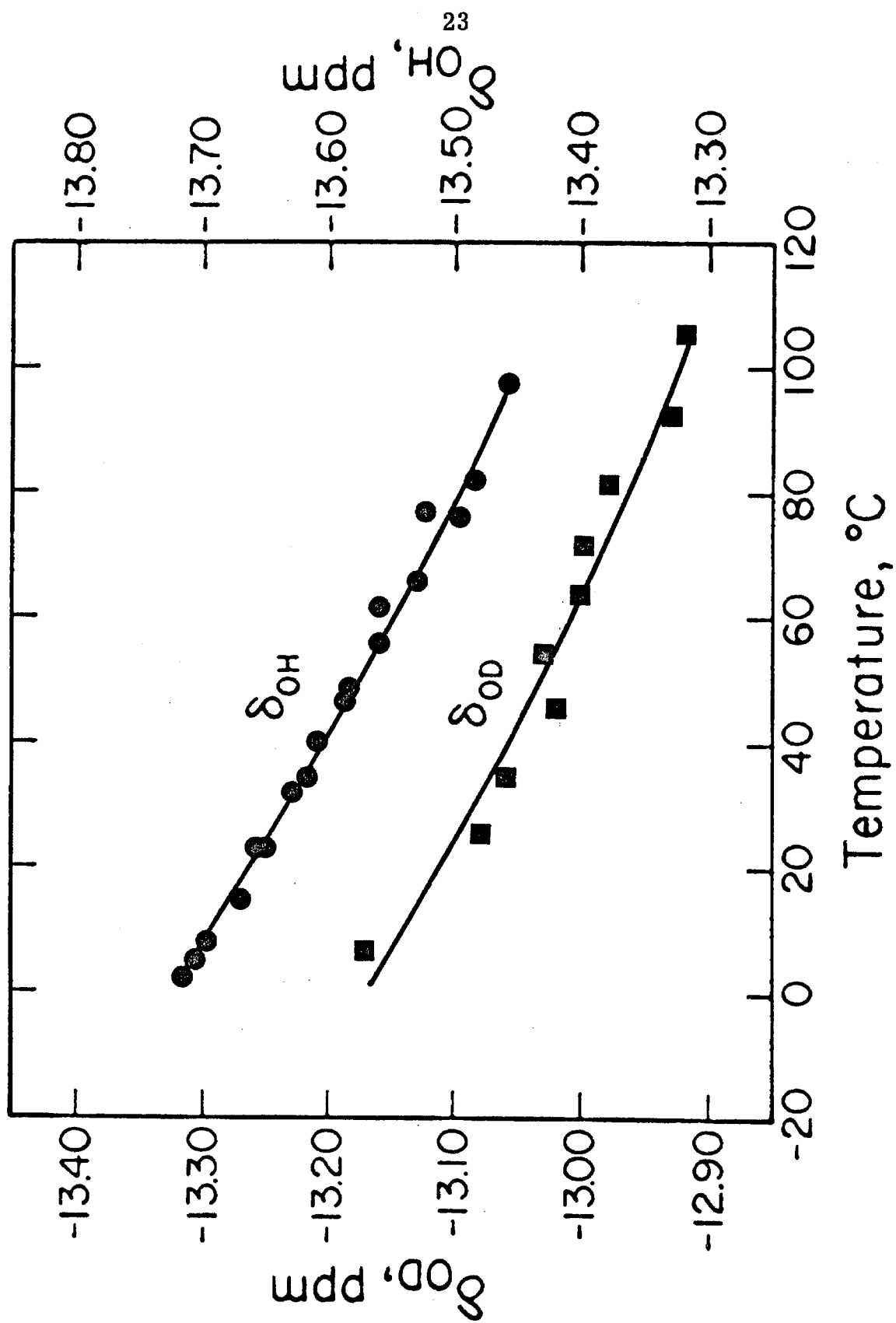


TABLE IV. A summary of the chemical shift of the bridge hydrogen as a function of the magnetic field.

<u>OH resonance (ppm)</u>	<u>OD resonance (ppm)</u>
(60 MHz) -13.646 ± 0.01	(6.5 MHz) -12.95 ± 0.1
(100 MHz) -13.641 ± 0.005	(15 MHz) -13.09 ± 0.03
(220 MHz) -13.656 ± 0.003	

3. Effect of Substitution

We have also observed an anomalous deuterium isotope effect on the chemical shift of the bridge hydrogen in several other β -diketones: 3-methyl-2,4-pentanedione, 1,3-diphenyl-1,3-propanedione and 1-phenyl-1,3-propanedione; and a temperature dependence of the chemical shift of the bridge hydrogen has also been noted in each case (Table V). However, in the case of β -keto esters, the chemical shift of the bridge hydrogen is known to be essentially temperature independent on the basis of previous work.⁽⁸⁾ Our measurements with neat ethyl acetoacetate reveal essentially no temperature effect, and as anticipated, no significant deuterium isotope effect on the chemical shift of the bridge hydrogen was observed (see Table II).

4. Solvent Effects

The chemical shift and the linewidth of the OH resonance of acetylacetone have been studied as a function of temperature in various solvents. The observed spectra are identical in cyclohexane and carbon tetrachloride with a linewidth of approximately 1.6 Hz at all temperatures between 0 and 60°C. When the solvent is n-butyl ether, the chemical shift of the OH resonance is identical to that observed in cyclohexane at low temperatures; but above 10°C, the OH resonance appears upfield from that observed in cyclohexane. This is shown in Fig. 6. Since the chemical shifts are measured relative to the enol methyl groups in both solvents, the observed difference in chemical shifts cannot be due to susceptibility effects. The difference in

FIGURE 6

Comparison of the temperature dependence of the proton and deuteron chemical shifts observed for the bridge hydrogen in the enol tautomer of acetylacetone in n-butyl ether and cyclohexane. δ_{OH} and δ_{OD} are measured relative to chemical shifts of enol methyl groups ($-\text{CH}_3$ and $-\text{CD}_3$, respectively).

--- 0.086 mole fraction of acetylacetone in cyclohexane in proton magnetic resonance experiments and 0.16 mole fraction in deuteron magnetic resonance experiments.

... 0.12 mole fraction of acetylacetone in n-butyl ether in both proton and deuteron experiments.

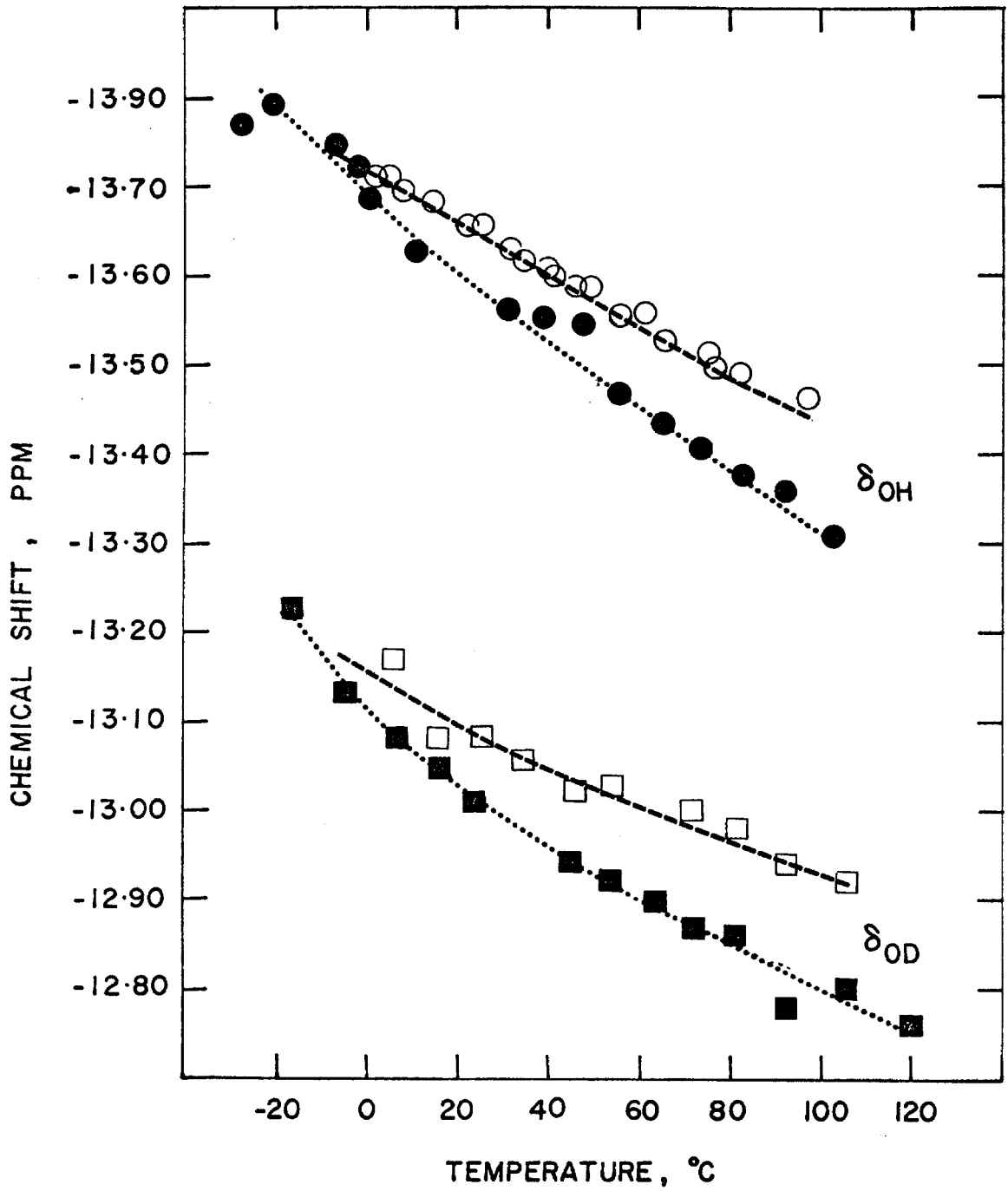


TABLE V. Temperature dependence of the chemical shifts of the bridge-hydrogen in several β -diketones and β -keto esters.

<u>Compound</u>	<u>Temperature Range, °C</u>	<u>Temperature Shift, ppm upfield</u>
Acetylacetone, anhydrous	5 - 82	0.22
3-Methyl-2,4-pentanedione	18 - 80	0.27
1,3-Diphenyl-1,3-propanedione	-17 - 64	0.38
1-Phenyl-1,3-butanedione	-14 - 76	0.20
Ethyl acetoacetate	30 - 92	0.06

chemical shift of the bridge hydrogen in the two solvents increases as the temperature is raised; for example, the chemical shift of the OH resonance in n-butyl ether at 100°C is 0.13 ppm upfield from that observed in cyclohexane.

We have also observed some unusual linewidth behavior of the OH resonance in n-butyl ether. The variation of the linewidth of the OH resonance at 100 and 220 MHz is shown in Fig. 7. At 100 MHz, the linewidth increases gradually from 2.5 Hz as the temperature is raised, reaching a maximum of 8 Hz around 20°C, and then decreases to a linewidth of 5 Hz above 60°C. This linewidth behavior is found to be frequency dependent. At 220 MHz, the linewidth increases from 3 Hz to a maximum of 16 Hz around 50°C, and decreases to a linewidth of 12 Hz above 100°C.

The linewidth of the OH resonance is also found to be dependent on the concentration of the solvent at low temperatures. The linewidth used here is the difference between the observed linewidth and the intrinsic linewidth of the resonance signal. A plot of the linewidth versus the concentration of n-butyl ether at 0°C is shown in Fig. 8. A straight line with a slope of $6.5 \text{ sec}^{-1} \text{ M}^{-1}$ is obtained.

FIGURE 7

Temperature dependence and frequency dependence of the reciprocal linewidth for the proton resonance of the bridge hydrogen in the enol tautomer of acetylacetone in n-butyl ether. The linewidth used here is the difference between the observed linewidth and the intrinsic linewidth of the resonance signal. Concentration of acetylacetone: 0.12 mole fraction.

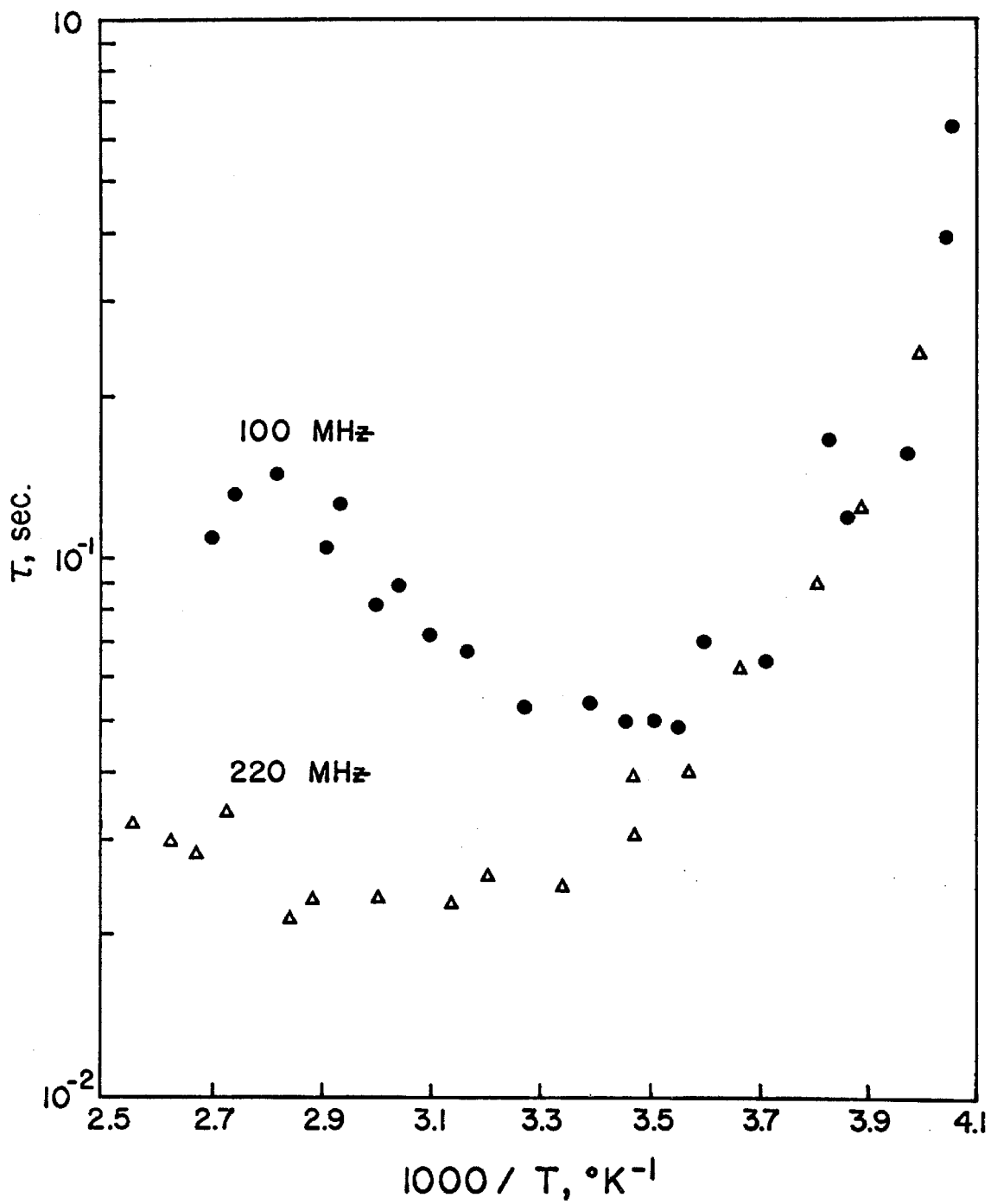
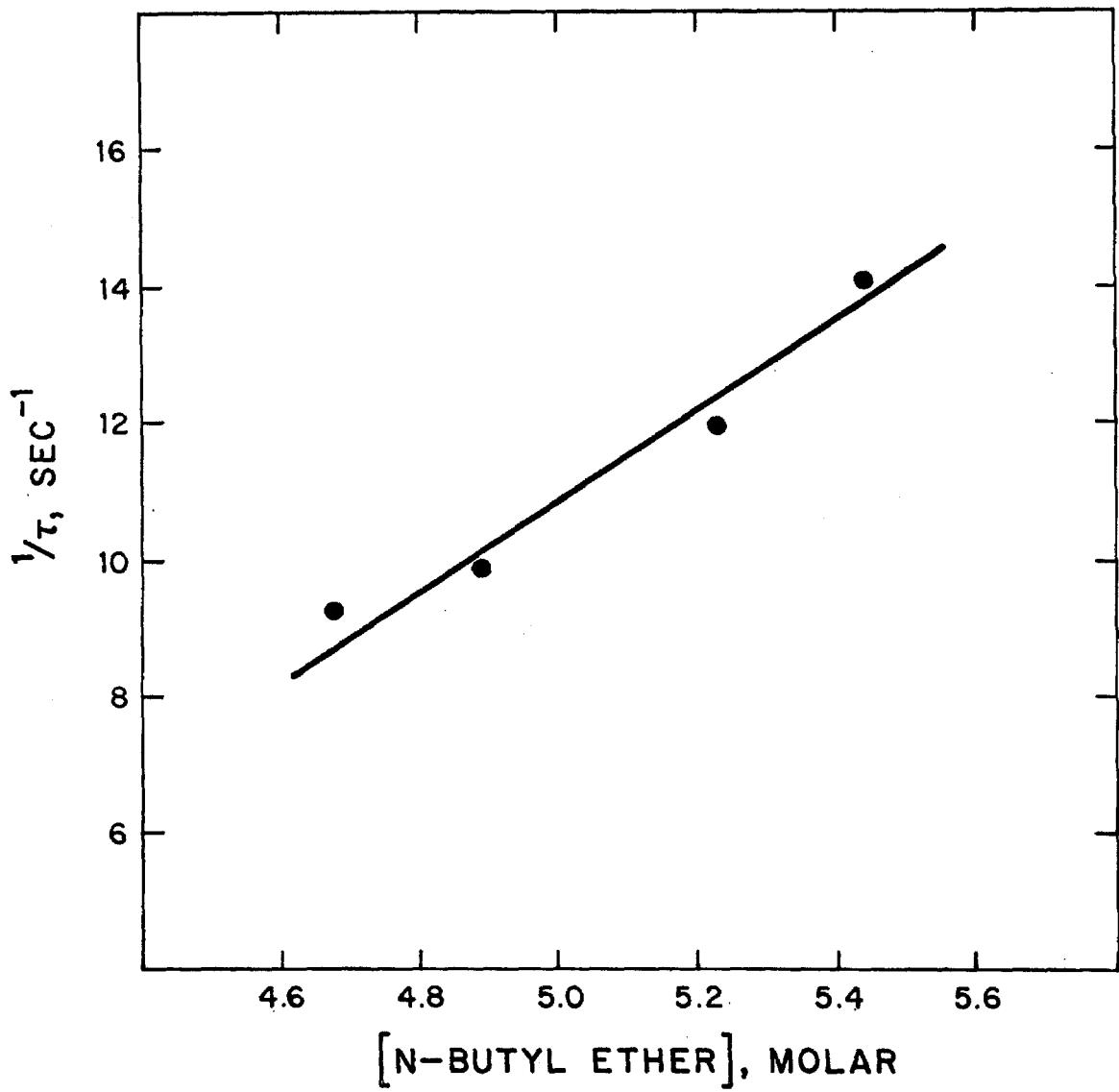


FIGURE 8

The dependence of the linewidth due to exchange on the concentration of n-butyl ether.



IV. DISCUSSION

1. Deuterium Isotope Effect

The chemical shift of the bridge hydrogen is a sensitive probe of the average electron density at the proton. In hydrogen-bonded systems, there is a reduction in the electron density of the proton upon formation of the hydrogen bond. This is reflected in a reduction of the magnetic shielding of the proton, which is observed as a down-field shift of the nmr signal.⁽²¹⁾ However, the measured chemical shift is in general only a vibrational average over the zero point vibrational motion. If the shielding constant (σ) is known as a function of the O-H bond distance (r) in a hydrogen-bonded system, then the vibrational average is given by the following:

$$(\sigma_{\text{H}})_{00} = \int \Psi_0^*(\text{H}) \sigma(r) \Psi_0(\text{H}) dr \quad (1)$$

where $\Psi_0(\text{H})$ is the vibrational wave function for the proton in the ground vibrational state.

When the proton is substituted by deuterium, we expect the modified vibrational motion of the molecule upon isotopic substitution to result in a change in the zero-point vibrational amplitude, and hence the average magnetic shielding of the deuteron. Since the wave function for the deuteron $\Psi_0(\text{D})$ is somewhat different, σ_{D} is expected to be different from that of the proton, where σ_{D} is given by:

$$(\sigma_{\text{D}})_{00} = \int \Psi_0^*(\text{D}) \sigma(r) \Psi_0(\text{D}) dr \quad (2)$$

From these expressions, we can see that if the deuterium isotope effect is large enough to be measurable, then it would provide some information about the nature of the potential function.

The effect of isotopic substitution on the magnetic shielding of nuclei have been known for some time,⁽²⁰⁾ but deuterium isotope effects on hydrogen chemical shifts are generally small, typically less than 0.05 ppm, as summarized in Table VI. From these deuterium isotope effects, it therefore appears that the observable is not sufficiently large to yield much information about the potential function. This is true even in hydrogen-bonded systems such as acetic acid and methanol (Table VII) where the anharmonicity of the potential well is expected to be larger. Thus, if the deuterium isotope effect is observed to be large, then either the vibrational motion of the proton and deuteron is characterized by quite different wave functions in their respective zero-point vibrational states; or two or more states exist in rapid equilibrium, each with quite a different vibrational wave function, and the deuterium substitution merely changes the energy spacings between them.

We now argue that the first possibility is unlikely. The potential function for the intramolecular hydrogen bond in acetylacetone could either be described as an -OH group hydrogen bonded to a ketone, in which case the potential function will be asymmetric; or the potential could be double minimum in nature if the intramolecular hydrogen bond is strong. For the first case, the potential function near the zero-point vibrational state can be approximated by a perturbed harmonic oscillator potential and the first few energy levels are non-degenerate. For

TABLE VI. Some typical deuterium isotope effect^a

	H	D
Chloroform and acetone	5.92	5.91
Water and acetone	2.84	2.87
Benzene and acetone	5.14	5.08
Benzene and water	1.75	1.74
Chloroform and water	2.56	2.61
Chloroform and benzene	0.82	0.86

^a P. Diehl and T. Leipert, Helv. Chim. Acta, 47, 545
(1964).

TABLE VII. Deuterium isotope effect in some hydrogen-bonded systems.

<u>Chemical shifts between</u> <u>OH and CH₃</u>	<u>H₂ resonance (ppm)</u>	<u>D₂ resonance (ppm)</u>
Acetic acid	9.24	9.16
Methanol	1.54	1.55

such a potential function, the isotope effect could only originate from changes in zero-point vibrational amplitude upon deuterium substitution; and we do not expect a sizable temperature effect since any excitation of the vibrational motion of the bridge hydrogen requires a quanta in excess of several thousand wave numbers which is much larger than kT . However, in view of the small deuterium isotope effect observed in OH stretching motions in both normal and hydrogen-bonded systems, this change in the zero-point vibrational motion is unlikely to account for the large deuterium isotope effect observed.

Similarly, we can rule out the first possibility even in the case when the intramolecular hydrogen bond is so strong that the potential well is double minimum. Here, we must consider two limiting cases, that where the central barrier is very high and that corresponding to a moderate barrier. The situation where the barrier is so low that the zero-point energy level is above the top of the barrier need not be considered here since the energy levels are non-degenerate and are quite widely separated, much larger than kT analogous to the asymmetric potential.

The energy levels of a symmetric double minimum potential are characterized as being either symmetric or antisymmetric with respect to reflection. When the barrier is very high, the lowest pair of the symmetric and antisymmetric states are degenerate for all practical purposes, and to a good approximation, their wave functions can be given by:

$$|0^+\rangle = \frac{1}{\sqrt{2}} (u_R + u_L) \quad (3)$$

$$|0^-\rangle = \frac{1}{\sqrt{2}} (u_R - u_L) \quad (4)$$

where u_R and u_L refer to the wave function on the right and left sides of the potential well respectively. For each of these states, the magnetic shielding is given by:

$$\begin{aligned} \langle 0^+ | \sigma(r) | 0^+ \rangle &= \frac{1}{2} \{ \langle u_R | \sigma(r) | u_R \rangle + \langle u_L | \sigma(r) | u_L \rangle \\ &\quad + \langle u_R | \sigma(r) | u_L \rangle + \langle u_L | \sigma(r) | u_R \rangle \} \quad (5) \end{aligned}$$

$$= \langle u_R | \sigma(r) | u_R \rangle \quad (6)$$

$$\begin{aligned} \langle 0^- | \sigma(r) | 0^- \rangle &= \frac{1}{2} \{ \langle u_R | \sigma(r) | u_R \rangle + \langle u_L | \sigma(r) | u_L \rangle \\ &\quad - \langle u_R | \sigma(r) | u_L \rangle - \langle u_L | \sigma(r) | u_R \rangle \} \quad (7) \end{aligned}$$

$$= \langle u_R | \sigma(r) | u_R \rangle \quad (8)$$

$$\text{since } \langle u_R | \sigma(r) | u_R \rangle = \langle u_L | \sigma(r) | u_L \rangle \quad (9)$$

$$\text{and } \langle u_R | \sigma(r) | u_L \rangle = \langle u_L | \sigma(r) | u_R \rangle \approx 0 \quad (10)$$

Also, both states are thermally populated when the central barrier is high, and $p_0^+ \approx p_0^- \approx 1/2$.

Therefore the average magnetic shielding is given by:

$$\sigma_{\text{ave}} = \langle u_R | \sigma(r) | u_R \rangle \quad (11)$$

Since u_R is not expected to change very much when the proton is substituted by deuterium, the deuterium isotope effect on the average magnetic shielding is probably too small to be observable, i. e.,

$$\sigma_{\text{ave}}^{\text{H}} = \langle u_R^{\text{H}} | \sigma(r) | u_R^{\text{H}} \rangle = \langle u_R^{\text{D}} | \sigma(r) | u_R^{\text{D}} \rangle = \sigma_{\text{ave}}^{\text{D}} \quad (12)$$

For moderate barrier heights, the magnitude of the splitting ($\Delta\epsilon$) will be of the order of kT . The aforementioned degeneracy between the 0^+ and 0^- states will then be lifted. Under these situations, the expectation values of $\sigma(r)$ for the 0^+ and 0^- states are represented by $\{\langle u_R | \sigma(r) | u_R \rangle + \langle u_R | \sigma(r) | u_L \rangle\}$ and $\{\langle u_R | \sigma(r) | u_R \rangle - \langle u_R | \sigma(r) | u_L \rangle\}$ respectively, and the average magnetic shielding is given by:

$$\sigma_{\text{ave}} = \frac{\{\langle u_R | \sigma(r) | u_R \rangle + \langle u_R | \sigma(r) | u_L \rangle\}}{1 + \exp(-\Delta\epsilon/kT)} + \frac{\{\langle u_R | \sigma(r) | u_R \rangle - \langle u_R | \sigma(r) | u_L \rangle\}}{1 + \exp(\Delta\epsilon/kT)} \quad (13)$$

We note that since $\langle u_R | \sigma(r) | u_L \rangle$ is expected to be much less than $\langle u_R | \sigma(r) | u_R \rangle$, the expectation value of $\sigma(r)$ is essentially the same in the two states. In fact, we expect the chemical shift difference between these two states to be smaller than the effective isotopic substitution since the effect of deuterium substitution generally leads to a change in energy which is much larger than kT .

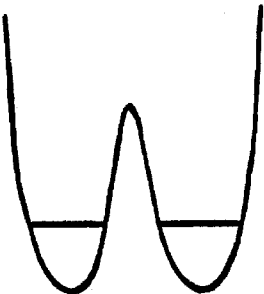
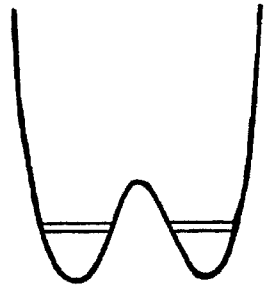
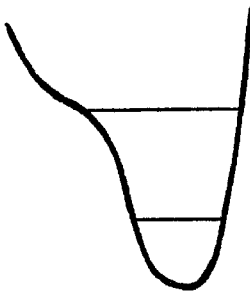
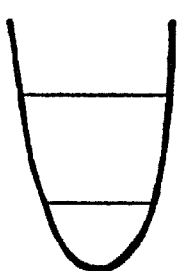
We are thus led to conclude that a single potential well would

not account for the large deuterium isotope effect observed. This then leaves us with the only other possibility for the origin of the large deuterium isotope effect, i. e., there are two or more states with quite different potential function for the hydrogen bond existing in rapid equilibrium and the deuterium isotope effect observed arises from the effect of deuteration on the energy spacing between the states. In the next section, we shall also show that the results of the temperature study are inconsistent with any model based on a single potential well.

2. Temperature Studies

We have shown in the previous section that the large deuterium isotope effect observed for the bridge hydrogen in acetylacetone is most likely not due to changes in the zero-point vibrational amplitude upon deuterium substitution; neither could it be due to the effect of deuterium substitution in the 0^+ and 0^- energy spacing in the symmetric double minimum potential well since the variation of $\sigma(r)$ with vibrational amplitude is not sufficiently large to exhibit such a large deuterium isotope effect. In Table VIII, we have summarized the type of isotope effect as well as temperature effect expected for the various single potential functions which we have described earlier in the previous section. Small isotope effects are indicated for all cases but we note that a temperature effect is expected only in case (B). This is the case where the potential function is symmetric double minimum in nature and the barrier is such that the energy spacing between the 0^+ and 0^- energy levels is comparable to kT . If this is the case, since $\sigma(r)$ is

TABLE VIII. Some properties associated with the nature of the potential function.

<u>Nature of the Potential Function</u>	<u>Magnitude of Energy Splitting between First Two Vibrational States</u>	<u>Isotope Effect</u>	<u>Temperature Effect</u>
(A) 	$\Delta\epsilon \ll kT$	small	no
(B) 	$\Delta\epsilon \approx kT$	small	yes
(C) 	$\Delta\epsilon \gg kT$	small	no
(D) 	$\Delta\epsilon \gg kT$	small	no

a monotonic function of r , the thermal population of the higher vibrational levels and the modification of the vibrational amplitudes by deuterium substitution are expected to have opposite effects on the observed magnetic shielding of the bridge hydrogen. Contrary to this, the temperature effect is found to be opposite in direction to the deuterium isotope effect since lowering the temperature moves the resonance downfield whereas the deuterium substitution moves the resonance upfield. So, the difference in the direction of the temperature effect and the deuterium isotope effect enables us to rule out this possibility.

We must therefore seek two states with quite different vibrational wave functions for the motion of the bridge hydrogen and which are both sufficiently thermally populated to give rise to a temperature effect. In view of the earlier discussion, the difference in the effect of deuterium substitution on the energy level of these structures must be large enough for the effect to manifest itself. Since the expectation values of $\sigma(r)$ for each state do not change very much upon deuterium substitution, a large deuterium isotope effect must reflect differences in the effect of deuterium substitution on the zero-point energies in these structures, which implies that the potential function associated with the motion of the bridge hydrogen must possess quite different anharmonicities. Such a situation could arise, for example, if there is an equilibrium between the intramolecular hydrogen-bonded cyclic structure and the "open" structure since the closed structure is significantly more anharmonic than the open structure. In fact, if the lower energy structure has a potential function for the O-H...O antisymmetric stretch which is double minimum with a potential barrier of the order

of 5000 cm^{-1} , the presence of this barrier will result in a deuterium isotope shift of the zero-point vibrational energy which is some $150\text{-}200 \text{ cm}^{-1}$ smaller than that expected for a more normal potential well, which is more representative of the open form. This scheme could readily account for the deuterium isotope effect and the temperature effect observed. A schematic representation of the zero-point energy levels is shown in Fig. 9. If the two structures are separated by $\Delta\epsilon_{\text{H}}^0$ and $\Delta\epsilon_{\text{D}}^0$ for the proton and deuterated compounds, and if δ_{I} , δ_{II} are the chemical shifts for the two states, and are essentially independent of the effect of deuterium substitution, then the proton chemical shift will be given by:

$$\delta_{\text{obs}}^{\text{H}} = \frac{\delta_{\text{I}}}{1 + \exp(-\Delta\epsilon_{\text{H}}^0/kT)} + \frac{\delta_{\text{II}}}{1 + \exp(\Delta\epsilon_{\text{H}}^0/kT)} \quad (14)$$

and the deuteron chemical shift will be given by

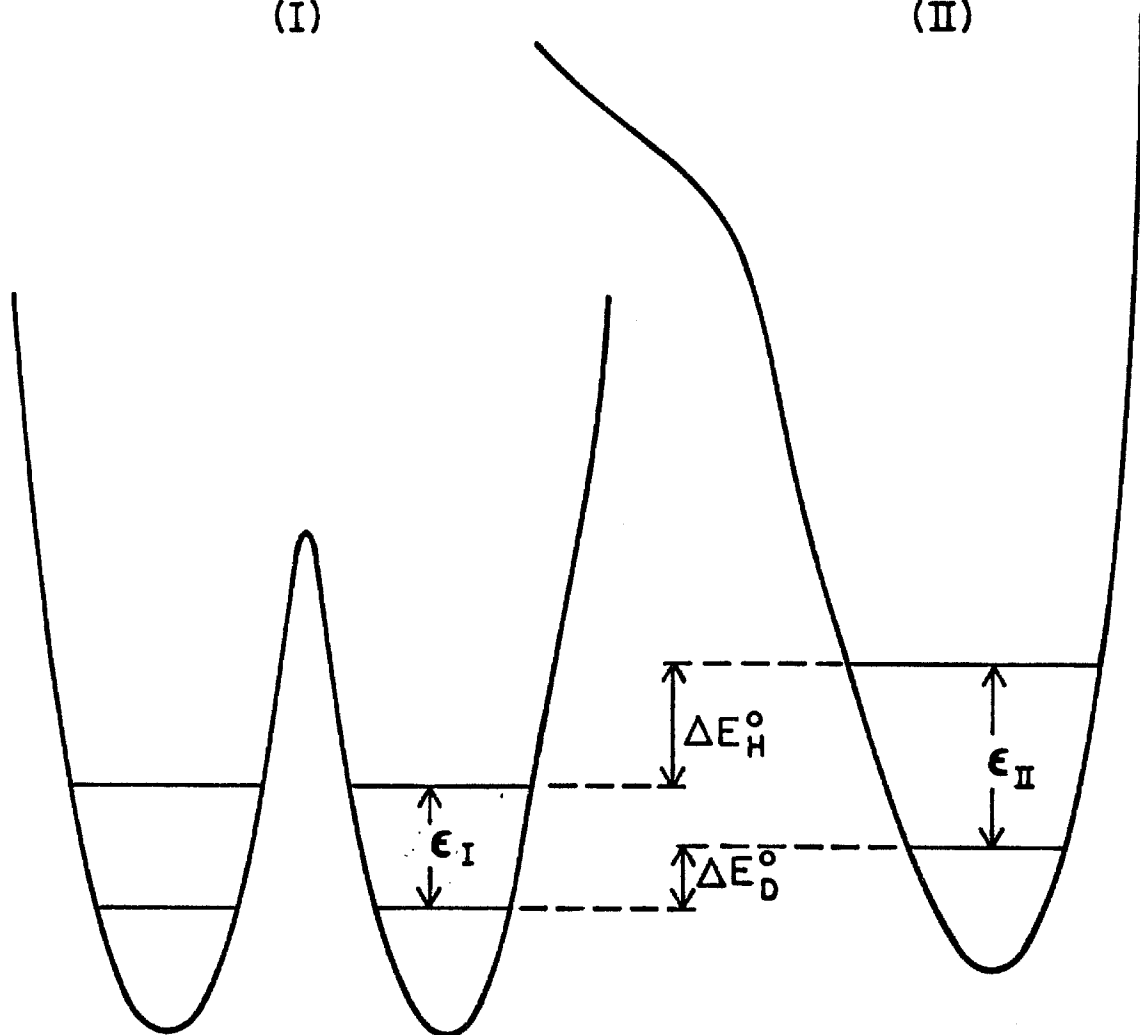
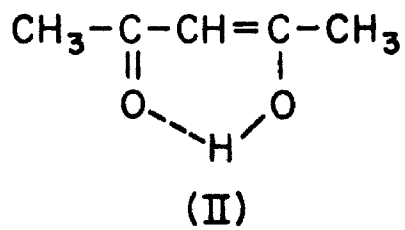
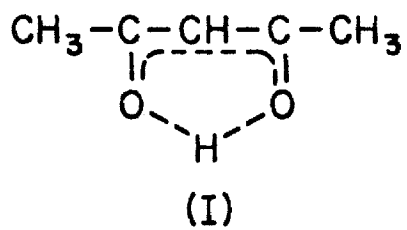
$$\delta_{\text{obs}}^{\text{D}} = \frac{\delta_{\text{I}}}{1 + \exp(-\Delta\epsilon_{\text{D}}^0/kT)} + \frac{\delta_{\text{II}}}{1 + \exp(\Delta\epsilon_{\text{D}}^0/kT)} \quad (15)$$

It is clear from these expressions that because of the difference in $\Delta\epsilon^0$ between the two states, a large deuterium isotope effect will result.

Unfortunately, there are some difficulties with this explanation due to the lack of any noticeable dependence of the chemical shift of the bridge hydrogen as well as the isotope effect on the basicity of the solvent. Moreover, if the deuterium isotope effect and the temperature dependence of the chemical shift of the bridge hydrogen observed for

FIGURE 9

A schématic representation of the zero-point energy levels for proton and deuterium in the symmetric double minimum potential function and the asymmetric potential function.



the β -diketones are to be interpreted in terms of this equilibrium, it is difficult to understand why this equilibrium is not also established in the case of β -keto esters, where the strength of the intramolecular hydrogen bond is presumably weaker, at least on the basis of the proton chemical shift. Additional evidence in support of this conclusion is provided by the broadening of the OH resonance observed in anhydrous n-butyl ether, a phenomenon which is not observed in cyclohexane or carbon tetrachloride. We have examined this line broadening as a function of temperature and at two different radiofrequencies. The results indicate that the broadening of the OH resonance is due to the presence of a small amount of the "open" form hydrogen bonded to the n-butyl ether, which is exchanging with the intramolecularly hydrogen-bonded species. Thus, we must seek an alternate interpretation elsewhere.

An alternate interpretation on the temperature dependence of the chemical shift on hydrogen-bonded systems in general has already been given by Muller and Reiter. (22) Their calculations have shown that the temperature dependence of the chemical shift of a proton in a hydrogen bond may have its origin in the anharmonicity of the low-frequency stretching vibration of $X-H \cdots Y$. As the temperature increases, the $H \cdots Y$ distance increases due to the increased populations of the excited vibrational levels of the symmetric mode. If δ_i is the chemical shift appropriate for the i^{th} vibrational state of the symmetric stretch, the observed chemical shift will be given by

$$\delta = \frac{\sum_i \delta_i \exp(-\epsilon_i/RT)}{\sum_i \exp(-\epsilon_i/RT)} \quad (16)$$

where the ϵ_i 's are the energy levels of the donor-acceptor vibration. The observed chemical shift would therefore be a function of temperature. This model also predicts a deuterium isotope effect on the proton involved in the hydrogen bond, but this isotope effect should be of the same order of magnitude as those observed in typical hydrogen-bonded systems.

The Muller and Reiter model has been used by Schaefer and Kotowycz to interpret the temperature dependence of the chemical shift of the bridge hydrogen in the case of 3,5-dichlorosalicylaldehyde.⁽²³⁾ However, the assumption of a low-frequency, asymmetric stretching vibration of the X-H...Y probably does not hold for a strong intramolecular hydrogen bond as in the case of acetylacetone, where the two oxygens involved in the hydrogen bond are connected by a chain of bonds. In fact, the lowest stretching frequency of the intramolecular hydrogen bond in acetylacetone as determined by Ogoshi and Nakamoto⁽¹⁸⁾ is 230 cm^{-1} in the infrared spectrum and the lowest stretching frequency observed in the Raman spectrum is 244 cm^{-1} ,⁽¹⁶⁾ which is too large (compare with kT) to give rise to the type of temperature variation observed within the framework of this theory. We must conclude therefore that these frequency effects are negligible in strong hydrogen-bonded systems and that the observed isotope effect as well as the temperature dependences observed for both the proton and deuteron resonances are inherent in the strong intramolecular hydrogen bond.

3. Model

It is clear from the deuterium isotope effect and the temperature studies that there are at least two energy states which are thermally populated at room temperature and which are associated with the motion of the bridge hydrogen. In principle, the states in question could either be close-lying vibrational levels of the O-H...O antisymmetric stretching vibration in the ground electronic state, or those of different molecular or electronic structures including tautomeric forms as well as low-lying electronic states. As we have shown, in view of the small energy difference between the two states and the pronounced effect of deuteration on their energy separation, it is clear that in the case of the first possibility, the potential energy function associated with the motion of the hydrogen in the O-H...O antisymmetric stretch must be double minimum in nature with a moderately high central barrier. While a double-minimum potential function for the O-H...O antisymmetric stretching vibration is not unexpected, it is, however, difficult to reconcile all our observations on the basis of this simple interpretation, since the thermal population of the higher vibrational levels, and the modification of the vibrational amplitudes by deuterium substitution are expected to have opposite effects on the observed average magnetic shielding of the bridge hydrogen. Contrary to this expectation, both deuterium substitution and raising the temperature increase the observed shielding of the bridge hydrogen. We are therefore more inclined to believe that the states are associated with different tautomeric or electronic structures, and that the large deuterium

FIGURE 10

One-dimensional potential curve and
energy levels for the hydrogen biacetate
ion.

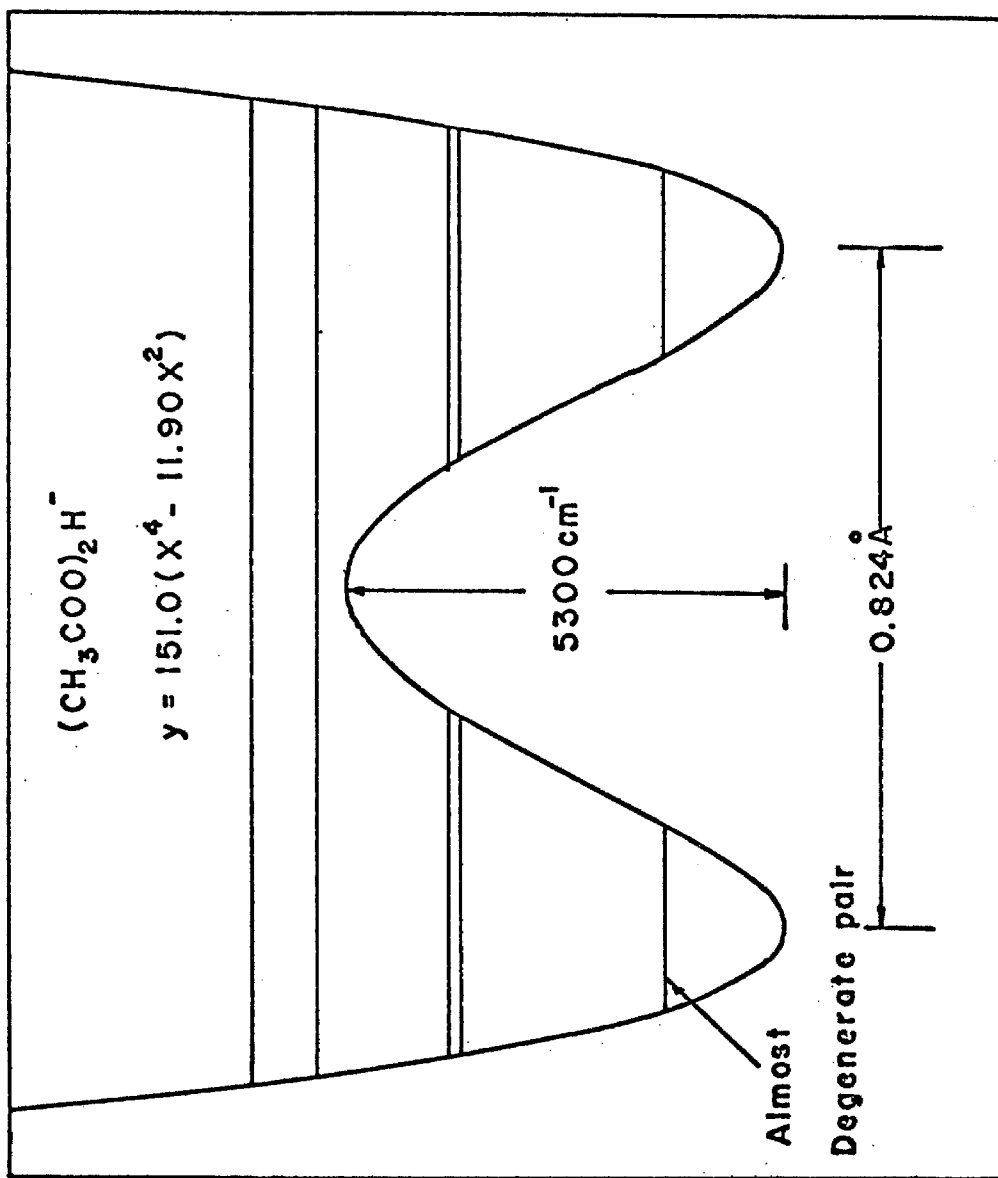
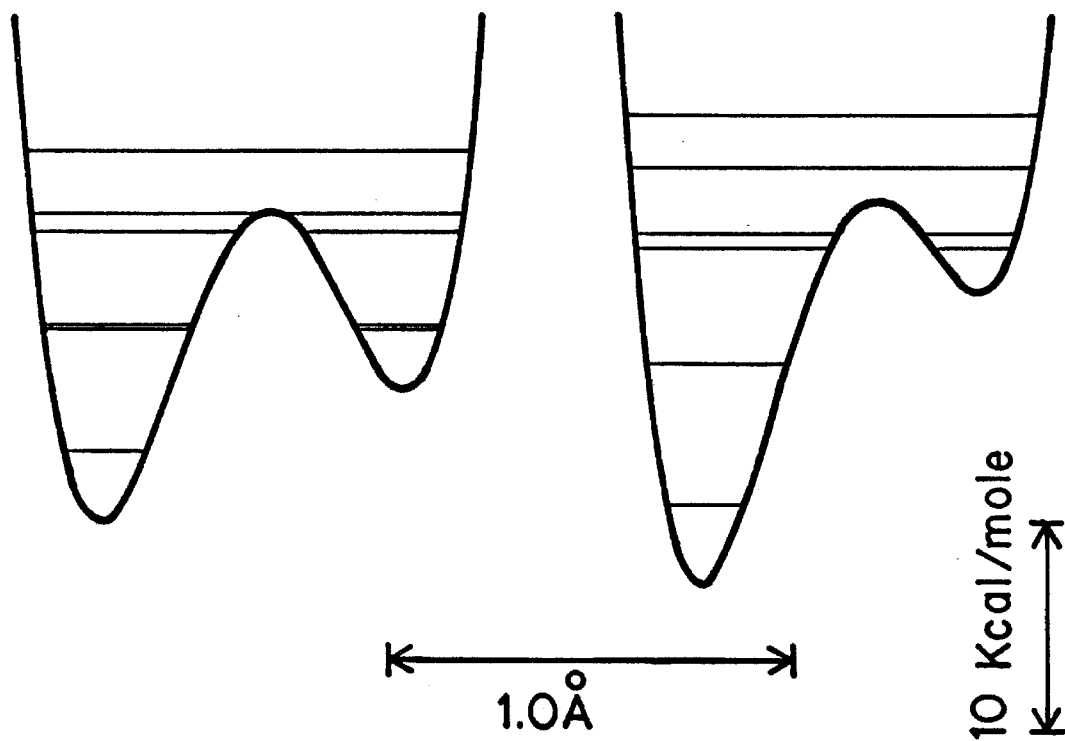


FIGURE 11

One-dimensional potential curves and energy levels of methanol and acetic acid hydrogen bonded to dioxane.

$\text{CD}_3\text{COOH}\cdots\text{dioxane } d_6$

$\text{CH}_3\text{OH}\cdots\text{dioxane}$



It is important to note that these two forms are not resonance structures, but tautomeric forms, since the geometry of the O-H...O bond is different in each case.

In view of this, the nature of the intramolecular hydrogen bond is expected to depend strongly on the coupling of the symmetric stretching vibration of the two oxygens with the antisymmetric O-H...O stretching vibration, and it is possible that the motions of the O-H and the donor-acceptor become less coupled at higher excitations of the donor-acceptor vibration. The hydrogen bond is probably strongest in the ground vibrational state of the donor-acceptor vibration, where the electrons in the enol ring are completely delocalized and the potential function of the bridge hydrogen is expected to be double minimum in nature. At higher excitations of the donor-acceptor vibration, the bridge hydrogen would tend to become more like a hydroxyl hydrogen-bonded to a ketone, in which case the potential function will be asymmetric. A reasonable speculation is that these tautomers correspond to the symmetric (I) and asymmetric (II) structures of the intramolecular hydrogen bond and that these two structures have their origin in the excitation of the donor-acceptor vibration. In the next section, we will examine the plausibility of this hypothesis by a CNDO calculation.

4. Molecular Orbital Calculations

An approximate method for determining the relative stability of the two enol structures is to compare their total energies using molecular orbital calculations. A qualitative description of the potential function associated with the bridge hydrogen in the hydrogen bond can also be obtained from such a calculation. The simplest approach would be to apply the extended Hückel method of Hoffman⁽²⁵⁾ to these systems. However, the results of some preliminary calculations carried out in this laboratory using the extended Hückel approximations indicate that the equilibrium geometrical configuration for the bridge hydrogen is only 0.485 Å away from one of the oxygen atoms. This is unlikely since the Van der Waal's radii have been determined to be 1.4 Å and 1.2 Å for oxygen and hydrogen atoms respectively.⁽²⁶⁾ The failure of the extended Hückel method in predicting the correct equilibrium internuclear distance probably arises from the approximation that the Hamiltonian is simply a sum of one-electron effective Hamiltonians and no specific considerations are given to the electron repulsion terms and the nuclear-nuclear repulsion terms.

Another less approximate self-consistent molecular orbital calculation is the CNDO/2 method proposed by Pople, Santry and Segal.⁽²⁷⁾ This method is based on the "complete neglect of differential overlap" approximation in which only the overlap distribution $\phi\mu(1)\phi\nu(1)$ of any two atomic orbitals $\phi\mu$ and $\phi\nu$ is neglected in all electron repulsion integrals. This method has been shown to predict correctly the relative stabilities of the cis- and trans- forms of

formic acid⁽²⁸⁾ and to successfully reproduce the approximate 1:2:3 ratio for the barriers in the three isoelectronic molecules CH_3OH , CH_3NH_2 and C_2H_6 .⁽²⁹⁾ The CNDO method also seems to be more effective in predicting the dissociation energies and proton potential functions of hydrogen bonds.⁽³⁰⁾ We have therefore used this method in order to obtain information on the potential function for the bridge hydrogen in the proposed symmetric and asymmetric structures of the enol tautomer in acetylacetone.

The full treatment of the CNDO method has been developed in detail by Pople and Segal^(27, 29, 31) and the several approximations used are summarized in the Appendix. The Hartree-Fock matrix F is constructed with the elements

$$F_{\mu\mu} = U_{\mu\mu} + (P_{AA} - \frac{1}{2} P_{\mu\mu}) \gamma_{AA} + \sum_{B(\neq A)} (P_{BB} \gamma_{AB} - V_{AB}) \quad (17)$$

$$F_{\mu\nu} = \beta_{AB}^0 S_{\mu\nu} - \frac{1}{2} P_{\mu\nu} \gamma_{AB} \quad (\mu \neq \nu) \quad (18)$$

where $P_{\mu\nu}$ is an element of the ordinary charge and bond order matrix; P_{AA} is the total electron density on atom A; γ_{AB} is the electron-interaction integral and β_{AB}^0 is an empirical bonding parameter depending only on the nature of the atoms A and B. The CNDO/2 parametrization of Pople and Segal⁽²⁹⁾ is used in this study without further modification.

The two different enol forms of acetylacetone are considered in this study. All calculations were carried out on an IBM 360/75 computer with the program provided by G. A. Segal. The input data

consist of the coordinates and atomic numbers of all nuclei in the molecule together with the number of valence electrons. Initial estimates of the LCAO coefficients were obtained from a Hückel-type theory using the matrix elements:

$$F_{\mu\mu}^{(0)} = -\frac{1}{2} (I_{\mu} + A_{\mu}) \quad (19)$$

$$F_{\mu\nu}^{(0)} = \beta_{AB}^0 S_{\mu\nu} \quad (20)$$

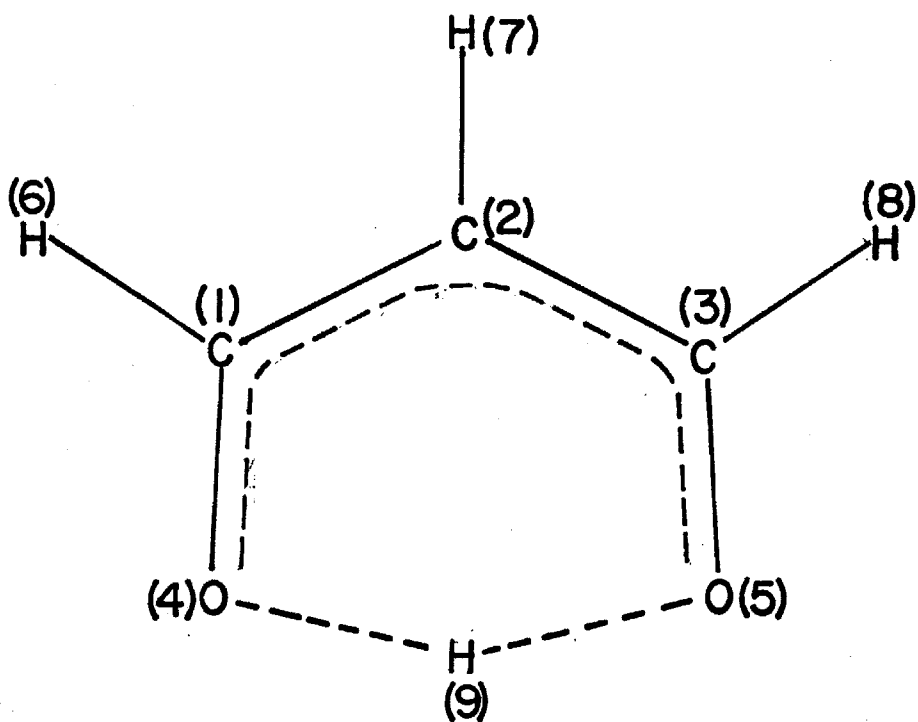
The coefficients obtained are combined with integral values already used to compute a new set of interaction elements which in turn yield a new set of coefficients. The cycling procedure is continued with a tolerance of 0.0001 or until the number of iterations reached 15.

The symmetric structure (I) and the asymmetric structure (II) used in the calculation are depicted in Fig. 12. An average C-C and C-O bond lengths of 1.378 Å and 1.266 Å were used for the symmetric structure whereas single and double C-C and C-O bond lengths were used in the asymmetric case. These parameters were chosen empirically as representative of the two structures. The acetylacetone molecule is greatly simplified in both cases by substituting a proton for each methyl group thereby reducing the order of the secular determinant from 36 to 24. It further simplifies the acetylacetone molecule into a planar configuration. The total computer time required for a complete run on one configuration of acetylacetone is accordingly reduced from 180 sec. to 60 sec. This simplification affects the total energy of the molecule considerably, but has little effect on the relative

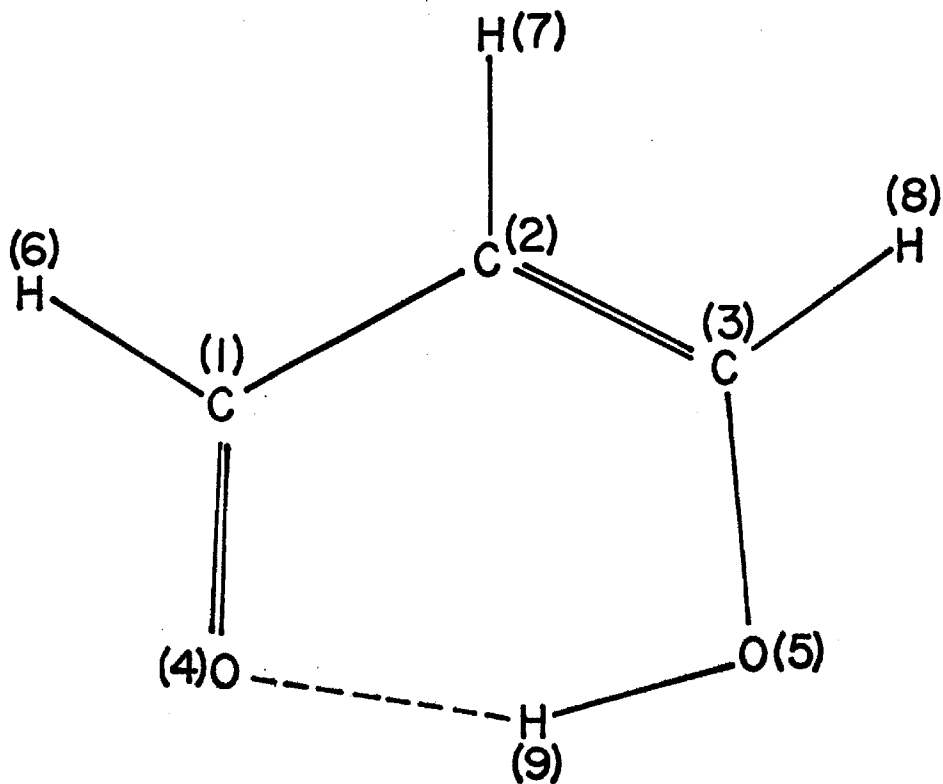
FIGURE 12

The symmetric (I) and asymmetric (II) structures of the enol tautomer of acetylacetone considered in the CNDO/2 calculations.

SYMMETRIC (I)



ASYMMETRIC (II)



energy changes.

The coordinate of the various atoms in the symmetric and asymmetric forms are listed in Table IX. CNDO/2 calculations on acetylacetone were carried out with variations in the atomic coordinate of the bridge hydrogen H(9), while the rest of the molecule is held fixed.

Two-dimensional total energy profiles for various coordinates of the bridge hydrogen are obtained as a result of these calculations. A symmetric double minimum potential was obtained for structure A (Fig. 13). The equilibrium configuration for the bridge hydrogen is centered at 0.96 Å from the oxygen atom and 0.4 Å below the O...O axis. The distance between the two minima corresponds to 0.85 Å. For the asymmetric case (Fig. 14), a sharp minimum is located at 1.0 Å from the oxygen atom and 0.3 Å below the O...O axis; another very broad minimum centered around 1.0 Å from the other oxygen atom is also located. The separation of the two centers of minimum energy in this case corresponds to 0.77 Å. The barrier in the case of the asymmetric potential was found to be 0.12 au while that of the double minimum was 0.05 au. The minimum energies obtained for these two forms at their equilibrium geometrical configuration, however, are comparable, being -60.96 au for the symmetric structure and -60.94 au for the asymmetric structure.

In view of the approximations involved in the calculation, the CNDO method cannot be expected to yield total energies which are in good agreement with experimental data. However, if the calculated energies were considered to be in arbitrary units, Wiberg⁽³²⁾ was able to show that a semi-empirical scaling factor may be determined

FIGURE 13

**A two-dimensional total energy profile
for the symmetric structure of the enol
tautomer.**

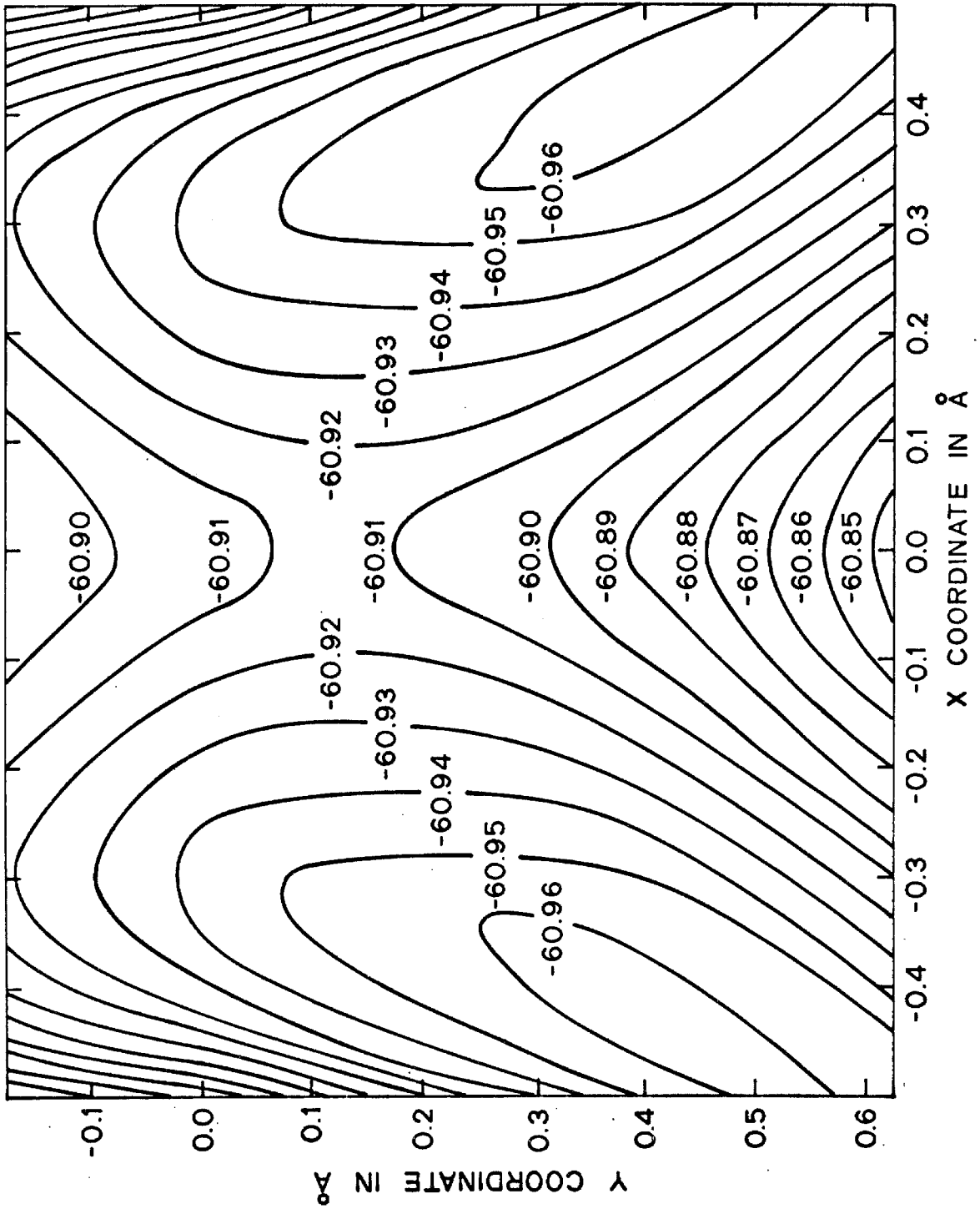


FIGURE 14

A two-dimensional total energy profile
for the asymmetric structure of the enol
tautomer.

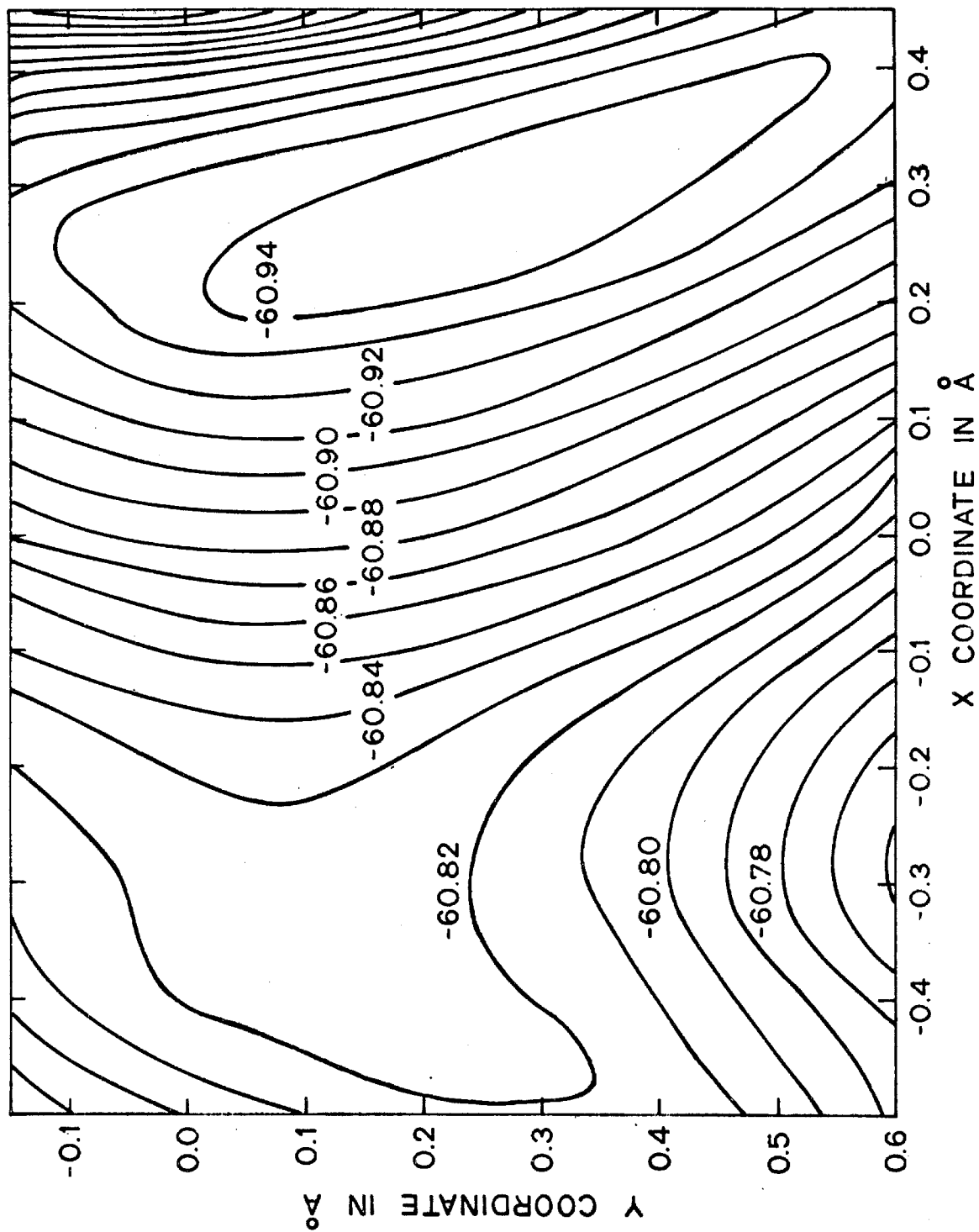


TABLE IX. The coordinate of various atoms in the symmetric and asymmetric structures proposed for the enol tautomer of acetylacetone.

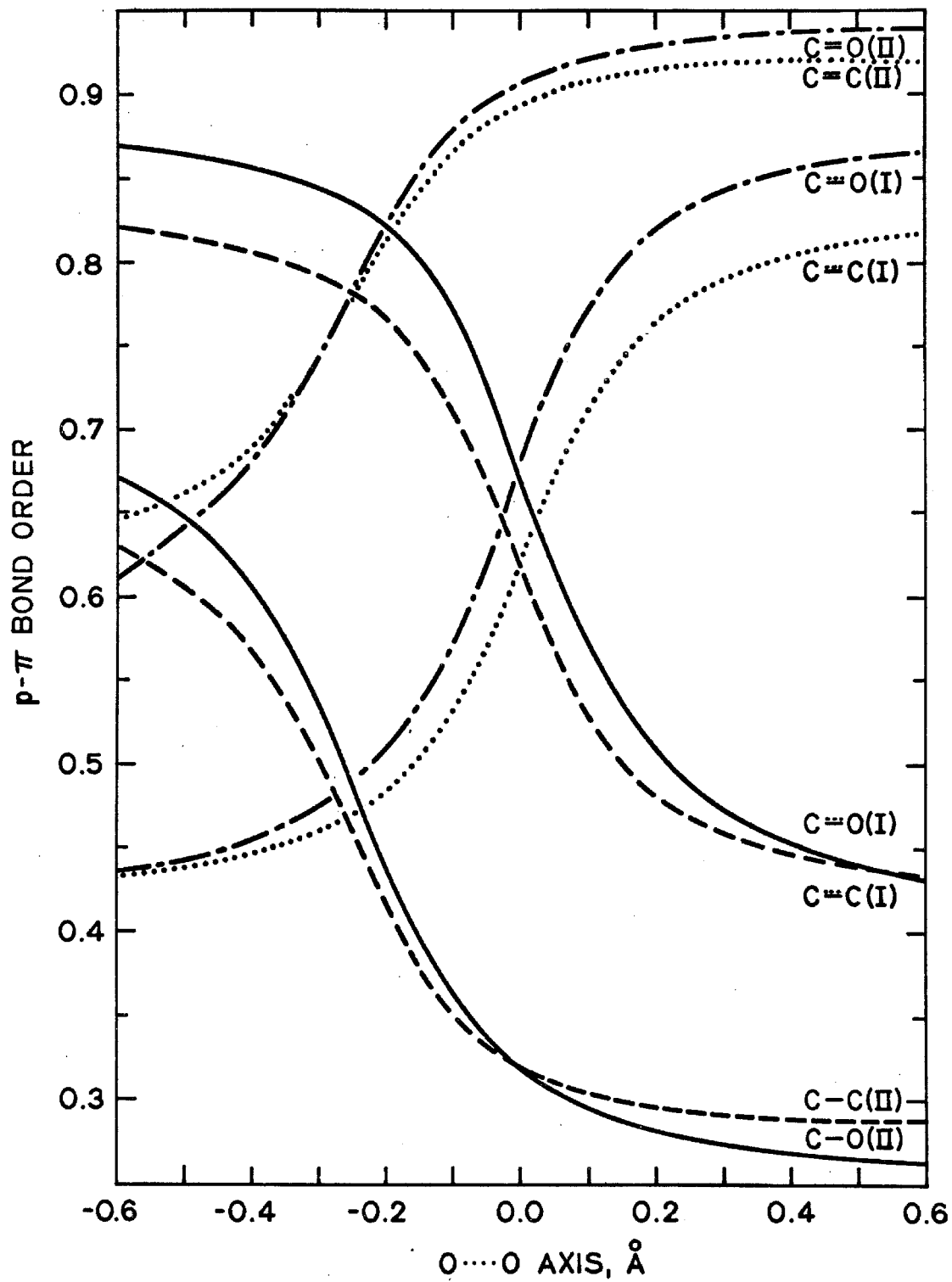
<u>Atom</u>	<u>Atomic Coordinate (Å)</u>					
	<u>Symmetric</u>			<u>Asymmetric</u>		
	X	Y	Z	X	Y	Z
C(1)	-1.2316	0.6181	0.0	-1.3764	0.6908	0.0
C(2)	0.0	0.0	0.0	0.0	0.0	0.0
C(3)	1.2316	0.6181	0.0	1.2065	0.6055	0.0
O(4)	-1.3850	1.8748	0.0	-1.4689	1.9072	0.0
O(5)	1.3850	1.8748	0.0	1.2991	2.0324	0.0
H(6)	-2.1192	0.0205	0.0	-2.2640	0.0932	0.0
H(7)	0.0	-1.0700	0.0	0.0	-1.0700	0.0
H(8)	2.1192	0.0205	0.0	2.0941	0.0079	0.0
H(9)	--	--	0.0	--	--	0.0

which permits the heats of atomization and heats of formation to be satisfactorily calculated. By comparing the experimental and calculated energies for a series of hydrocarbons, radical cations, free radicals and cations, the conversion factor was determined to be 220 kcal/mole/atomic unit of energy. Using this conversion factor, the height of the barriers obtained in this calculation correspond to 3800 cm^{-1} for the double minimum potential and 9200 cm^{-1} for the asymmetric case. Calculations by Brickmann and Zimmermann⁽³³⁾ have indicated that the lingering time τ , which is the average time that a proton lingers in one of the two wells before it tunnels into the other, increases by a factor of 100 for a barrier height of 10,000 cm^{-1} as the energy difference between the two minima increased from 0 to 100 cm^{-1} . Therefore, the bridge hydrogen is expected to be strongly localized in the asymmetric potential well while there is rapid tunnelling in the symmetric case.

We have also examined the $p\pi$ -bond orders of the enol ring $(\text{O}=\overset{\cdot}{\text{C}}-\text{CH}-\overset{\cdot}{\text{C}}-\text{O})^-$ as the bridge hydrogen is moved along the $\text{O}\cdots\text{O}$ axis. The motion of the bridge hydrogen has a large effect on the electronic distribution in the enol ring. The results are summarized in Fig. 15. In the symmetric structure, the degree of conjugation is highest when the bridge hydrogen is at the mid-point of the $\text{O}\cdots\text{O}$ axis; the degree of conjugation is much less in the asymmetric case. Comparison of the $p\pi$ -bond order of the two carbonyl groups in the asymmetric structure indicates that the hydrogen-bonded carbonyl carbon has a high $p\pi$ -bond order of 0.93 compared with the low bond order of 0.27 for the olefinic carbon bearing a hydroxyl; the bond orders for the two

FIGURE 15

Summary of the $p\pi$ -bond orders of the enol ring system in acetylacetone as the bridge hydrogen is moved along the O...O distance.



carbonyl groups for the symmetric form are 0.85 and 0.45 at the equilibrium geometrical configuration. The total atom densities are listed in Table X.

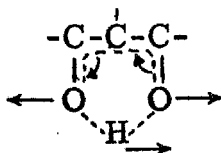
On the basis of this calculation, we can conclude that the symmetric and asymmetric forms of the hydrogen bond have quite similar energies. Naively, one can consider them in the following way: in order to go from the asymmetric structure to the symmetric structure, one must hybridize one of the lone pairs so that it can undergo conjugation with the π electrons of the enol ring system. The energy required to hybridize the oxygen orbital will be compensated by the energy resulted from conjugation. In view of this, the energy required for the conversion of the two structures must be rather small. In fact, the motion of the donor-acceptor groups may be sufficient to change the potential function from one form to the other. The motion of the bridge hydrogen also causes changes in the electron density in the π system suggesting that there is strong coupling of the electron density to the motion of the bridge hydrogen in the intramolecular hydrogen bond.

TABLE X. Total atom electron densities of the symmetric and asymmetric structures.

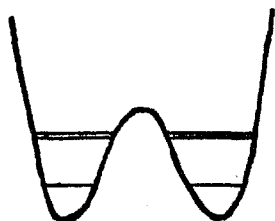
<u>Atom</u>	<u>Total atom electron densities</u>	
	<u>Symmetric</u>	<u>Asymmetric</u>
C(1)	3.7306	3.7510
C(2)	4.1786	4.1253
C(3)	3.7375	3.8223
O(4)	6.3285	6.2437
O(5)	6.2136	6.2480
H(6)	1.0432	1.0265
H(7)	0.9837	0.9788
H(8)	1.0024	0.9858
H(9)	0.7813	0.8179

5. The Nature of the Two States

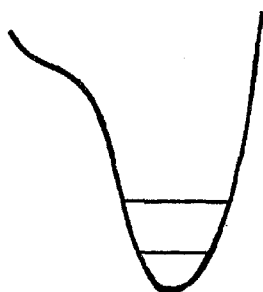
The results of the CNDO/2 calculations described in the previous section have shown that the motion of the bridge hydrogen is strongly coupled to the electronic distribution in the enol ring system. As the bridge hydrogen moves closer to the oxygen in the C=O group, these calculations show that there is an increase in the $p\pi$ -bond order in the other C-O group. This is also true for the C-C and C=C groups, so that there is a continuous displacement of the electron charge density in the enol ring system. The CNDO/2 calculations also indicate that the energy difference between the symmetric and asymmetric forms of the intramolecular hydrogen bond is quite small. This suggests that the excitation of the symmetric stretching motion may lead to a slightly different O...O distance and this may be sufficient to produce a charge shift in the system which would then alter the effective symmetry of the potential function for the hydrogen bond. When the molecule is excited, an O-H...O symmetric vibrational stretch would move the two oxygen atoms apart. Since the bridge hydrogen would tend to follow the movement of the oxygen in the C-O group, this will again initiate a continuous displacement of the electron charge density in the ring system in the opposite direction, leading to the asymmetric structure II. Some of the dynamics involved in the interconversion are summarized in the diagram below.



If the above hypothesis is correct, then we are proposing the following: when the donor-acceptor vibration is in the ground vibrational state, the potential is symmetric double minimum in nature;



and when it is in the first vibrational excited state of the donor-acceptor vibration, there exists the possibility that the potential function is asymmetric.



Since the energy difference between these two structures is so small, it is possible that by exciting the donor-acceptor vibration by one quanta, the effective potential function for the bridge hydrogen would be changed from one form to another.

The existence of an equilibrium between the symmetric (I) and asymmetric (II) structures would readily account for our proton and deuteron magnetic resonance observations. These two structures would be in rapid equilibrium on the NMR time scale, but relatively slow in the IR time scale. Since the magnetic shielding experienced

by the bridge hydrogen is quite different in these two structures, the chemical shift of the bridge hydrogen would be temperature dependent if the energy separation is about the order of magnitude of kT . To ascertain the isotope effect, we would have to determine the effect of deuterium substitution on the zero-point vibrational energy level of the proton and deuteron in the O-H...O antisymmetric stretch. As we had indicated earlier, the effect of deuterium substitution on the energy spacing between the zero-point vibrational energy levels of the two forms is expected to be quite large if the potential function is symmetric in one form and asymmetric in another.

These are some of the considerations which prompted us to examine the Raman spectra of acetylacetone and to look for the symmetric stretch. This band is expected to be Raman active but relatively weak in the infrared. The complete Raman spectra of acetylacetone and partially deuterated acetylacetone have recently been reported by Ernstbrunner.⁽¹⁶⁾ For a totally symmetric vibration, the Raman scattering will be completely polarized only if the derivatives of the polarizability $\partial \alpha_{xx}/\partial q_k$, $\partial \alpha_{yy}/\partial q_k$, $\partial \alpha_{zz}/\partial q_k$ are all equal by symmetry.⁽³⁴⁾ Otherwise these three derivatives may have different values leading to an arbitrary, but frequently very small degree of depolarization. In the case of acetylacetone, these polarizability derivatives for the O-H...O symmetric vibration are not identical by symmetry. The motion of the bridge hydrogen is mainly along the O...O axis rather than along the perpendicular direction. We therefore anticipate a partially depolarized band in the Raman spectrum for this transition, and that the degree of depolarization

should decrease upon deuterium substitution since the amplitude of vibration is smaller in the latter case. The Raman bands arising from the enol form in the region 500 cm^{-1} to 200 cm^{-1} are listed in Table XI. The two lowest frequency bands which are depolarized are the 418 cm^{-1} band in the normal compound and the 230 cm^{-1} band in the deuterated molecule. Both of these bands are depolarized, but the Raman band in the deuterated compound is less depolarized and more intense than the band in the normal molecule. These two transitions therefore correspond to the energy difference between the symmetric (I) and asymmetric (II) structures in the proton and the deuterated compounds. The deuterium isotope effect observed here is 188 cm^{-1} which would result in the large deuterium isotope effect observed in our proton and deuteron magnetic resonance studies.

6. Analysis of the NMR Data in Terms of the Two-State Model

In this section we shall attempt to place the results of the temperature study on the bridge hydrogen and the bridge deuterium on a more quantitative basis. We have proposed that there are two enol structures in dilute solutions of acetylacetone in non-hydrogen bonding solvents, the symmetric structure (I) and the asymmetric structure (II). The vibrational potential function for structure I is symmetric double minimum in nature, while that for structure II is asymmetric. The zero-point energy differences are denoted by ΔE_{H}^0 for the normal molecule and ΔE_{D}^0 for the deuterated molecule. A schematic representation of energy levels is shown in Fig. 9. The ΔE^0 's are the

TABLE XI. Raman spectra of the enol form of acetylacetone and partially deuterated acetylacetone below 500 cm^{-1} .

<u>Acetylacetone</u>	<u>($^2\text{H}_2$) Acetylacetone</u>
503 m, p	504 m, p
418 w, dp	465 w, p
391 w, p	399 w, dp?
244 m, p	368 w, p
	321 vw, dp
	230 m, dp?

vibrational quanta for exciting the O-H...O vibration which enables the potential function to change from one form to another and we now show that the deuterium isotope effect is merely a reflection of the change in the free energy difference between the two enol tautomers in the normal and deuterated molecules.

In order to determine the energy difference between structures I and II based on the results of the temperature study, it is first necessary to determine whether there is any difference in entropy between these two structures. If we ignore the higher vibrational states in the discussion, then there will be two "ground" vibrational energy states for structure I corresponding to the well-known symmetric and anti-symmetric states. However, these two vibrational states are probably degenerate unless the central barrier is very low. There are also two states of interest for structure II, i. e., the one depicted in Fig. 9 and its mirror image. These states are also degenerate since the potential barrier to go from one to the other is very high and the resonance between the two wells has no effect on the energy. These considerations clearly indicate that there is no entropy difference between these two structures and we can assume that

$$\Delta G^0 = \Delta H^0 = \Delta E^0 \quad (21)$$

It therefore follows that

$$K = e^{-\Delta G^0/kT} = e^{-\Delta E^0/kT} \quad (22)$$

The chemical shift observed for the bridge hydrogen in acetylacetone is the weighted average of the chemical shifts of the two

structures since they undergo rapid exchange throughout the temperature range studied. The observed chemical shift may be expressed as follows:

$$\delta_{\text{obs}} = \delta_{\text{I}} F_{\text{I}} + \delta_{\text{II}} F_{\text{II}} \quad (23)$$

where F_{I} and F_{II} represent the mole fractions of structures I and II respectively, and δ_{I} and δ_{II} are the chemical shifts for structures I and II. Assuming a Boltzmann distribution, equation (17) can be rewritten as:

$$\delta_{\text{obs}} = \frac{\delta_{\text{I}}}{1 + \exp(-\Delta E^{\circ}/kT)} + \frac{\delta_{\text{II}}}{1 + \exp(\Delta E^{\circ}/kT)} \quad (24)$$

For the normal compound, $\Delta E^{\circ} = \Delta E_{\text{H}}^{\circ}$ and for the deuterated compound, $\Delta E^{\circ} = \Delta E_{\text{D}}^{\circ}$. From the temperature dependence of the experimentally observed proton and deuteron chemical shifts shown in Fig. 5, a non-linear least squares computer program was used to extract the best values of δ_{I} , δ_{II} , and ΔE° .

The results of an analysis of the OH temperature data in terms of a two-state model indicate an energy separation of 405 cm^{-1} between the two states. A similar analysis of the OD temperature data yields an energy separation of 215 cm^{-1} between the corresponding states in the deuterated system. The chemical shifts obtained for the OH proton and the OD deuteron in the lower and upper states are identical, being -14.15 and -10.10 ppm (relative to the methyl resonance of the enol tautomer) for the lower and upper states respectively. These results are summarized in Table XII. The effect of deuteration upon the

TABLE XII. Chemical shifts and thermodynamic parameters for bridge hydrogen (deuterium) states.

	<u>Proton</u>	<u>Deuteron</u>
δ_{I} ppm	-14.15	-14.15
δ_{II} ppm	-10.10	-10.10
F_{I} @ 25°C	0.87	0.74
F_{II} @ 25°C	0.13	0.26
ΔH° (cm ⁻¹)	405	215
ΔS° (e. u.)	0	0
Standard Error (Hz)	0.58	0.20

bridge hydrogen has therefore resulted in a decrease in the energy separation between the states by 190 cm^{-1} . This deuterium isotope effect is in excellent agreement with that observed in the Raman spectra, where the transitions of interest are 418 cm^{-1} for the normal molecule and 230 cm^{-1} for the deuterated molecule.

7. Potential Function

One of the primary objectives of this work is to determine the potential energy function for the bridge hydrogen in the enol tautomer of acetylacetone. We have concluded from the previous sections that the potential function for the O-H...O antisymmetric stretch in the ground vibrational state is double minimum in nature while that for the first vibrational excited state is asymmetric and that the anomalous deuterium isotope effect and the pronounced temperature dependence have their origin in the differences in the energy spacings between the two structures. It is possible to calculate theoretically the energy levels of the two potential functions proposed for the two structures I and II if there is sufficient data in the infrared spectrum on the OH stretching region of acetylacetone, and in general the accuracy of the potential functions used in the calculation can be confirmed by the isotope effect observed in the infrared spectrum of the partially deuterated molecule.

In general, one may write the vibrational Hamiltonian for the A-H stretching motion in the following form:

$$H = p^2/2\mu + V \quad (25)$$

where μ is the mass of hydrogen, and

$$V = \sum_n a_n x^n \quad (26)$$

is a Taylor expansion of the potential function. The constant term in (25) can be neglected since it displaces all energy levels by the same amount. Moreover, one of the coefficients a_n ($n \neq 0$) can be generally set equal to zero by a simple coordinate translation. For most molecular vibrations of small amplitude, the harmonic potential $V = a_2 x^2$ is usually sufficient. More complicated forms of the potential function have been suggested, but their applications are mostly limited to diatomic molecules. In special cases, e. g., the inversion of ammonia, the puckering of small rings, etc., where the potential well may be double minimum, the potential is quite different from the usual harmonic or Morse type function. It is necessary to include higher powers in the Taylor expansion even to account for the transitions between the lowest energy levels. The simplest symmetrical double minimum potential function takes the form

$$V = ax^4 + bx^2 \quad (27)$$

where b is negative.

Somorjai and Hornig have done energy calculations for this potential using twenty harmonic oscillator wave functions as basis. ⁽³⁵⁾ Chan and coworkers have also carried out similar calculations for anharmonic potential functions. ⁽³⁶⁾ These workers have shown that the harmonic oscillator basis is, in general, rather unsatisfactory for

such calculations due to slow convergence. Instead, they demonstrated that extremely rapid convergence was obtained when the quartic oscillator basis was used as a starting point for the variational calculations. We shall therefore use the quartic oscillator basis in this work.

For the simplification of computations, the displacement coordinate and its conjugate momentum are transformed into dimensionless space:

$$X = (8\mu a/\hbar^2)^{1/6} x \quad (28)$$

$$P = (8/\mu a\hbar^4)^{1/6} p \quad (29)$$

The Hamiltonian then becomes:

$$H = A (P_\eta^2 + X_\eta^4 + \eta X_\eta^2) \quad (30)$$

where

$$A = (a\hbar^4/64\mu^2)^{1/3} \quad (31)$$

$$\eta = (k^3\mu/a^2\hbar^2)^{1/3} \quad (32)$$

The energy level calculations are straightforward. The matrix elements developed for the quartic oscillator by Chan et al. ⁽³⁶⁾ have been used to set up the energy matrix, which was then diagonalized to give the energy eigenvalues λ_n and eigenfunctions Ψ_n . The present computations were carried out using 20×20 matrices on an IBM 360/75 computer. The convergence of the eigenvalues and eigenfunctions are all satisfactory. For the eigenfunction of the n th level, we have

$$\Psi_n = \sum_k a_k \phi_k \quad (33)$$

where the ϕ_k 's are the quartic oscillator wave functions. In principle, A and η can be varied in the calculation to make the eigenvalues of the Hamiltonian (30) fit the lowest transitions observed for the hydrogen bonded complex. However, ratios of successive energy-level spacings, i. e., $\left[(W_{1-} - W_{0+}) - (W_{1+} - W_{0-}) \right] / (W_{1-} - W_{0+})$, are independent of the scaling factor $(a\hbar^4/64)^{1/3}$; thus η can be unambiguously determined if the experimental ratio is known.

The resonance splitting of the O-H... vibrational levels had been studied in detail by Shigorin et al. (17) They have reported that the broad O-H...O stretch in the region of 2700 cm^{-1} splits into two bands at 2622 and 2675 cm^{-1} ($\Delta = 53 \text{ cm}^{-1}$) at low temperatures. A plot of $\left[(W_{1-} - W_{0+}) - (W_{1+} - W_{0-}) \right] / (W_{1-} - W_{0+})$ is given in Fig. 16 over the region of $\eta = -11.0$ to -13.0 . Experimentally, the ratio of the splitting over the lowest transition was observed to be 0.198 . Reference to Fig. 16 then yields a value of -12.5 for η in acetylacetone. By scaling the energy levels to reproduce the 0-3 transition, we obtained the transition frequencies presented in Table XIII.

The accuracy of the potential function can also be checked by comparing the isotope effect when the bridge hydrogen is substituted by deuterium, since it is reasonable to assume that the potential is changed only slightly with deuterium substitution. The energy levels for the deuterium bond can then be determined from the potential function for the corresponding hydrogen bond using the following relationships without the introduction of additional empirical parameters:

FIGURE 16

A plot of $\left[(W_{1-} - W_{0+}) - (W_{1+} - W_{0-}) \right] / (W_{1-} - W_{0+})$
ratio for the lowest two vibrational levels of the poten-
tial function $V(X) = A(X^4 - \eta X^2)$ in the region $\eta = -11.0$
to -13.0 .

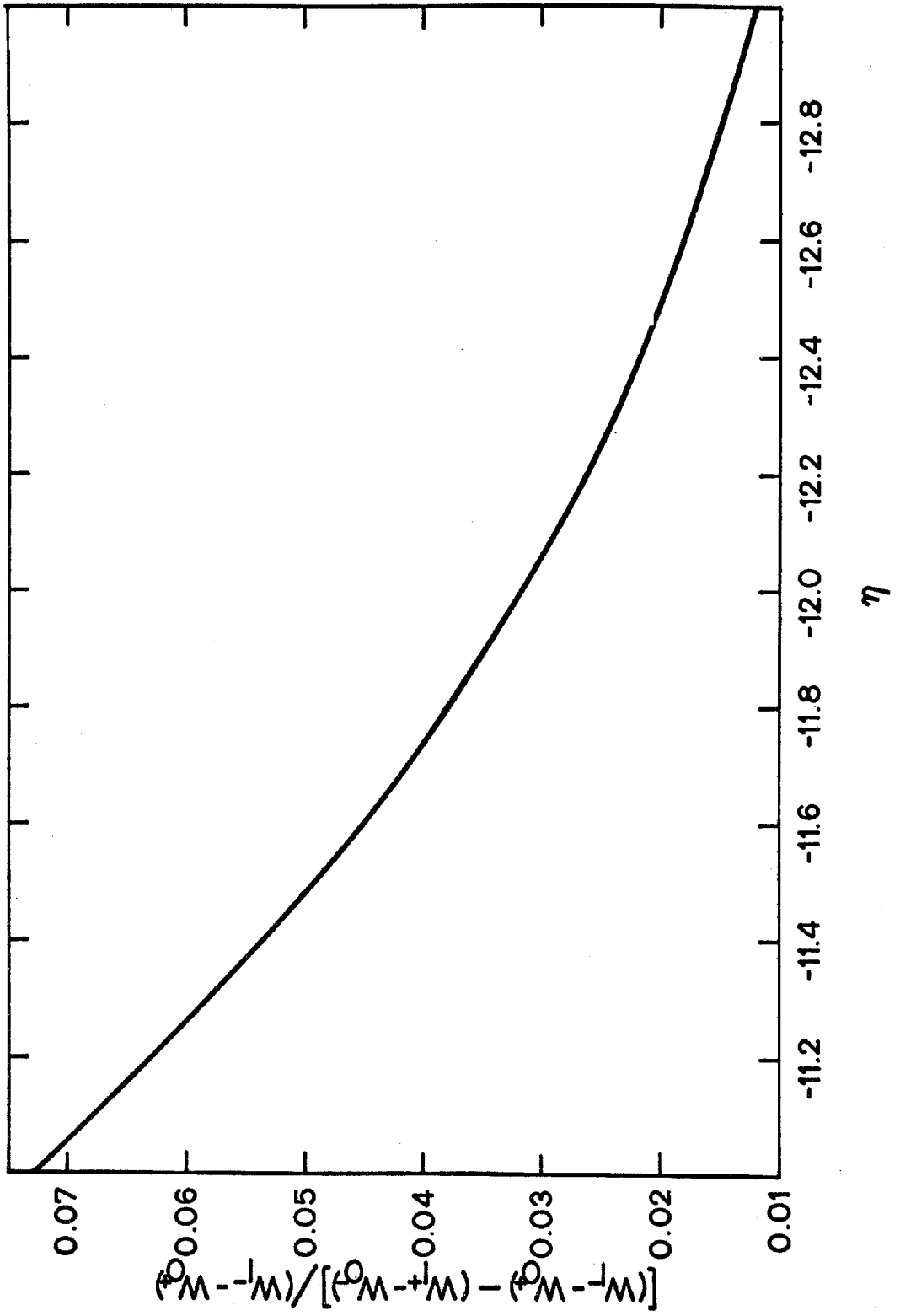


TABLE XIII. The calculated infrared spectrum of the OH and OD stretching region in acetylacetone.

	OH	OD
η	-12.5	-15.7
$\epsilon(0^+)$	-4427	-4830
$\epsilon(0^-)$	-4427	-4830
$\epsilon(1^+)$	-1805	-2855
$\epsilon(1^-)$	-1752	-2858
A	150.5	95.3
$0^+ - 1^-$	2675	1972
$0^- - 1^+$	2623	1975

$$A_D/A_H = (\mu_H/\mu_D)^{2/3} \quad (34)$$

$$\eta_D/\eta_H = (\mu_D/\mu_H)^{1/3} \quad (35)$$

The potential function for the O-H...O stretching vibration in acetylacetone is given in Fig. 17. In terms of the reduced coordinate X,

$$V(X) = 150.5 (X^4 - 12.5 X^2) \text{ cm}^{-1} \quad (36)$$

for the normal molecule and

$$V(X) = 95.3 (X^4 - 15.7 X^2) \text{ cm}^{-1} \quad (37)$$

for the deuterated molecule.

The height of the central barrier is 5900 cm^{-1} and the distance between the potential minima is 0.83 \AA . Two pairs of energy levels lie below the top of the central barrier. The energy splitting for the first pair of levels is 53 cm^{-1} . Upon deuterium substitution, the most dramatic effect for the symmetric double minimum potential is the coalescence of each pair of symmetric and antisymmetric levels below the top of the barrier. This behavior simply reflects the difference in the effect of the central barrier in the wave functions of the symmetric and antisymmetric states. From the zero-point energies of the normal molecule and the deuterated molecule, the zero-point energy difference (ϵ_I) can be calculated to be 403 cm^{-1} .

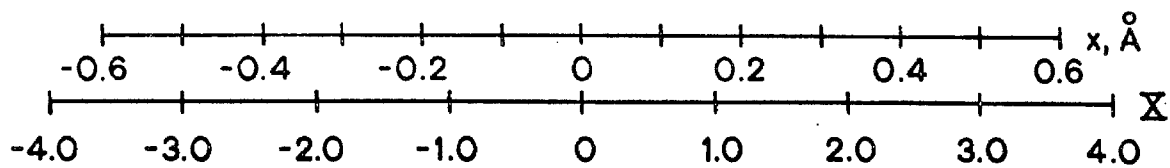
For the asymmetric potential proposed for structure II, the central barrier is very high so that for the ground vibrational state, it is adequate to assume that the isotope shift is given by:

FIGURE 17

Lower portion of the potential energy function
 $V(X) = 150.5 (X^4 - 12.5 X^2) \text{ cm}^{-1}$ for the donor-
acceptor vibration of the bridge hydrogen in the
enol tautomer of acetylacetone.

$- 3000 \text{ cm}^{-1}$ $- 2000$ $- 1000$

0

 $--1000$ $--2000$ $--3000$ $--4000$ $--5000$ $--6000$ $V(H) = |^-$ $V(H) = |^+$ $V(D) = |^\pm$ $V(H) = 0^\pm$ $V(D) = 0^\pm$ 

$$\nu_{\text{H}}/\nu_{\text{D}} = (\mu_{\text{D}}/\mu_{\text{H}})^{1/2} \quad (38)$$

If we denote the energy difference between the zero point energy of the normal and deuterated molecules as ϵ_{II} , then it is clear that

$$\epsilon_{\text{II}} = \frac{1}{2} (\nu_{\text{H}} - \nu_{\text{D}}) = 0.146 \nu_{\text{H}} \quad (39)$$

The fundamental frequency for the OH stretch in intramolecular hydrogen bonded compounds without resonance stabilization are known to result in the formation of single-bridge hydrogen bonds similar to those of the intermolecular hydrogen bonds. The OH stretch usually occurs as a relatively weak absorption in the range 3570-3450 cm^{-1} ,⁽³⁷⁾ for example, that of ethyl acetoacetate has been reported to be 3480 cm^{-1} by Fèvre and Welsh.⁽³⁸⁾ If ν_{H} is around 3500 cm^{-1} , then the zero point energy difference is approximately given by:

$$\epsilon_{\text{II}} = 0.146 \times 3500 \text{ cm}^{-1} = 511 \text{ cm}^{-1} \quad (40)$$

The energy difference between the two energy spacings corresponds to the observed deuterium isotope effect. The isotope effect is therefore

$$\epsilon_{\text{II}} - \epsilon_{\text{I}} = \Delta E_{\text{H}}^0 - \Delta E_{\text{D}}^0 = 108 \text{ cm}^{-1} \quad (41)$$

Considering the approximations involved in this calculation, the results are in reasonable agreement with the Raman results of 188 cm^{-1} .

8. Effect of Substitution

Examination of the results on the deuterium isotope effect and the temperature effect on the chemical shift of the bridge hydrogen in some substituted β -diketones and β -keto esters have revealed an apparent correlation between the temperature dependence and the deuterium isotope effect in these systems (Table XIV). A large isotope effect is in general accompanied by a pronounced temperature dependence; and this temperature dependence is large only in β -diketone systems and not in β -keto esters. The only exception to this generalization is the case of hexafluoroacetylacetone, where the absence of a temperature effect for the bridge hydrogen is probably due to the strong electron-withdrawing property of the CF_3 groups, which have a dominating effect on the electron density at the two oxygens so that an excitation of the donor-acceptor vibration cannot produce any change in the effective potential function for the bridge hydrogen.

The chemical shift of the β -diketone systems are also observed to be more sensitive to the effect of substituent groups on the enol ring than those of β -keto esters. This effect of substituent groups on the chemical shift of the bridge hydrogen in β -diketones is a direct reflection of the high degree of electron delocalization in the ring. This type of electron delocalization can be demonstrated by comparing the inductive effect of substituent groups on the enol ring. In the case of trifluoroacetylacetone, for example, the strong electron-withdrawing property of the CF_3 group will increase the double-bond character of the $\text{C}=\text{O}$ bond and weaken the $\text{C}-\text{C}$ bond. Since the CH_3 group is slightly

TABLE XIV. Correlation of the proton chemical shifts of the bridge-hydrogen in the enol tautomer of several pure β -diketones and β -keto esters with the effects of temperature and deuterium substitution.

<u>Compound</u>	<u>Chemical Shift (Enol OH)^a</u>	<u>Temperature Effect</u>	<u>Anomalous Deuterium Isotope Effect</u>
Acetylacetone	-15.57	yes ^{b, c}	yes ^c
α -Chloroacetylacetone	-15.37	yes ^b	
1, 3-Diphenyl-1, 3-propanedione	-17.00	yes ^c	yes ^c
Hexafluoroacetylacetone	-13.00	no ^b	
1-Phenyl-1, 3-butanedione	-16.33	yes ^c	yes ^c
3-Methyl-1, 4-pentanedione	-16.50	yes ^{b, c}	yes ^c
Trifluoroacetylacetone	-14.12	yes ^b	
Butyl acetoacetate	-12.17	no ^b	
t-Butyl acetoacetate	-12.22	no ^b	
t-Butyl α -chloroacetoacetate	-12.45	small ^b	
Ethyl acetoacetate	-12.17	no ^b	no ^c
Ethyl benzoylacetate	-12.83	small ^b	
Ethyl α -bromoacetoacetate	-12.73	no ^b	
Ethyl α -n-butylacetoacetate	-12.85	no ^b	
Ethyl α -chloroacetoacetate	-12.28	small ^b	
Ethyl α -cyanoacetoacetate	-13.45	small ^b	
Ethyl α -ethylacetoacetate	-12.73	no ^b	
Ethyl trifluoroacetoacetate	-12.00	small ^b	
Ethyl α -methylacetoacetate	-12.63	no ^b	

^a Data taken from J. L. Burdett and M. T. Rogers, *J. Amer. Chem. Soc.*, **86**, 2105 (1964). Chemical shifts are room temperature values and are in ppm from internal TMS.

^b J. L. Burdett and M. T. Rogers, *J. Phys. Chem.*, **70**, 939 (1966).

^c This work.

electron donating, its effects on the enol ring occur in the opposite direction. It follows that the oxygen atom in C=O of acetylacetone is more basic than that of trifluoroacetylacetone, the former forms a stronger O...H bond and a weaker O-H bond than the latter. This is evidenced by the chemical shift of the two bridge hydrogens, which occur at -15.57 ppm for acetylacetone and -14.12 ppm for trifluoroacetylacetone. Recently, Yoshida et al. ⁽³⁹⁾ studied the effect of substituent effect on the enol ring on the chemical shifts of the bridge hydrogen, and the stronger electron-withdrawing resonance effect of the substituent was observed to result in a lower downfield shift of the bridge hydrogen.

It is also interesting to note that acetylacetone gives a uv spectrum markedly different from simple conjugated ketones. ⁽⁴⁰⁾ In ethyl acetoacetate, for example, a strong band occurs at 2340 Å which corresponds to the π - π band noted by many investigators for the conjugated system. Acetylacetone however exhibits a very strong band with a maximum at 2700 Å, and molar extinction coefficient $\sim 10,000$. This is where bands for simple unconjugated ketones are usually found, but these bands are much weaker (molar extinction coefficient ~ 20). ⁽¹²⁾

All of these observations can be readily accounted for if the enol tautomer of the β -keto esters exist predominantly in the asymmetric structure, whereas acetylacetone and related β -diketones exist predominantly in the symmetric structure. It is perhaps no coincidence that the chemical shift of the bridge hydrogen in β -keto esters does not exhibit any significant temperature dependence or isotope effect with deuterium substitution, and that it is also invariably found to be

3 to 4 ppm upfield from that observed in the β -diketones.

9. Solvent Effect

We have observed that the chemical shift and linewidth behavior of the bridge hydrogen is quite different when the solvent is n-butyl ether. The data at 100 MHz indicate that at low temperatures slow chemical exchange is occurring and as the temperature is increased, the intermediate and finally the fast exchange regions are encountered. Due to the increase in observing frequency, the linewidth behavior at 220 MHz indicates only the slow and intermediate regions. Examination of Figures 6 and 7 show that at approximately 10°C, the chemical shift of the OH resonance in n-butyl ether departs from that observed in cyclohexane and the linewidth of the resonance has broadened appreciably. Thus, the results indicate that a minor species, whose chemical shift is at higher field, is present in small quantity and is exchanging with the major species. Analysis of these results by adding an additional term in Equation (23) ($\delta_{\text{III}} F_{\text{III}}$) and using the data which approximate the fast chemical exchange region indicates that this third species is present to the extent of approximately 1% in n-butyl ether. The chemical shift for the OH in this tautomer is predicted to occur approximately 5 ppm downfield from the enol methyl resonance. The most likely candidate for this minor species is an enol form of acetylacetone in which the intramolecular hydrogen bond has been broken and the OH group is rotated out of the molecular plane. In this configuration, conditions are favorable for the ether oxygen group

of the solvent molecule to form a hydrogen bond with the bridge hydrogen.

It is well known that if a molecule can exist in two distinct molecular environments B and C, where B is acetylacetone in the enol tautomer and C is the acetylacetone ether complex, the chemical shift(s) and the linewidth(s) of the resulting nmr signal(s) will be determined by the ratio of the rate of chemical exchange to the chemical shift difference between the two environments (the nmr time scale). When the exchange is fast compared to the nmr time scale, only the weighted average signal is observed and its linewidth is given by⁽⁴¹⁾

$$\Delta\nu_{\text{obs}} = \Delta\nu_0 + 4\pi P_B^2 P_C^2 \Delta^2 (\tau_B + \tau_C) \quad (42)$$

where $\Delta\nu_{\text{obs}}$ is the observed linewidth; $\Delta\nu_0$ is the weighted average linewidth in the absence of chemical exchange; τ_B and τ_C denote their pre-exchange lifetimes; Δ is the chemical shift difference of the proton between the two environments; P_B and P_C are the relative populations of the two exchanging species and are related by the standard free energy difference between the two species:

$$P_C/P_B [\text{Ether}] = e^{-\Delta G/RT} \quad (43)$$

It is clear that in this limit, increasing the temperature will decrease the linewidth, since both τ_B and τ_C decrease with temperature. In the slow exchange limit, i. e., when the exchange is slow on the nmr time scale, we expect to see two separate signals, provided that the populations of both species are large enough and their resonances narrow

enough to enable them to be observed. The linewidth of the resonances due to species B is, for example, given by⁽⁴¹⁾

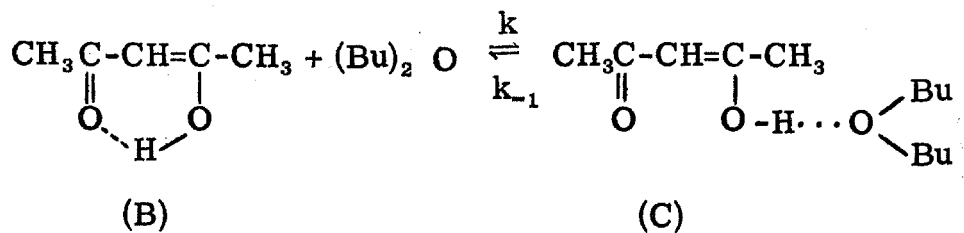
$$(\Delta\nu_{\text{obs}})_B = (\Delta\nu_0)_B + 1/\pi \tau_B \quad (44)$$

Here $(\Delta\nu_0)_B$ is the resonance linewidth of species B in the absence of chemical exchange. Note that because of the reciprocal dependence on τ_B , the linewidth increases with temperature in this limit. As expected, in the intermediate exchange region, where the exchange is taking place at a rate comparable to the nmr time scale, maximum broadening occurs. Thus, as the exchange rate increases from the slow to the fast exchange limit, the resonance broadens to a maximum width, and then decreases in width.

We also note that since Δ , the chemical shift difference of the bridge hydrogen between the two magnetic environments, is directly proportional to the magnetic field strength in the limit of fast exchange, we expect the exchange linewidth to be proportional to the square of the magnetic field (cf. Eq. (42)). In the limit of slow exchange, however, the linewidth should be independent of the magnetic field (cf. Eq. (44)). Our experimental data show that in the high temperature region, the linewidth of the bridge hydrogen increases by a factor of two to four (depending on temperature) as the magnetic field is increased from 23.5 Kilogauss (100 MHz) to 51.7 Kilogauss (220 MHz).

We have also observed that the linewidth due to exchange at low temperatures is a linear function of the concentration of the solvent n-butyl ether. A mechanism which is consistent with this concentration dependence is the formation of the acetylacetonate-ether

complex. The exchange process may be summarized as follows:



In this case,

$$-\frac{d[\text{Acetylacetone}]}{dt} = k [\text{Acetylacetone}][\text{Ether}] \quad (45)$$

and it follows that

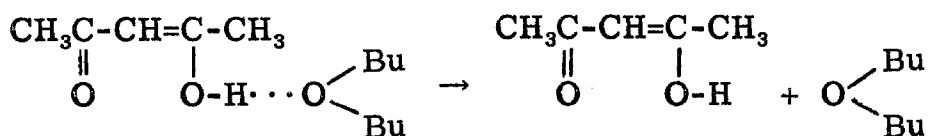
$$\frac{1}{\tau} = -\frac{d[\text{Acetylacetone}]}{[\text{Acetylacetone}] dt} = k [\text{Ether}] \quad (46)$$

Since the line broadening of the bridge hydrogen arises from the chemical exchange between B and C, the linewidth of the bridge hydrogen can be calculated for a given k if the relative populations between the two species as well as the chemical shift difference Δ , is known. We have carried out such calculations for the bridge hydrogen using the Dynamic NMR Program provided by G. Binsch and D. A. Kleier.⁽⁴²⁾ It is possible to extract the rate constant k from the experimental linewidth for a given assumed Δ and ΔG° . At a given temperature, the observed linewidths at 100 MHz and 220 MHz must, however, yield the same k and this correspondence must apply over the whole temperature range if Δ and ΔG° are to be unique. Since the chemical shift of acetylacetone is a function of temperature in inert solvents, this temperature dependence has to be taken into

consideration in the choice of Δ . As a result of a number of iterations, we have found that $\Delta = 850$ Hz at 100 MHz at 20°C and $\Delta G^\circ = 3.87$ Kcal gave the best fit to our data.

A comparison of the observed linewidth at the two frequencies with the theoretically expected linewidth is depicted in Figs. 18 and 19. It is observed that the theoretical linewidths deviate from the experimental data at high temperatures. This is apparent only in the 220 MHz data where the exchange rate is still in the intermediate exchange region at the highest temperature studied. The 100 MHz line shapes are less sensitive at high temperatures where the exchange is rapid. This is indicated by the variation of linewidths with rate constants at different population ratios in two observing frequencies. These results are shown in Figs. 20 and 21.

It is conceivable that the reaction is more complicated at high temperature. One probable reaction is the break-up of the intermolecular hydrogen bond in the acetylacetone-ether complex to give another "open" species:



The thermodynamic parameters for this process cannot be derived in this study. Presumably, this free OH proton would be the most shielded of all forms of acetylacetone considered. Due to the increase in frequency separation between the exchanging species, the experimental linewidth is expected to be broader than the theoretical value.

FIGURE 18

A comparison of the calculated and observed linewidth of the bridge hydrogen at 100 MHz. Concentration of acetylacetone in n-butyl ether: 0.12 mole fraction.

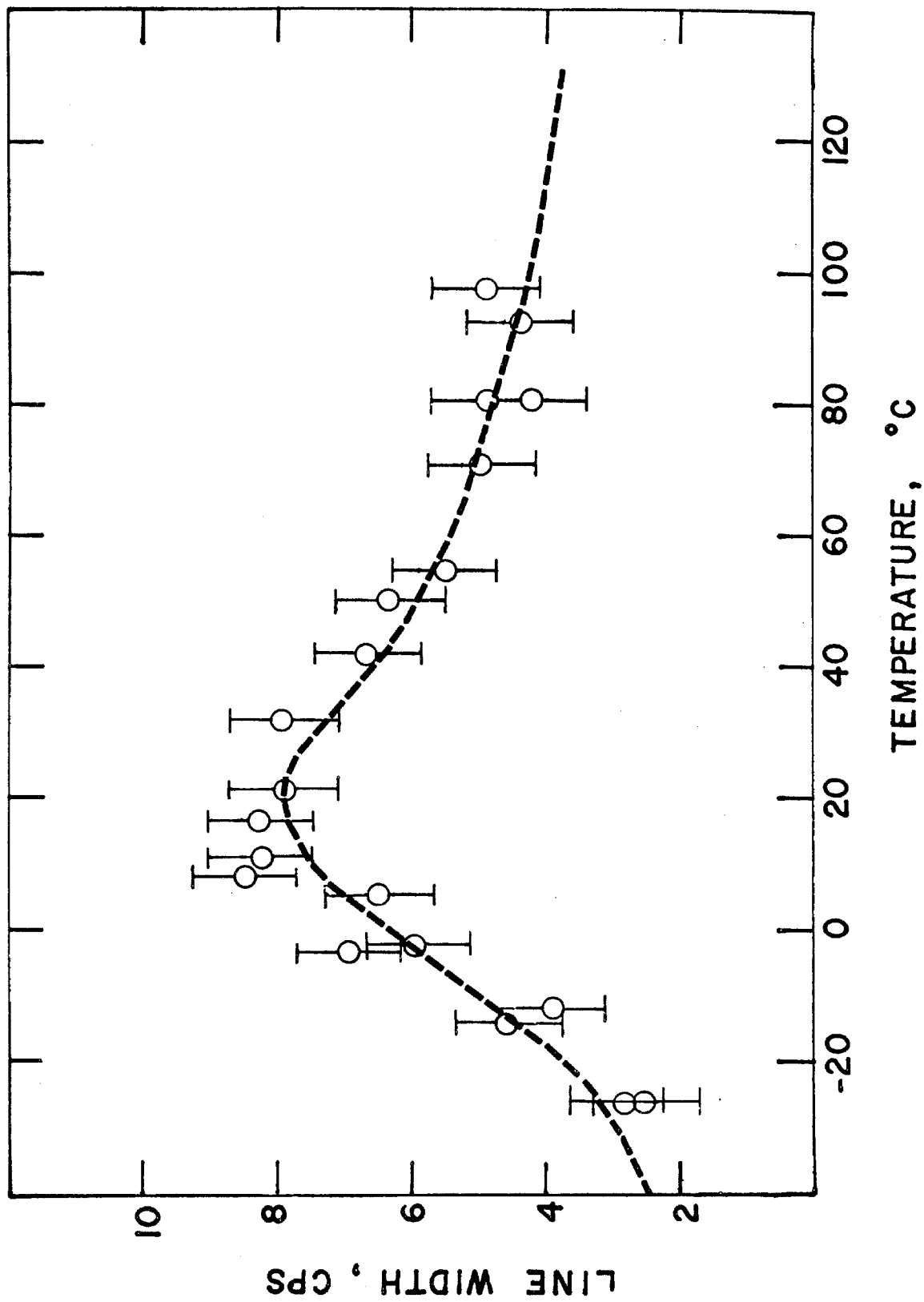


FIGURE 19

A comparison of the calculated and observed linewidth of the bridge hydrogen at 220 MHz. Concentration of acetylacetone in n-butyl ether: 0.12 mole fraction.

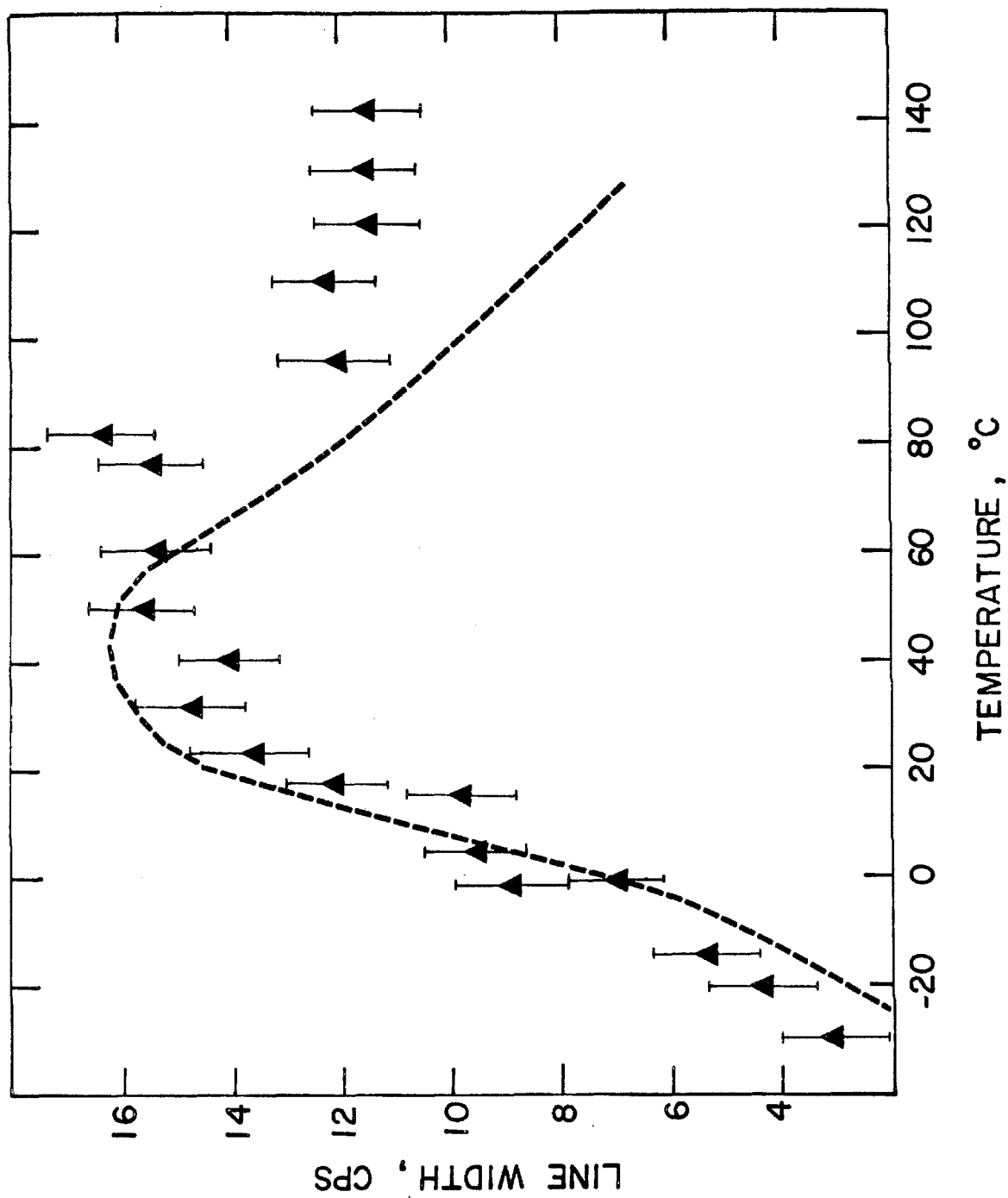


FIGURE 20

Calculated dependence of the linewidth of the bridge hydrogen at 100 MHz on the exchange rate constant for a range of population ratios.

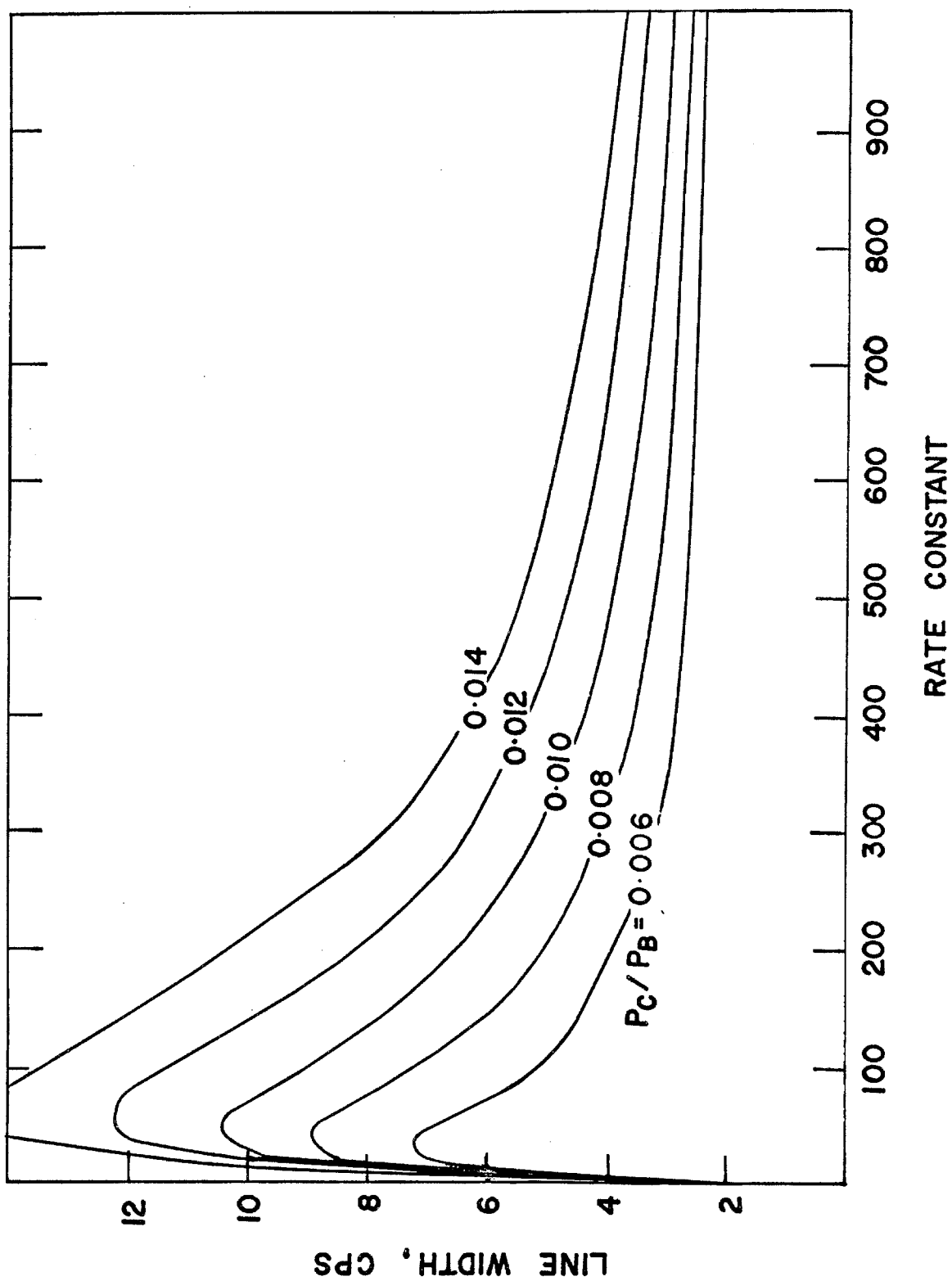
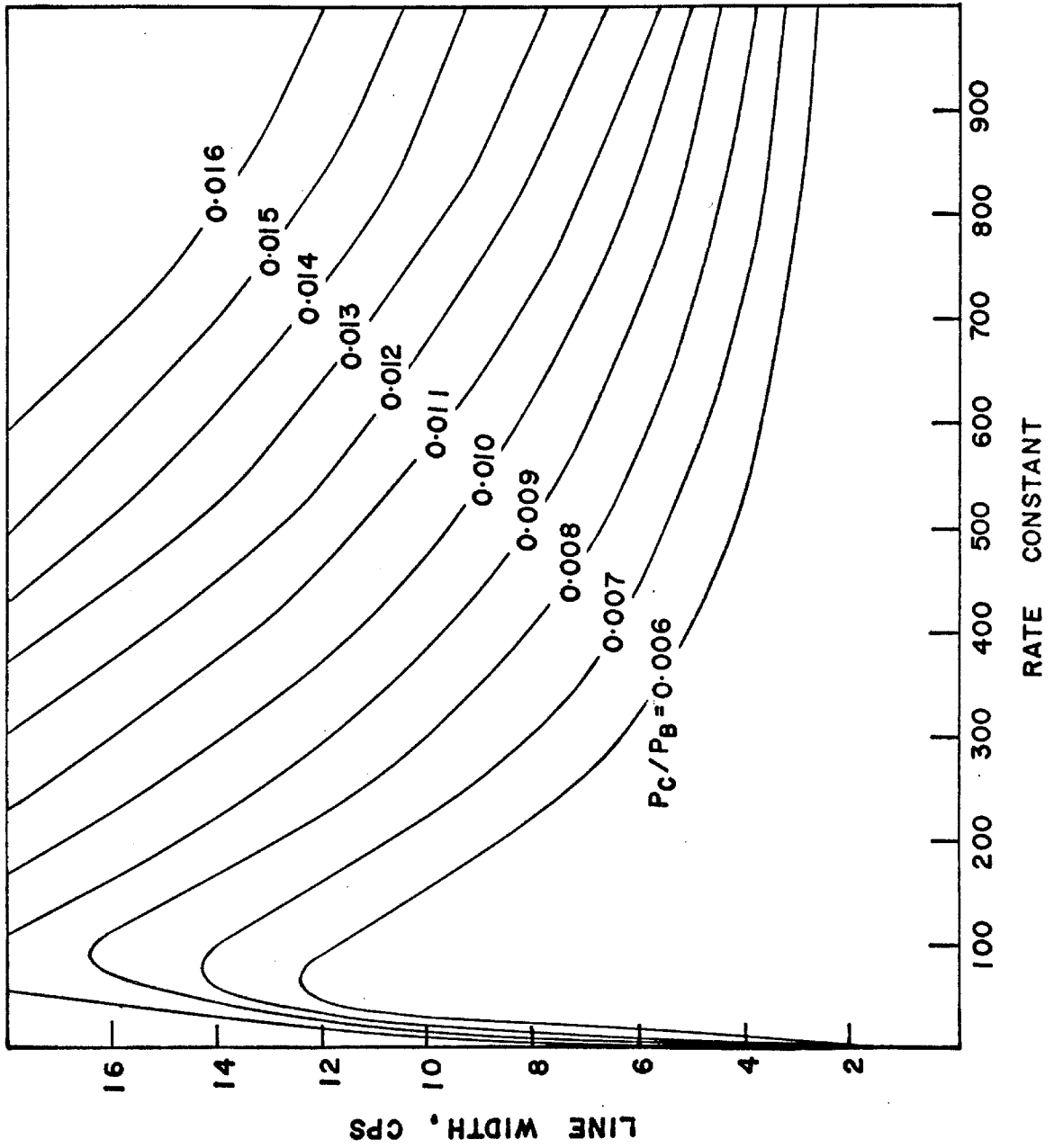


FIGURE 21

Calculated dependence of the linewidth of the bridge hydrogen at 220 MHz on the exchange rate constant for a range of population ratios.

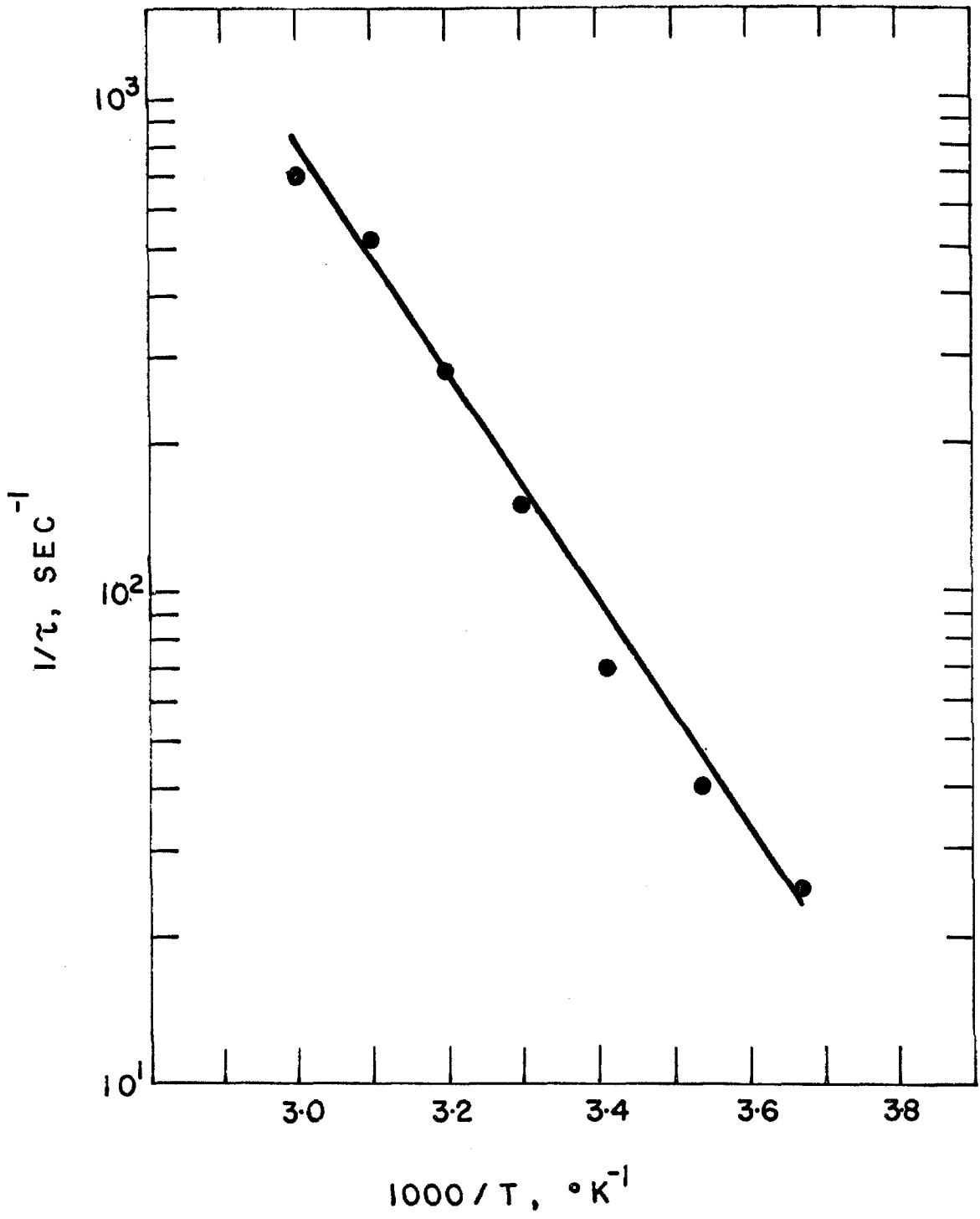


In Fig. 22, we have plotted the log of the rate constant so extracted versus the reciprocal temperature in the range 0 to 60°C. The slope yields an activation energy of 10.5 Kcal for the conversion of B to C. The life time of the bridge hydrogen in a 0.12 mole fraction of acetylacetone in n-butyl ether is found to be 1.4×10^{-2} sec. at 20°C. The second order rate constant for this process is $13 \text{ sec}^{-1} \text{ M}^{-1}$ at 20°C.

There is no physical evidence that this "open" form of acetylacetone exists in cyclohexane since the deuterium isotope effect on the OH chemical shift is the same in cyclohexane and n-butyl ether throughout the temperature range studied. In addition, the linewidth behavior is very different in the presence of the open form. We must conclude therefore that the observed isotope effect as well as the temperature dependences observed for both the proton and deuteron resonances are inherent in the strong intramolecular hydrogen bond of acetylacetone.

FIGURE 22

A plot of the log of the rate constant versus
the reciprocal temperature.



V. CARBON-13 NMR STUDIES

In a comprehensive study of ^{13}C chemical shifts in a variety of molecular systems, Lauterbur⁽⁴³⁾ first reported a downfield shift of about 5 ppm in the carbonyl carbon in methyl salicylate, and attributed this shift to the effect of intramolecular hydrogen bonding between the carbonyl oxygen atom and the hydroxyl hydrogen. This interpretation is further elaborated by Maciel and Savitsky⁽⁴⁴⁾ who were able to distinguish the "carbonyl carbon" ($\text{C}=\text{O}\cdots\text{H}$) and the "hydroxyl carbon" ($=\text{C}-\text{O}-\text{H}$) by examining the carbon-13 nmr spectra of a series of compounds in which strong intramolecular hydrogen bonds are known to exist between a carbonyl group attached to a benzene ring and a hydroxyl group situated ortho to the carbonyl group. It was found that the intramolecular hydrogen bond shifts the "carbonyl carbon" downfield by amounts ranging from 3 to 7 ppm; while the "hydroxyl carbon" is shifted upfield by 2 to 5 ppm. These hydrogen bonding shifts are summarized in Table XV.

The results of our molecular orbital calculations on the enol tautomer of acetylacetone have indicated that the motion of the bridge hydrogen is strongly coupled to the electronic charge distribution in the enol ring system. In view of the large effect of the intramolecular hydrogen bond on the chemical shifts of the carbonyl groups, the ^{13}C chemical shifts of the ring carbons are expected to exhibit a temperature dependence, since the ratio of the asymmetric structure of the enol tautomer is known to increase with temperature and upon deuterium substitution. An examination of the ^{13}C nmr signals of the ring

TABLE XV. ^{13}C chemical shifts of carbonyl groups in some aromatic systems demonstrating effects of intramolecular hydrogen bonding.^a

COMPOUND	LINE POSITIONS ^a			Δ^b
			15.8 C=O	
			11.4 X 19.6 Y	-4.4
			12.8 C=O	-3.0
	-13.1 C=O	-2.2 C=O	17.2 C-OCH3	
	-20.6 C=O	-9.5 C=O	19.8 C-OH	-7.3
		-14.9 C=O		
	-22.0 C=O		18.3 C-OH	-7.1
		-13.8 C=O		
	-20.2 C=O		20.4 C-OH	-6.4
	δ^c ppm			

^a G. E. Maciel and G. B. Savitsky, J. Phys. Chem., **68**, 438 (1964).

carbons should provide additional insight into the structure of the symmetric and asymmetric forms of the enol tautomer.

A typical ^{13}C spectrum of neat acetylacetone in natural abundance at a normal probe temperature of 18°C is shown in Fig. 23. The sensitivity is greatly improved in this spectrum by deriving it as the Fourier transform of the free induction signal after a strong radio-frequency pulse. The carbonyl region of interest is shown in detail in Fig. 24. Since acetylacetone has an enol content of 76-80% in the neat liquid, ⁽³⁾ the two signals in this region of the ^{13}C spectrum can be readily assigned to the C=O keto and C=O enol carbon from the observed intensities. The weaker downfield signal is assigned to the keto form and is used as reference in chemical shift measurements. The more intense peak at 10.8 ppm upfield, which is about four times as intense as the lower field signal, must be due to the enol form. The fact that only a single strong band can be attributed to the C=O enol does not enable us to differentiate the symmetric and asymmetric structures. Due to the rapid tunnelling rate of the bridge hydrogen and the high degree of symmetry in the acetylacetone molecule, the observed peak position is an average of the chemical shift for a carbon nucleus in two different environments, the "carbonyl carbon" and the "hydroxyl carbon". We shall show later that the deuterium isotope effect and the temperature study provide additional evidence to the existence of these two structures. The CH resonance is found at 101.9 ppm upfield from the C=O keto with a coupling constant of 167 Hz. The CH_2 resonances centered at 144.2 ppm are rather weak due to the low abundance of the keto form and the spin coupling of the protons. Two

FIGURE 23

A Fourier Transform ^{13}C spectrum of
neat acetylacetone in natural abundance.

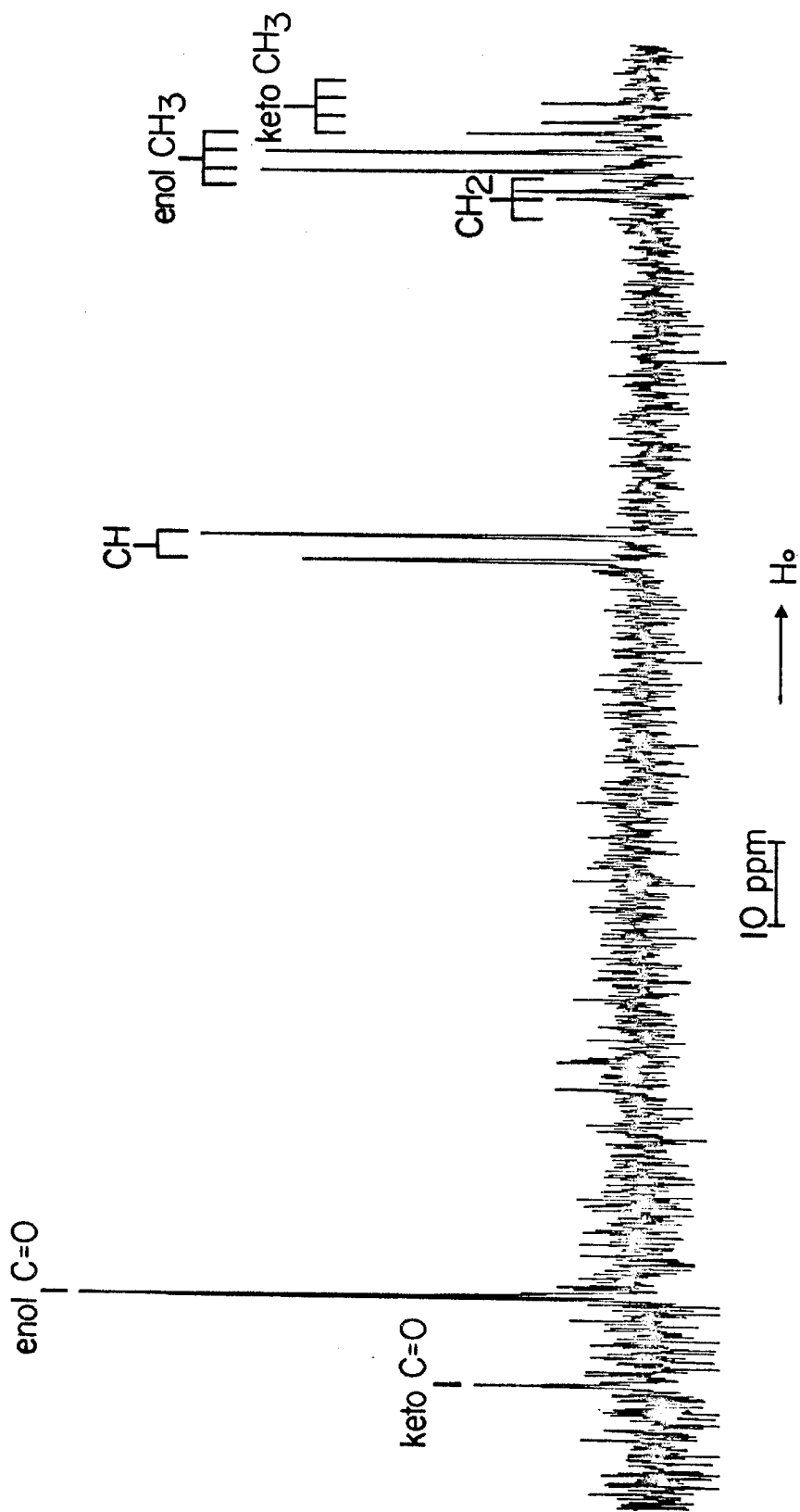
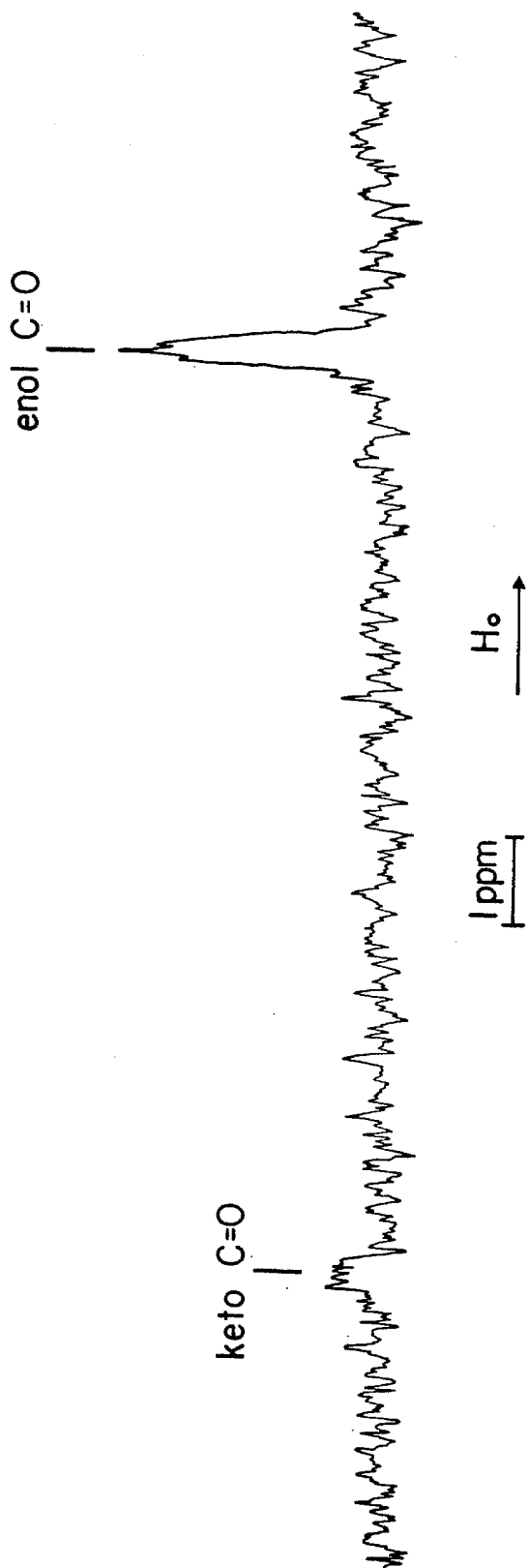


FIGURE 24

The ^{13}C NMR spectrum of the carbonyl region in neat acetylacetone.



groups of methyl resonances are observed arising from the enol and the keto forms. The chemical shifts are 148.7 ppm and 154.6 ppm for the enol and keto methyl groups, and a coupling constant of 127 Hz is observed in each case. The assignment in the methylene and methyl regions are different from the work of Stothers and Lauterbur⁽⁴⁶⁾ who first reported and assigned the ^{13}C nmr spectrum of acetylacetone. The methylene peak was not observable in their spectrum and the assignments of the enol and keto methyl resonances were reversed.

In the partially deuterated acetylacetone, two resonances are observed in the C=O enol region, in addition to the C=O keto resonance. A spectrum of the carbonyl region is shown in Fig. 25. The downfield resonance at 10.9 ppm may be assigned to the residual C=O...H resonance in comparison with the spectrum of neat acetylacetone. The resonance ~ 40 Hz upfield from it (11.6 ppm) is therefore assigned to the C=O...D resonance. In the presence of a trace amount of water, the two C=O...H and C=O...D resonances collapse into one signal indicating that there is rapid exchange between the bridge proton and the deuterium.

Temperature Study

The results of the temperature study on the carbonyl shift of acetylacetone and partially deuterated acetylacetone are shown in Fig. 26. A downfield shift of 50 Hz is observed when the temperature increases from -10°C to 90°C . The results of our previous proton temperature study indicate that the amount of the asymmetric structure increased from 10% to 17% as the temperature increases

FIGURE 25

The ^{13}C NMR spectrum of the carbonyl region in neat partially deuterated acetylacetone.

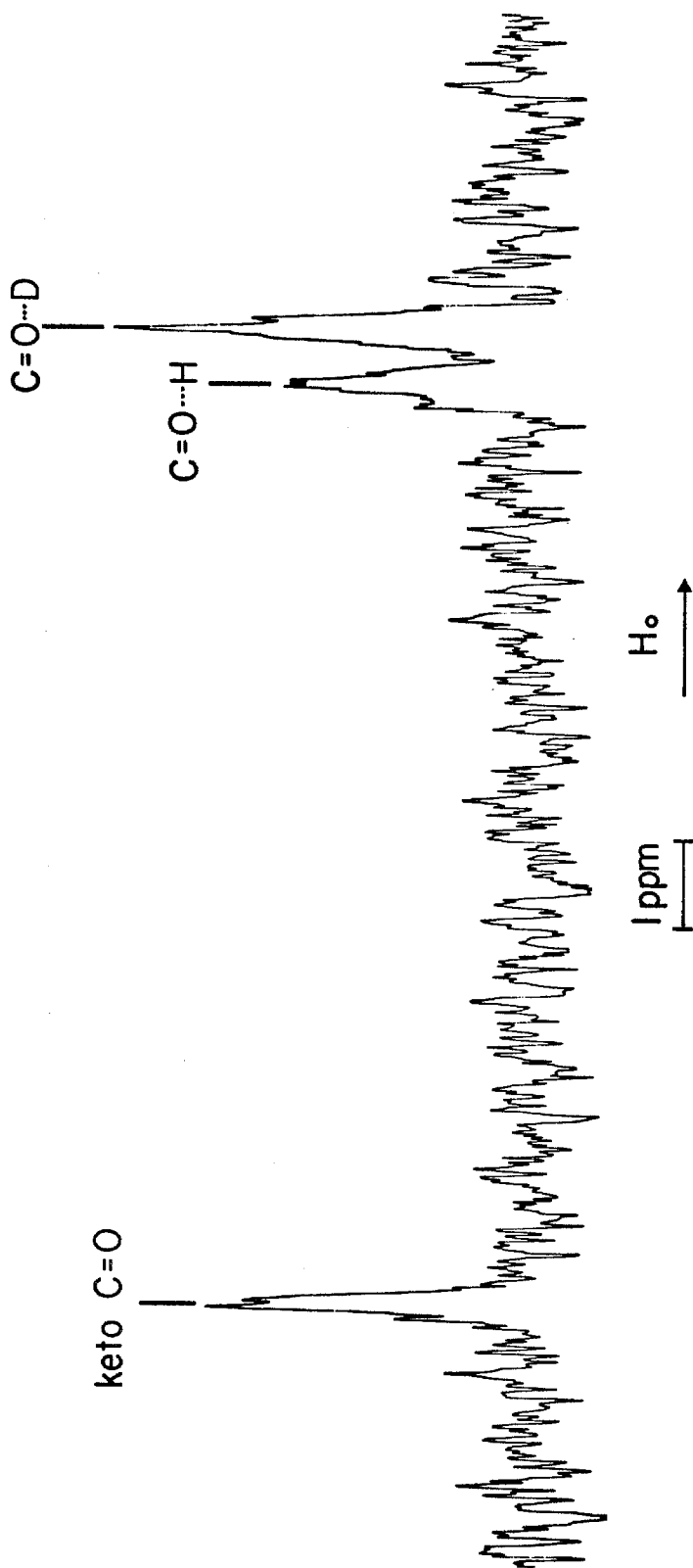
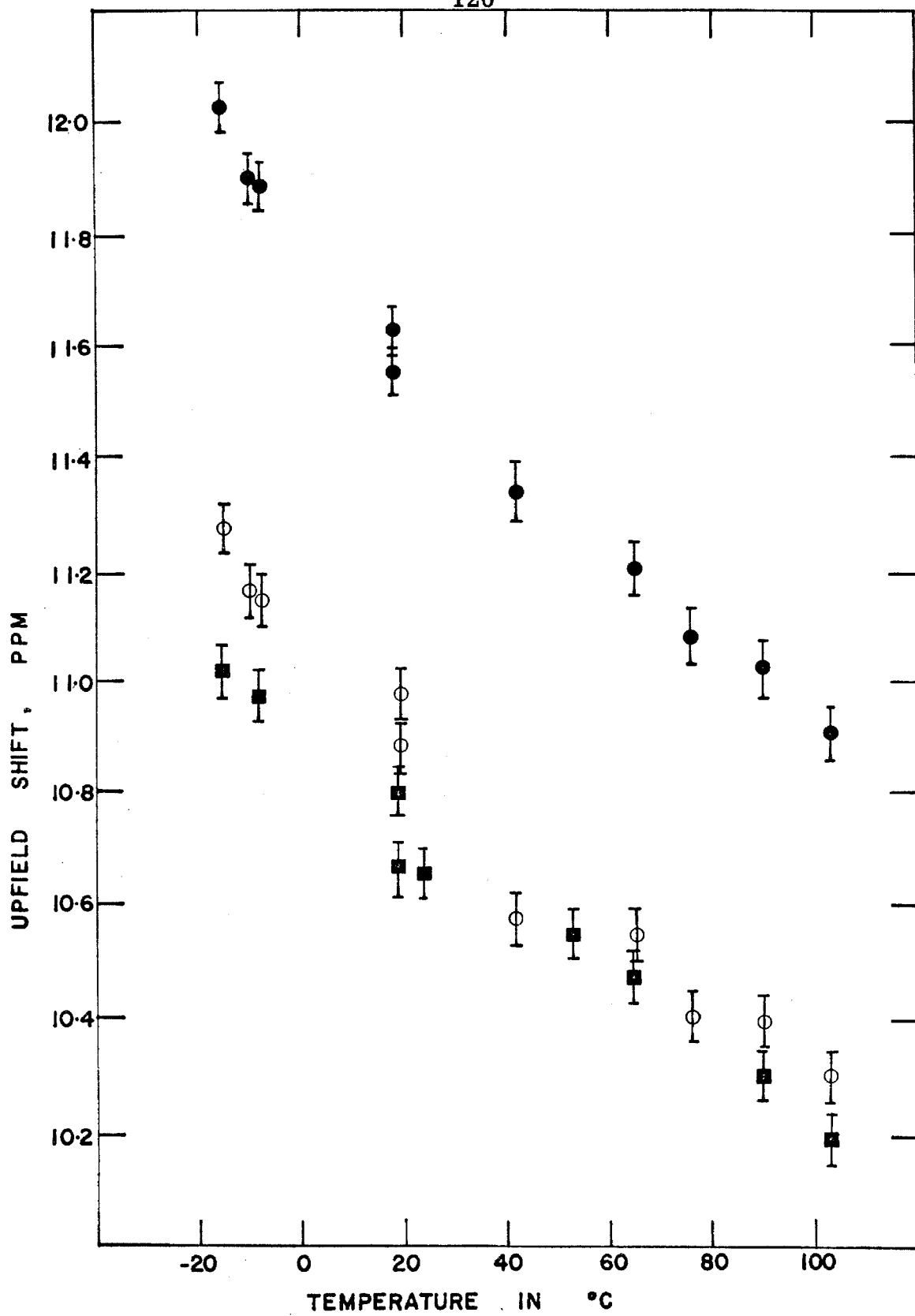


FIGURE 26

Variation of the chemical shift of C=O enol resonance
as a function of temperature.

- C=O···D in neat partially deuterated acetylacetone.
- C=O···H in neat partially deuterated acetylacetone.
- C=O···H in neat acetylacetone.



from -10°C to 90°C , and the deuterium temperature study indicates that this percentage increased from 24 to 30 over this temperature range. Since deuterium substitution and raising the temperature both increase the percent of the asymmetric structure, one would expect the C=O enol resonance to be shifted in the same direction in these experiments. However, our results indicate that deuterium substitution shifts the C=O enol resonance upfield whereas raising the temperature shifts the resonance downfield.

This apparent contradiction can be resolved if we take into consideration the isotope shift induced on the ^{13}C resonance when the bridge hydrogen is substituted by deuterium. In most cases, heavy isotopic substitution shifts the nmr signal of a nearby nucleus toward a higher magnetic field, i. e., deuterium substitution would result in an increase in shielding of the neighboring nuclei. The magnitude of the isotope shift is known to depend on the range in chemical shifts of the resonant nucleus; therefore a large upfield isotope shift is to be expected since the ^{13}C chemical shifts range over 350 ppm. A study of the carbonyl resonance in CH_3COOH and CD_3COOD indicate an upfield shift of 90 Hz upon deuterium substitution. We therefore conclude that, on the average, the symmetric structure has a C=O enol resonance upfield from that of the asymmetric structure, so that a downfield shift of the C=O enol resonance is observed with increasing temperature. Upon deuterium substitution, the ratio of the asymmetric structure increases, but the observed chemical shift is dominated by the large isotope shift which moves the resonance upfield.

Results of the CNDO calculations on the CO pi-bond order are

also consistent with the carbon-13 results. Since the average shift of the two carbonyls are observed experimentally, the average bond order of the two carbonyls in each of the symmetric and asymmetric forms must be considered. Fig. 15 shows a summary of the bond orders in the ring system as the bridge hydrogen is moved along the O...O distance in both the symmetric and asymmetric forms. The hydrogen-bonded "carbonyl carbon" has a high CO pi-bond order of 0.93 compared with the "hydroxyl carbon" which has a low bond order of 0.27. These calculations also indicate that on the average, the enol carbonyls in the symmetric structure have a higher bond order than the asymmetric structure.

The polarity of the carbonyl pi bond has been correlated to the carbonyl chemical shifts by Maciel and Natterstad.⁽⁴⁵⁾ A reduction in the polarity of the pi-bond results in an increase in electron density which screens the C=O carbon nucleus. Since the carbonyls on the symmetric structure have a higher bond order on the average, the ¹³C resonance would be expected to occur upfield to the asymmetric form. Stothers and Lauterbur⁽⁴⁶⁾ also concluded from a study of substituent effects on carbonyl chemical shifts that conjugation tends to shield the carbonyl carbon. This prediction is therefore consistent with the change in direction of the C=O enol chemical shift with temperature.

We have been able to interpret the results of this study in terms of the two-state model proposed in the previous sections. The fact that only one resonance is observed for the carbonyl groups in neat acetylacetone is a direct reflection on the rapid tunnelling rate of the bridge

hydrogen and its effect on the electronic distribution in the ring system. This strong coupling between the motion of the bridge hydrogen and the electronic distribution in the ring system is essential to the fundamental difference between the structure of the symmetric and asymmetric form in the enol tautomer of acetylacetone.

VI. CONCLUSION

The nature of the intramolecular hydrogen bond in acetylacetone has been studied in detail. Our results suggest that there are two tautomers for the enol form of acetylacetone, the symmetric structure (I) and the asymmetric structure (II). The difference between these two structures arises from difference in the π electron distribution in the enol ring. When the donor-acceptor vibration is in the ground vibrational state, the potential function is symmetric double minimum in nature, and when it is in the first vibrational excited state of the donor-acceptor vibration, then the potential function is asymmetric. These two structures are in rapid equilibrium on the NMR time scale; but relatively slow on the IR time scale. Analysis of the NMR temperature data in terms of the two-state model result in an energy difference of 405 cm^{-1} between the two states, and this energy difference is reduced to 215 cm^{-1} in the deuterated case. These changes in the zero-point vibrational amplitude upon isotopic substitution in the two different potential functions give rise to the anomalous deuterium isotope effect observed for the bridge hydrogen. The transitions between the ground state and the first excited state of the donor-acceptor vibration are observed to correspond to two depolarized Raman bands observed for the normal and deuterated acetylacetone. The interconversion of these two tautomers can be brought about by a symmetric $\text{O} \cdots \text{O}$ stretch which could produce a charge shift in the π system which then alters the effective symmetry of the potential function for the hydrogen bond.

REFERENCES

1. K. H. Meyer, Ann. Physik, 380, 212 (1911); Ber. 44, 2718 (1911); 45, 2843 (1912); 47, 826, 832 (1914).
2. H. S. Jarett, M. S. Sadler and J. N. Shoolery, J. Chem. Phys., 21, 2092 (1953).
3. L. W. Reeves, Can. J. Chem., 35, 1351 (1957).
4. L. W. Reeves and W. G. Schneider, Can. J. Chem., 36, 793 (1958).
5. F. J. Balta Calleja, Compt. Rend., 249, 1102 (1959).
6. J. L. Burdett and M. T. Rogers, J. Amer. Chem. Soc., 86, 2105 (1963).
7. M. T. Rogers and J. L. Burdett, Can. J. Chem., 43, 1516 (1965).
8. J. L. Burdett and M. T. Rogers, J. Phys. Chem., 70, 939 (1966).
9. G. Allen and R. A. Dwek, J. Chem. Soc. (B), 161 (1966).
10. R. Mecke and E. Funck, Z. Elektrochem., 60, 1124 (1956).
11. G. C. Pimentel and A. L. McClellan, "The Hydrogen Bond", W. H. Freeman and Co., San Francisco, 1960, p. 167.
12. R. S. Rasmussen, D. D. Tunnicliff and R. R. Brattain, J. Amer. Chem. Soc., 71, 1068 (1949).
13. G. G. Smith, J. Amer. Chem. Soc., 75, 1134 (1953).
14. L. J. Bellamy and L. Beecher, J. Chem. Soc., 4487 (1954).
15. S. Bratoz, D. Hadzi and G. Rossy, Trans. Faraday Soc., 52, 464 (1956).
16. E. E. Ernstbrunner, J. Chem. Soc. (A), 1558 (1970).
17. D. N. Shigorin, A. P. Skoldinov, T. S. Ryabchikova and G. A. Golder, Zhur. Fizicheskoi Khimii, 38, 1996(1964).

18. H. Ogoshi and K. Nakamoto, J. Chem. Phys., 45, 3113 (1966).
19. P. Diehl and T. Leipert, Helv. Chim. Acta, 47, 545 (1964).
20. H. Batiz-Hernandez and R. A. Bernheim, "Progress in Nuclear Magnetic Resonance Spectroscopy", Vol. 3, Pergamon Press, Oxford, 1967, p. 63.
21. J. A. Pople, W. G. Schneider and H. J. Bernstein, "High-Resolution Nuclear Magnetic Resonance", McGraw-Hill, New York, 1959, p. 407.
22. N. Muller and R. C. Reiter, J. Chem. Phys., 42, 3265 (1965).
23. T. Schaefer and G. Kotowycz, Can. J. Chem., 46, 2865 (1968).
24. B. M. Fung, Thesis, California Institute of Technology, 1967.
25. R. Hoffman, J. Chem. Phys., 39, 1397 (1963).
26. L. Pauling, "The Nature of the Chemical Bond", Cornell University Press, New York, 1960, p. 260.
27. J. A. Pople, D. P. Santry and G. A. Segal, J. Chem. Phys., 43, S 129 (1965).
28. A. S. N. Murthy, R. E. Davis and C. N. R. Rao, Theoret. Chim. Acta, (Berl.), 13, 81 (1969).
29. J. A. Pople and G. A. Segal, J. Chem. Phys., 43, S 136 (1965).
30. A. S. N. Murthy, R. E. Davis and C. N. R. Rao, Chem. Phys. Lett., 2, 123 (1968).
31. J. A. Pople and G. A. Segal, J. Chem. Phys., 44, 3289 (1966).
32. K. B. Wiberg, J. Amer. Chem. Soc., 90, 59 (1968).
33. J. Brickmann and H. Zimmermann, J. Chem. Phys., 50, 1608 (1969).
34. K. S. Pitzer, "Quantum Chemistry", Prentice-Hall, Inc., New

Jersey, 1953, p. 237.

35. R. L. Somorjai and D. F. Hornig, J. Chem. Phys., 36, 1980 (1962).
36. S. I. Chan and D. Stelman, J. Mol. Spectry., 10, 278 (1963); S. I. Chan, D. Stelman and L. E. Thompson, J. Chem. Phys., 41, 2828 (1964); S. I. Chan, T. R. Bergers, J. W. Russell, H. L. Strauss and W. D. Gwinn, ibid., 44, 1103 (1966).
37. L. J. Bellamy, "The Infra-red Spectra of Complex Molecules", John Wiley and Sons, Inc., New York, 1958, p. 102.
38. R. J. W. Le Fèvre and H. Welsh, J. Chem. Soc., 2230 (1949).
39. Z. Yoshida, H. Ogoshi and T. Tokumitsu, Tetrahedron, 26, 5691 (1970).
40. R. M. Silverstein and G. C. Bassler, "Spectrometric Identification of Organic Compounds", John Wiley and Sons, Inc., New York, 1963, p. 159.
41. J. A. Pople, W. G. Schneider and H. J. Bernstein, "High Resolution Nuclear Magnetic Resonance", McGraw-Hill, New York, 1959, p. 218.
42. G. Binsch and D. A. Kleier, "The Computation of Complex Exchange-Broadened NMR Spectra Computer Program DNMR", Quantum Chemistry Program Exchange, 1969.
43. P. C. Lauterbur, Ann. N. Y. Acad. Sci., 70, 841 (1958).
44. G. E. Maciel and G. B. Savitsky, J. Phys. Chem., 68, 438 (1964).
45. G. E. Maciel and J. J. Natterstad, J. Chem. Phys., 42, 2752 (1965).
46. J. B. Stothers and P. C. Lauterbur, Can. J. Chem., 42, 1563 (1964).

APPENDIX

Molecular Orbital Calculations

An ideal solution to quantum mechanical problems is to find the wave function Ψ , which are solutions to the Schrödinger equation $H\Psi = E\Psi$, in which the Hamiltonian operator, H , includes all interaction terms for electrons and nuclei. If the nuclei are assumed to be fixed, the Hamiltonian for the electrons is represented as follows:⁽¹⁾

$$\mathcal{H}_e = -\frac{\hbar^2}{8\pi^2 m} \sum_i \nabla_i^2 - \sum_i \frac{Z_e}{r_i} + \sum_{i>j} \frac{e^2}{r_{ij}} \quad \text{A-1}$$

where the successive terms represent operators for the kinetic energy of the electrons (i), the nuclear-electronic attraction, and the repulsion between electrons. Unfortunately, the solution for this Hamiltonian becomes too complicated for any but the simplest molecules, unless some method of approximation is used.

The Hückel method⁽²⁾ consists in the approximate determination of the molecular orbitals and the associated energy values for one electron in a potential field corresponding to the molecule. The total energy is then considered to be the sum of the energies of all the electrons, distributed among the more stable molecular orbitals with no more than two electrons per orbital. The application of this method is limited because no specific considerations are given to the electron repulsion terms.

The CNDO/2 method proposed by Pople, Santry and Segal⁽³⁾

is used in the calculations on acetylacetone. The main improvement of the CNDO method over the simpler Hückel calculations is that it includes explicit rather than averaged electron repulsion terms in the Hamiltonian. This inclusion removed important conceptual deficiencies of earlier semi-empirical molecular orbital methods. The calculations are in general more complex than the simpler Hückel methods because this calculation is based upon self-consistent orbital equations⁽⁴⁾ and therefore the single determinant functions should also be made internally self-consistent.

In the LCAO MO method, the i^{th} molecular orbital is expressed in terms of the atomic orbitals:

$$\Psi_i = \sum_{\mu} C_{i\mu} \varphi_{\mu} \quad \text{A-2}$$

where the equations which determine the μ -th atomic orbital coefficients are, under the variation principle,

$$\sum_{\nu} F_{\mu\nu} C_{i\nu} = \epsilon_i \sum_{\nu} S_{\mu\nu} C_{i\nu} \quad \text{A-3}$$

where

$$F_{\mu\nu} = \mathcal{H}_{\mu\nu} + G_{\mu\nu} \quad \text{A-4}$$

In these equations, ϵ_i is the orbital energy for the molecular orbital Ψ_i . $\mathcal{H}_{\mu\nu}$ is the matrix element of the one-electron Hamiltonian including the kinetic energy and the potential energy in the electrostatic field of the core. $G_{\mu\nu}$ is the matrix element of the potential due to other valence electrons and includes electron repulsion terms.

The total electronic energy of the valence electrons is given by:

$$\epsilon_{\text{electronic}} = \frac{1}{2} \sum_{\mu, \nu} P_{\mu\nu} (H_{\mu\nu} + F_{\mu\nu}) \quad \text{A-5}$$

where $P_{\mu\nu}$ is the charge density and bond-order matrix:

$$P_{\mu\nu} = 2 \sum_i^{\text{occ}} C_{i\mu} C_{i\nu} \quad \text{A-6}$$

The total energy of the molecule is obtained by adding the repulsion energy between cores.

$$E_{\text{total}} = \epsilon_{\text{electronic}} + \sum_{A < B} \sum \frac{Z_A Z_B}{R_{AB}} \quad \text{A-7}$$

where Z_A is the core charge of atom A and R_{AB} is the A-B internuclear distance.

The full treatment of the CNDO method has been developed in detail by Pople and Segal. (3, 5, 6) The several approximations used are briefly described below:

- (1) The overlap distribution $\phi_{\mu}(1) \phi_{\nu}(1)$ of any two atomic orbitals ϕ_{μ} and ϕ_{ν} is neglected in all electron repulsion integrals.
- (2) All electron interaction integrals are neglected other than

$$\gamma_{\mu\nu} = \iint [\phi_{\mu}(1) \phi_{\nu}(2) \phi_{\mu}(1) \phi_{\nu}(2) / r_{12}] dv_1 dv_2 \quad \text{A-8}$$

- (3) The electron-interaction integrals $\gamma_{\mu\nu}$ are assumed to depend only on the average repulsion between an electron in a valence atomic orbital on A and another in a valence orbital on B and not to the

actual type of orbital.

(4) Integrals $(\mu | V_B | \nu)$ where ϕ_μ and ϕ_ν belong to atom A are assumed to be zero if $\mu \neq \nu$. In the case when $\mu = \nu$, the integral has a fixed value for all valence atomic orbitals on atom A.

(5) Off-diagonal core matrix elements between atomic orbitals on different atoms are estimated by a formula

$$\mathcal{H}_{\mu\nu} = \beta_{\mu\nu} = \beta_{AB}^0 S_{\mu\nu} \quad \text{A-9}$$

where $S_{\mu\nu}$ is the overlap integral and β_{AB}^0 is an empirical bonding parameter depending only on the nature of the atoms A and B.

Under these approximations, the pertinent matrix elements become:

$$F_{\mu\mu} = H_{\mu\mu} + \frac{1}{2} P_{\mu\mu} \gamma_{\mu\mu} + \sum_{\sigma(\neq\mu)} P_{\sigma\sigma} \gamma_{\mu\sigma} \quad (\text{Approx. 1 \& 2}) \quad \text{A-10}$$

$$= H_{\mu\mu} - \frac{1}{2} P_{\mu\mu} \gamma_{AA} + P_{AA} \gamma_{AA} + \sum_{(B \neq A)} P_{BB} \gamma_{AB} \quad \text{A-11}$$

(Approx. 3)

where μ belongs to atom A and P_{BB} is the total valence electron density on atom B.

$$P_{BB} = \sum_{\nu}^B P_{\nu\nu} \quad \text{A-12}$$

$$H_{\mu\mu} = (\mu | -\frac{1}{2} \nabla^2 - V_A | \mu) - \sum_{B(\neq A)} (\mu | V_B | \mu) \quad \text{A-13}$$

$$= U_{\mu\mu} - \sum_{B(\neq A)} (\mu | V_B | \mu) \quad \text{A-14}$$

$$= U_{\mu\mu} - \sum_{B(\neq A)} V_{AB} \quad (\mu \text{ on atom A}) \quad (\text{Approx. 4}) \quad \text{A-15}$$

$$F_{\mu\nu} = H_{\mu\nu} - \frac{1}{2} P_{\mu\nu} \gamma_{\mu\nu} \quad (\mu \neq \nu) \quad (\text{Approx. 1 \& 2}) \quad \text{A-16}$$

$$H_{\mu\nu} = (\mu | -\frac{1}{2} \nabla^2 - V_A | \nu) - \sum_{B(\neq A)} (\mu | V_B | \nu) \quad \text{A-17}$$

$$= 0 \quad (\mu \neq \nu, \text{ but both on the same atom}) \quad (\text{Approx. 4}) \quad \text{A-18}$$

$$= \beta_{AB}^0 S_{\mu\nu} \quad (\mu \neq \nu, \text{ but both on different atoms}) \quad \text{A-19}$$

(Approx. 5)

Hence, the matrix elements now reduce to the following form:

$$F_{\mu\mu} = U_{\mu\mu} + (P_{AA} - \frac{1}{2} P_{\mu\mu}) \gamma_{AA} + \sum_{B(\neq A)} (P_{BB} \gamma_{AB} - V_{AB}) \quad \text{A-20}$$

$$F_{\mu\nu} = \beta_{AB}^0 S_{\mu\nu} - \frac{1}{2} P_{\mu\nu} \gamma_{AB} \quad (\mu \neq \nu) \quad \text{A-21}$$

Using the same approximations, the total energy is given by:

$$E_{\text{total}} = \sum_A E_A + \sum_{A < B} E_{AB} \quad \text{A-22}$$

where

$$E_A = \sum_{\mu}^A P_{\mu\mu} U_{\mu\mu} + \frac{1}{2} \sum_{\mu}^A \sum_{\mu}^A (P_{\mu\mu} P_{\nu\nu} - \frac{1}{2} P_{\mu\nu}^2) \gamma_{AA} \quad \text{A-23}$$

and

$$E_{AB} = \sum_{\mu}^A \sum_{\mu}^B (2 P_{\mu\nu} \beta_{\mu\nu} - \frac{1}{2} P_{\mu\nu}^2 \gamma_{AB}) \quad \text{A-24}$$

$$+ (Z_A Z_B R_{AB}^{-1} - P_{AA} V_{AB} - P_{BB} V_{BA} + P_{AA} P_{BB} \gamma_{AB})$$

The minimum basis set of Slater-type orbitals for the valence shell is used in the calculation. The Slater Z' value of 1.2, 3.25 and 4.55 are used for hydrogen, carbon and oxygen respectively. The overlap integrals $S_{\mu\nu}$ are all calculated explicitly from formulas given by Mulliken et al. (7) The electron repulsion integrals $\gamma_{\mu\nu}$ are calculated using two-center Coulomb integral involving valence s electrons. Formulas for these integrals are listed by Roothaan. (8)

The calculation of V_{AB} and $U_{\mu\mu}$ in this study follows the CNDO/2 version as given by Pople and Segal. (5) This version is different from the general CNDO method in two ways: (1) Certain penetration-type terms which led to excess bonding between formally nonbonded atoms has been omitted in the CNDO/2 version. This corresponds to expressing the repulsion energy term as follows:

$$V_{AB} = Z_B \gamma_{AB} \quad \text{A-25}$$

There is no justification for this correction, but it results in more accurate bond lengths and binding energies by introducing an error similar to those introduced through the neglect of overlap populations but is of opposite sign. (2) The local core matrix elements which were obtained from atomic ionization potential I_μ previously are chosen empirically using data on both atomic ionization potential and electron affinities, A_μ .

REFERENCES

1. H. Eyring, J. Walter, and G. E. Kimball, "Quantum Chemistry", John Wiley & Sons, Inc., New York, 1967, p. 190.
2. A. Streitwieser, Jr., "Molecular Orbital Theory", John Wiley & Sons, Inc., New York, 1961, p. 33.
3. J. A. Pople, D. P. Santry and G. A. Segal, J. Chem. Phys., 43, S 129 (1965).
4. C. C. J. Roothaan, Rev. Mod. Phys., 23, 61 (1951).
5. J. A. Pople and G. A. Segal, J. Chem. Phys., 43, S 136 (1965).
6. J. A. Pople and G. A. Segal, J. Chem. Phys., 44, 3289 (1966).
7. R. S. Mulliken, C. A. Rieke, D. Orloff, and H. Orloff, J. Chem. Phys., 17, 1248 (1949).
8. C. C. J. Roothaan, J. Chem. Phys., 19, 1445 (1951).

PROPOSITION I

NMR STUDY OF THE INTERACTION BETWEEN
PURINE AND STEROIDS

Abstract: It is proposed to study the possible complexation of steroid and purine in aqueous medium using high resolution proton magnetic resonance spectroscopy.

It has been reported⁽¹⁾ that some polycyclic aromatic carcinogenic hydrocarbons, such as dibenzcarbazoles, form complexes with caffeine and other purines, although the nature of the interaction is yet unknown. If the complex-forming properties of purines extend to include steroids, which are also polycyclic compounds, it is conceivable that the broad spectrum of physiological activities of steroids, both desirable and adverse, could be mediated by the formation of complexes with adenine nucleotides, since the activities of enzyme systems containing adenine nucleotides, the nucleic acids, or both, might thereby be altered.

The solubilities of progesterone, deoxycorticosterone, and testosterone in water have been found to increase in the presence of adenine, adenosine and the isomers of adenosine monophosphate.⁽²⁾ This effect was considered to be due to an interaction between the steroids and purine. Munck et al.⁽³⁾ studied this interaction using the method of partition equilibrium. A water/heptane system was used in which the concentration of steroid in water and in water solution of coenzyme derivatives were determined by ultraviolet absorbance.

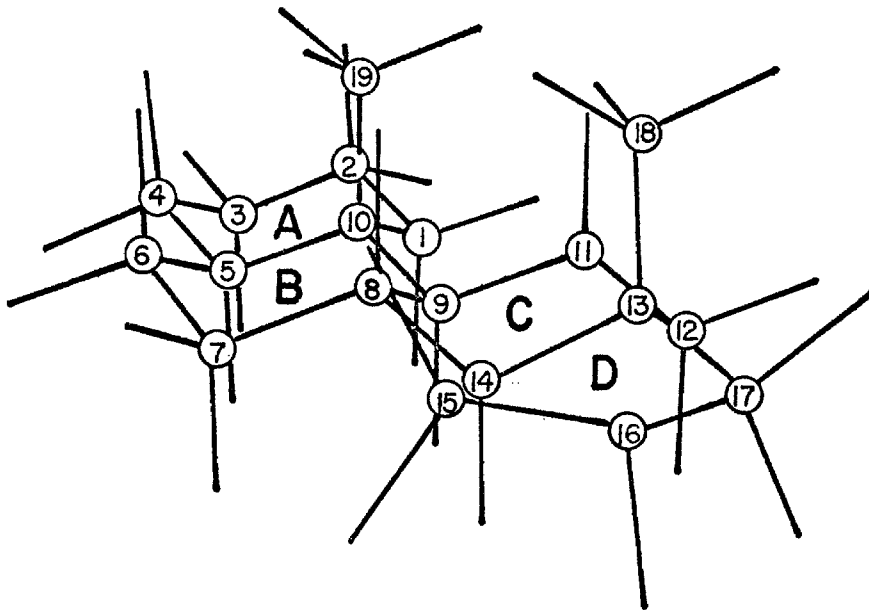
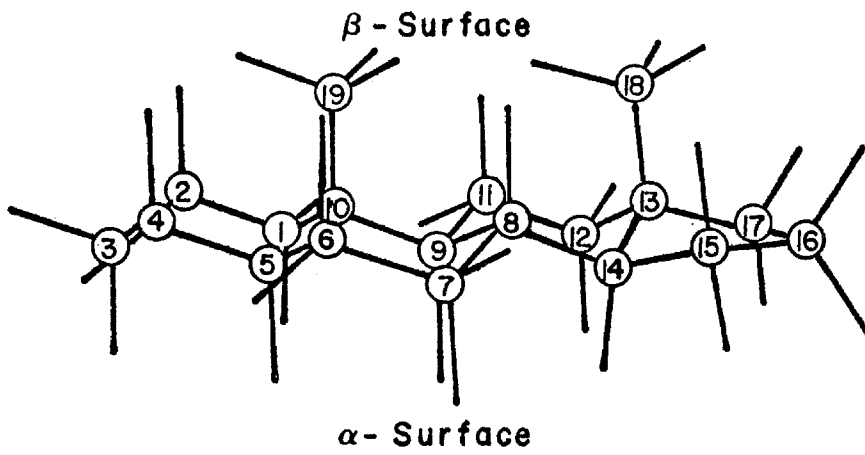
A series of twelve steroids were studied; the results obtained gave a qualitative pattern for the interaction of purine and steroids. They postulated that the α -surface presented by the axial hydrogen atoms in rings C and D and part of ring B were involved in the interaction (see Figure 1 for steroid structure). The forces involved were assumed to be of the London-Van der Waals dispersion type, but specific experimental evidence for the nature of the interaction was not given.

Tsutsui et al.⁽⁴⁾ have shown that certain steroids have an inhibitory action on glucose-6-phosphate dehydrogenase, and they all possess a ketone group in the C-17 or C-20 position. The same conclusion is reached in a recent study on the specificity of steroid interaction with glucose-6-phosphate dehydrogenase.⁽⁵⁾ Estrone and estradiol have been observed to have a rate-accelerating effect on isocitric dehydrogenase.^(6, 7) Studies on glutamic dehydrogenase also revealed that corticosterone and cortisol have a stimulating effect on the initial rate of the reaction.⁽⁸⁾ All of these reactions require nicotinamide adenine dinucleotides, and it is not clear whether the substrate specificity or the effect on the reaction rate is dependent on the enzyme, the coenzyme or a combination thereof.

In view of the lack of more conclusive experimental evidence on the details of the interaction between steroid hormones and purine-containing coenzymes, a high resolution nuclear magnetic resonance (NMR) study of these compounds in solution is highly desirable. This would provide not only direct evidence for the existence of the complex, but can also be used to uncover the geometry of the complex and the nature of the interaction. NMR has been found to be a useful method

FIGURE 1

Models of androstane showing the numbering of carbon atoms and rings A, B, C, and D.



for studying interactions between purine bases and nucleosides, and has allowed hydrogen bonding to be distinguished from base stacking. (9-11)

The first classical study of the NMR spectra of steroids was carried out by Shoolery and Rogers in 1958. (12) They were able to show that the resonance of angular methyl protons is dependent on both the nature and orientation of substituent groups in the steroid skeleton and their effects are additive. Numerous studies of steroids using NMR have since appeared, (13) and deuterated chloroform is the common solvent used. Solvent effects due to pyridine and benzene have also been investigated. (14, 15) It was shown that when the carbonyl group is relatively near C-19, but remote from C-18, the shielding effect on passing from deuterated chloroform to benzene solution is greater on C-19. Alternatively, for compounds where the carbonyl group is in ring D, there is a larger shielding effect on C-18. Also, axial methyl resonances suffer an appreciable upfield shift (0.2 ppm) on passing from deuterated chloroform to benzene solution, but equatorial methyl groups suffer a small downfield shift (0.06 ppm). These results are consistent with the formation of a collision complex in which the π -electrons of the benzene ring interact with the partial positive charge on the carbonyl carbon atom.

It is proposed that the possible complexation of steroid and purine be studied in deuterated water medium using high resolution proton magnetic resonance spectroscopy. The scope of this study will include three series of steroids: the pregnanes (21-C's), the androstanes (19-C's) and the estranes (18-C's). Since steroids are relatively insoluble in water, the soluble salts of the sulfate, phosphate or succinate

esters must be used. Among the three series of steroids under study, sodium sulfate salts of the estrane and androstane derivatives are commercially available. Most of the sodium phosphate and sodium succinate salts of the pregnane derivatives are also commercially available; others can be prepared by esterification of the C-21 primary alcohol.⁽¹⁶⁾ A list of the steroids under study are presented in Figs. 2-4. The substituents and degrees of unsaturation of the steroids chosen are varied in a systematic fashion so that their effects on the interaction may be studied. The pregnane series includes the adrenocortical and progestational hormones. From the list of seven steroids chosen, this study would elucidate the effects of the OH-groups on C-17 and C-11, of the keto-group on C-11, and of the presence of double bonds on ring A. The androstane series is chosen because it represents the nucleus of the male sex hormones, some of which are carcinogenic. These compounds would enable us to study the effect of unsaturation on ring B, and to compare the α and β -configurations of the hydrogen on position 5 of the steroid nucleus. The estrane series represents the female estrogenic hormones, and provides examples to study the effect of conjugation in rings A and B.

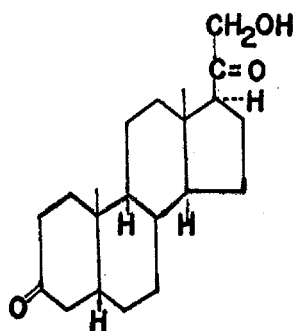
Solutions of steroids in phosphate buffer, pD 7.0 will be prepared in different concentrations of purine, and the NMR spectra will be taken by using a Varian HR-220 spectrometer. The Varian C-1024 time-averaging computer will be used in conjunction with the spectrometer when necessary. If a molecular complex were formed between a steroid and purine in water as hypothesized by Munck *et al.*,⁽³⁾ the resonances of all protons involved in the interaction should shift

FIGURE 2

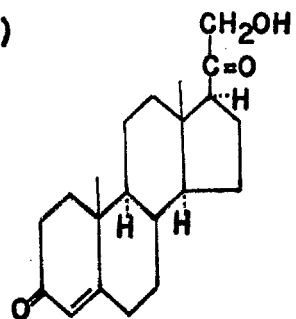
Pregnane Series

- (I) pregnane-21-ol-3, 20-dione
- (II) 4-pregnene-21-ol-3, 20-dione
- (III) 4-pregnene-17 α , 21-diol-20-one
- (IV) 4-pregnene-11 β , 21-diol-3, 20-dione
- (V) 4-pregnene-11 β , 17 α , 21-triol-3, 20-dione
- (VI) 4-pregnene-17 α , 21-diol-3, 11, 20-trione
- (VII) 1, 4-pregnadiene-11 β -17 α , 21-triol-3, 20-dione

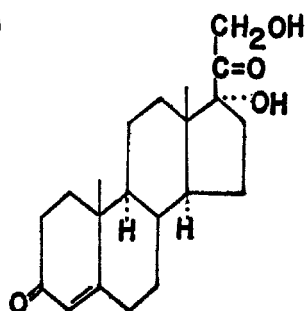
(I)



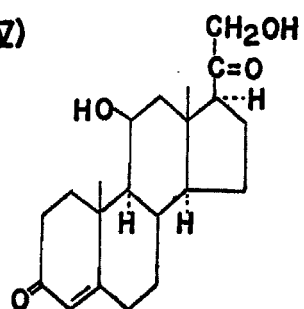
(II)



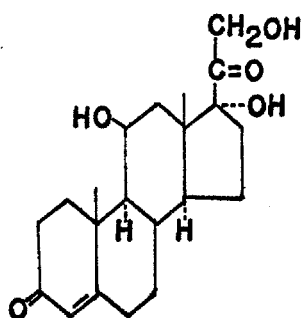
(III)



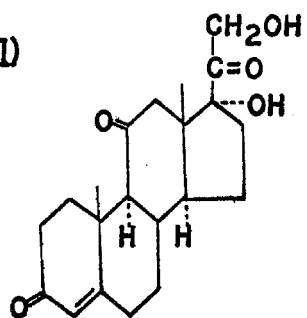
(IV)



(V)



(VI)



(VII)

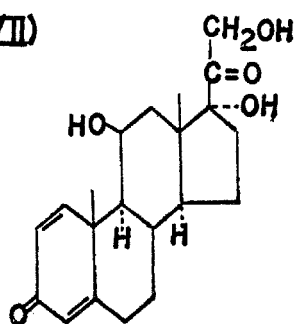
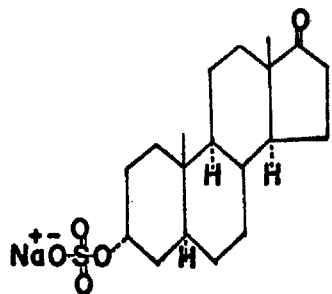


FIGURE 3

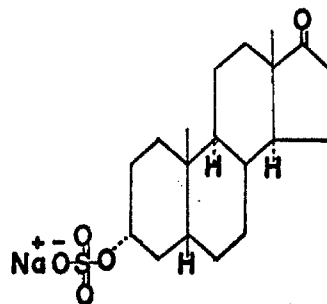
Androstane Series

- (I) 3 α -hydroxy-5 α -androstane-17-one sulfate, sodium salt
- (II) 3 α -hydroxy-5 β -androstane-17-one sulfate, sodium salt
- (III) 3 α -hydroxy-5 α -androstane-11, 17-dione sulfate,
sodium salt
- (IV) 3 α -hydroxy-5 β -androstane-11, 17-dione sulfate,
sodium salt
- (V) 3 β -hydroxy-5-androstane-17-one sulfate, sodium salt

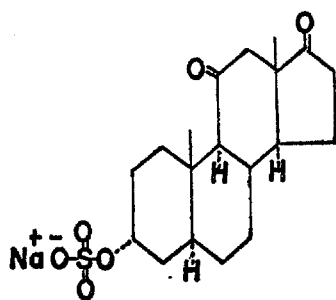
(I)



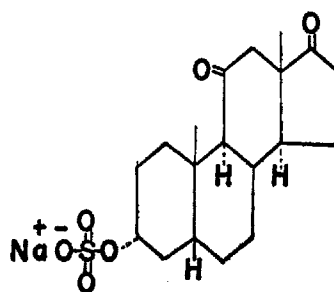
(II)



(III)



(IV)



(V)

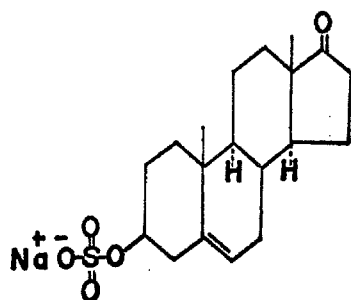
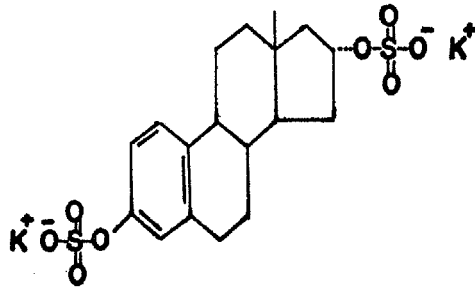


FIGURE 4

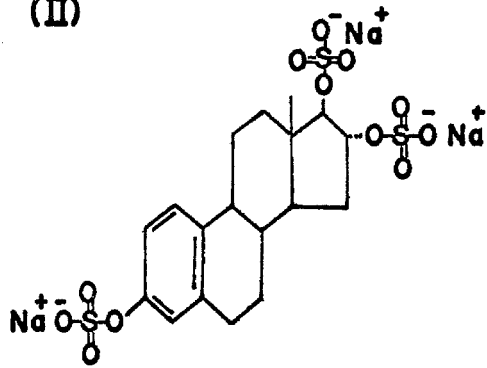
Estrane Series

- (I) 1, 3, 5-estratriene-3 β , 11 α -diol-disulfate,
dipotassium salt
- (II) 1, 3, 5-estratriene-3 β , 16 α , 17 β -triol
trisulfate, trisodium salt
- (III) 1, 3, 5(10), 6, 8(9)-estrapentaene-3 β -ol-17-
one sulfate, sodium salt

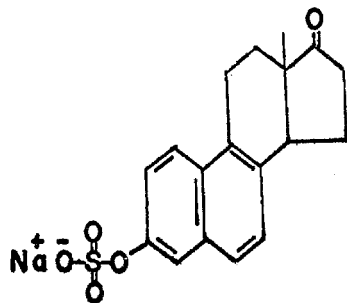
(I)



(II)



(III)



upfield. Such upfield shifts have been shown to result from base stacking in several studies of purine binding to bases, nucleosides and nucleotides, and are a consequence of the ring current magnetic anisotropy of purine. (17-19) In this study, it is conceivable that purine would form a stronger complex with steroids having less interfering substituents such as hydroxy groups. It is tempting to speculate that part of the specificity of steroid hormone actions might be due to steroid-coenzyme interactions, which might in turn alter protein synthesis and metabolism.

REFERENCES

1. J. Booth and E. Boyland, Biochim. Biophys. Acta, 12, 75 (1953).
2. J. F. Scott and L. L. Engel, Biochim. Biophys. Acta, 23, 665 (1957).
3. A. Munck, J. F. Scott, and L. L. Engel, Biochim. Biophys. Acta, 26, 404 (1957).
4. E. A. Tsutsui, P. A. Marks, and P. Reich, J. Biol. Chem., 237, 3009 (1962).
5. R. Raineri and R. H. Levy, Biochemistry, 9, 2233 (1970).
6. P. Ralalay and H. G. Williams-Ashman, Proc. Nat. Acad. Sci., U.S., 44, 15 (1958).
7. C. A. Villee and D. D. Hagerman, J. Biol. Chem., 233, 42 (1958).
8. L. L. Engel and J. F. Scott, 'Recent Progress in Hormone Research' Vol. 16, 79 (1962).
9. S. I. Chan, M. P. Schweizer, P. O. P. Ts'o, and G. K. Helmkamp, J. Amer. Chem. Soc., 86, 4182 (1964).
10. M. P. Schweizer, S. I. Chan, and P. O. P. Ts'o, J. Amer. Chem. Soc., 87, 5241 (1965).
11. A. D. Broom, M. P. Schweizer, and P. O. P. Ts'o, J. Amer. Chem. Soc., 89, 3612 (1967).
12. J. N. Shoolery and M. T. Rogers, J. Amer. Chem. Soc., 80, 5121 (1958).
13. N. S. Bhacca and D. H. Williams, "Applications of NMR Spectroscopy in Organic Chemistry. Illustrations from the Steroid Field," Holden-Day, Inc., San Francisco (1964).

14. N. S. Bhacca and D. H. Williams, Tetrahedron Letters, 42, 3127 (1964).
15. G. Slomp and F. Mackellar, J. Amer. Chem. Soc., 82, 999 (1960).
16. G. I. Poos, R. Hirschman, G. A. Bailey, F. A. Culter, Jr., L. H. Sarett, and J. M. Chemerda, Chem. and Ind. 1260 (1958).
17. S. I. Chan, B. W. Bangerter, and H. H. Peter, Proc. Nat. Acad. Sci., 55, 720 (1966).
18. B. W. Bangerter and S. I. Chan, Biopolymers, 6, 983 (1968).
19. B. W. Bangerter and S. I. Chan, Proc. Nat. Acad. Sci., 60, 1144 (1968).

PROPOSITION II

METALLIC DMSO COMPLEXES AND THEIR
BIOLOGICAL TRANSPORT PROPERTIES

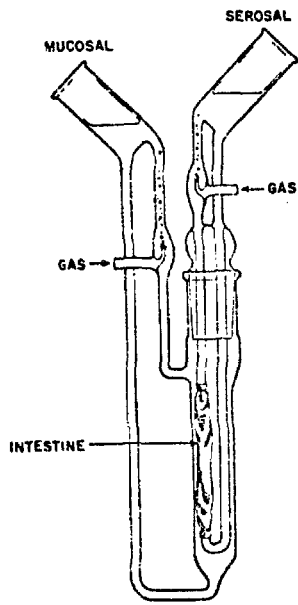
Abstract: It is proposed to extend the DMSO transport experiments to determine the effect of various essential ions on the transport phenomenon, and to study the extent of competitive solvation of ions in DMSO-water mixtures by proton magnetic resonance spectroscopy.

There have been numerous investigations on the biological actions of DMSO in the past few years.⁽¹⁾ The extraordinary solvent and penetrating properties of DMSO⁽²⁾ led to its agricultural use for aiding nutritive element transport in plants. The influence of DMSO on the permeability of biological membranes has also been studied by various workers. Despite all these investigations, the mechanism by which DMSO goes across biological barriers such as the intestine is not yet understood.

Recently, we have conducted several experiments in this laboratory to provide information on the transport mechanism of DMSO and the influence of metallic ions on the transport phenomenon.⁽³⁾ By using intestinal segments excised from albino rats and mounted on a modified Wiseman's apparatus⁽⁴⁾ (Fig. 1), the transport of DMSO across the segment has been shown to be passive with a first order rate constant of 2×10^{-7} mole min⁻¹ for a DMSO concentration of 5×10^{-3} M. This passive diffusion was found to be facilitated by the presence of calcium ions. In addition, we have observed that the

FIGURE 1

A modified Wiseman apparatus for
transport studies.



transport of calcium ions is facilitated by the presence of DMSO. Radioactivity assay of ^{14}C -labelled DMSO and ^{45}Ca was used in these experiments. The results are summarized in Tables I and II.

It is tempting to speculate that complex formation between DMSO and calcium ions may play an important role in the facilitative transport process. The preparation of a large number of metallic complexes of DMSO have been reported, ^(5, 6) and oxygen is usually the donor atom in the DMSO molecule. In cases where concentrated aqueous solutions of the salts are used in the preparation, the complexes obtained were reported to contain water as well as DMSO. Apparently, both water and DMSO compete for places in the coordination sphere and it is only necessary that the concentration of water be low for it to be excluded. Thus, it is unlikely that these DMSO complexes would be stable in aqueous solution, but their behavior in the biological membrane is still open to conjecture.

It is proposed to continue this study in two approaches: (1) An extension of the transport studies to determine the influence of other essential ions in the transport properties of DMSO. The ions of particular interest in this study are:

- (a) Sodium
- (b) Potassium
- (c) Iron
- (d) Magnesium
- (e) Manganese
- (f) Copper

It is important for the understanding of the transport mechanism

TABLE I. The effect of calcium ions on the transport of DMSO at 37°C.

<u>Molar Concentration of DMSO</u>	<u>Molar Concentration of Calcium Ions</u>	<u>K (liter minute⁻¹)</u>	<u>Average Rate (mole minute⁻¹)</u>
2×10^{-3}	0	1.02×10^{-5}	2.04×10^{-8}
2×10^{-3}	1×10^{-2}	1.77×10^{-5}	3.54×10^{-8}
2×10^{-3}	1.2×10^{-1}	1.87×10^{-5}	3.74×10^{-8}

TABLE II. The effect of DMSO on the rate of transport of calcium ions at 37°C.

<u>Molar Concentration of Calcium</u>	<u>Molar Concentration of DMSO</u>	<u>K (liter minute⁻¹)</u>	<u>Average Rate (mole minute⁻¹)</u>
2×10^{-3}	0	3.34×10^{-6}	6.88×10^{-9}
2×10^{-3}	2×10^{-3}	5.76×10^{-6}	1.15×10^{-8}
2×10^{-3}	2×10^{-2}	7.28×10^{-6}	1.56×10^{-8}

to determine the influence of DMSO on the transport properties of the ions mentioned above, and to determine if this effect is the same with respect to the direction in which these molecules are moving. In general, both influx and efflux kinetics are identical for simple diffusion processes.

In these experiments, the solution of interest at 37°C and at proper concentration will be placed on the outer or luminal side of the intestine, and normal Tyrode's solution on the inner or serosal side. At regular intervals of time, samples will be taken from the serosal side for assay. The two solutions will be reversed in experiments where the asymmetry of the membrane is studied. ¹⁴C-labelled DMSO will be used in some of these experiments; and the concentration of the ions will be assayed by atomic absorption spectroscopy.

(2) To obtain information concerning the extent of competitive solvation of ions in DMSO-water mixtures. The application of the technique of nuclear magnetic resonance spectroscopy to studies of electrolytic solutions has provided information concerning the electrostatic interactions that occur in these systems. (7, 8) When an electrolyte is added to an aqueous solvent mixture, the hydrogen bonds already existing in solution are partially destroyed but the loss of structure will be compensated by an ionic solvation which subsequently occurs. In general, this is accompanied by an upfield displacement in chemical shift in the first case and a downfield displacement of the chemical shift in the latter. Thus, in a solvent mixture, if a downfield displacement of the water signal occurs in the presence of an ion, this will indicate that solvation dominates. By comparing the change in chemical

shift of the water resonance and the methyl resonance in DMSO in the presence of various ions, information about the competition in the coordination sphere under various conditions can be obtained. A variety of solvent mixtures will be used in this study to provide additional insight into the mechanism of action of DMSO in the biological system.

REFERENCES

1. C. D. Leake, Ann. N. Y. Acad. Sci., 141, 1 (1967).
2. S. W. Jacobs, M. D. Bischel and R. J. Herschler, Cur. Ther. Res., 6, 193 (1964).
3. P. K. Dea, S. I. Chan, and F. J. Dea, manuscript in preparation.
4. P. Saltman, J. Chem. Educ., 42, 682 (1965).
5. F. A. Cotton and R. Francis, J. Amer. Chem. Soc., 82, 2986 (1960).
6. V. Sislov, Glas. Hem. Tehnol. Bosne Hercegovine, 15, 91 (1967).
7. J. F. Hinton, Chem. Rev., 67, 367 (1967).
8. A. Fratiello and D. P. Miller, Mol Phys., 11, 37 (1966).

PROPOSITION III

CIRCULAR DICHROISM AND OPTICAL ROTATORY
DISPERSION STUDIES OF dAT OLIGOMERS

Abstract: Recently, a series of deoxyoligonucleotides with the repeating self-complementary base sequence ATAT have been prepared. It is proposed to study the CD and ORD of the different conformations of $d(A-T)_i$ oligomer.

Recent advances in instrumentation and theory on circular dichroism (CD) and optical rotatory dispersion (ORD) have provided a new and powerful approach for determining the conformation of molecules in solution. ⁽¹⁾ In general, optical rotation is observed when a medium transmits the left and right circularly polarized components of a beam of plane polarized light with unequal velocity. If in addition to unequal velocity, there is a difference in the absorption coefficient for left and right circularly polarized light, the emergent light will be elliptically polarized. This unequal absorption is referred to as "circular dichroism", and the combined phenomenon of circular dichroism and optical rotation is known as the "Cotton" effect. ⁽²⁾ The Cotton effect is found to occur near optically active absorption bands; thus any chromophore may exhibit a Cotton effect when located in an asymmetric environment.

In nucleic acids, the optically inactive base chromophores are induced to produce Cotton effects when they are attached to the optically active sugars. Tinoco and his coworkers ⁽³⁻⁵⁾ have proposed a theory which successfully explains the hypochromism observed for

polynucleotides as mainly due to the coulombic interactions between electrons in neighboring base pairs because of their proximity and parallel stacking along the chain. The general ORD profile of all oligomers and polynucleotides consists of two peaks and one trough centered around the 260 m μ absorption bands, and their CD has positive and negative bands above 220-230 m μ . Additional Cotton effects have also been observed below this region. Both the CD and ORD spectrum, like the absorption spectrum, have been shown to exhibit sequence dependence of the bases and is very sensitive to any conformation change of the molecule in solution, such as changes induced by temperature and pH variations.

Most of the CD and ORD studies have been done on synthetic polynucleotides as a necessary step to understand the more complicated natural nucleic acids which contain a multiplicity of bases and base sequences. Recently, polydeoxyribonucleotides and polyribonucleotides of defined base composition and sequence have become available. A series of deoxyoligonucleotides with the repeating, self-complementary base sequence ATAT ... have been prepared by digestion of the dAT copolymer with pancreatic DNase, followed by preparative electrophoresis in concentrated acrylamide gels. The details of the synthetic procedure has been outlined by Elson and Jovin.⁽⁶⁾ Scheffler et al.⁽⁷⁾ have shown by using molecular weight measurements that at low counter ion (Na⁺) concentration, the oligomers form single hairpin helices while at high counter ion concentrations and low temperatures, the single-chain helices are slowly converted to two-chain helices with base pairing between dA and dT in the opposing strands. There is no

evidence yet to determine whether the two-chain helices are straight-chain or double-hairpin helices. The $d(\text{T-A})_i$ oligomers can also form single-strand circles by means of the DNA ligase when $i \geq 16$; ⁽⁸⁾ and these single-strand circles have been shown to form a base-paired double helix with a loop at each end. Analysis of the melting curves has shown that the T_m of an open hairpin depends on chain length and that the closed hairpins are more stable than the open hairpins. ⁽⁹⁾

An ORD study of the $d(\text{T-A})_i$ polymer from two sources has been carried out by Ts'o et al. ⁽¹⁰⁾; one synthetic as described and one natural, isolated from *Cancer antennarius*. Comparison of the temperature effect on the ORD curves of natural $d(\text{T-A})_i$ and synthetic $d(\text{T-A})_i$ shows that around the $285 \text{ m}\mu$ peak, rotation of the natural $d(\text{T-A})_i$ is not affected by temperature until the melting temperature is reached (53°C). Rotation of the synthetic $d(\text{T-A})_i$ is only 60% of that of natural $d(\text{T-A})_i$, but increases with temperature up to the level of synthetic $d(\text{T-A})_i$ just before the onset of melting. This phenomenon was thought to be due to some difference in the secondary structure of these two polymers at room temperature.

In view of the recent characterization of the $d(\text{A-T})_i$ polymer, it is proposed to examine in detail the CD and ORD spectrum of the $d(\text{A-T})_i$ polymer under conditions of a single hairpin, a double helix and the single-strand circles made from them. CD and ORD spectra can be recorded using a Cary Model 60 spectropolarimeter with 6001 circular dichroism accessory. The standard buffers employed to give a 100-fold range of counter ion (Na^+) concentrations as used by Scheffler et al. ⁽⁷⁾ would be appropriate for this study, and

variable temperature measurements are usually achieved using water-jacketed fused quartz cells with an attachment for thermostatic control. The results of this study on the $d(A-T)_i$ polymer would be valuable as a model system to further our understanding of the forces involved in maintaining the secondary structure of nucleic acids in general. The heterogeneity and variation of composition of DNA and RNA are sufficiently complex such that studies of the interactions between bases and their effects on secondary structure cannot be made with certainty without preliminary information from simpler model systems.

REFERENCES

1. J. T. Yang and T. Samejima, Prog. Nucleic Acid Research and Mol. Biol., 9, 223 (1969).
2. C. Djerassi, "Optical Rotatory Dispersion", McGraw-Hill, New York, 1960.
3. I. Tinoco, Jr., R. W. Woody, and D. F. Bradley, J. Chem. Phys., 38, 1317 (1963).
4. D. F. Bradley, I. Tinoco, Jr., and R. W. Woody, Biopolymers, 1, 239 (1963).
5. I. Tinoco, Jr., Radiation Res., 20, 133 (1963).
6. E. Elson and T. Jovin, Analyt. Biochem., 27, 193 (1969).
7. I. E. Scheffler, E. L. Elson, and R. L. Baldwin, J. Mol. Biol., 36, 291 (1968).
8. B. M. Olivera, I. E. Scheffler, and I. R. Lehman, J. Mol. Biol., 36, 275 (1968).
9. I. E. Scheffler, E. L. Elson, and R. L. Baldwin, J. Mol. Biol., 48, 145 (1970).
10. P. O. P. Ts'o, S. A. Rapaport, and F. J. Bollum, Biochemistry, 5, 4153 (1966).

PROPOSITION IV

A PROPOSED MECHANISM OF CELLULAR INVASION
BY METASTATIC CARCINOMA CELLS

Abstract: A mechanism is proposed in which faulty RNA from malignant tumor cells may escape to invade a normal cell, in which abnormal proteins are then synthesized, causing further malignant proliferation of the cell. An experiment which would provide evidence for the metastatic mechanism is also described.

The distinguishing characteristic of tumor cells compared with normal cells is that their growth is no longer subject to regulation. ⁽¹⁾ The mechanism of cellular regulation is still relatively unknown; but both DNA and non-DNA-containing kinds of interactions have been proposed. ⁽²⁾ In the case with DNA-containing tumor viruses, neoplastic transformation requires the incorporation of the viral DNA into the genome of the host cell. ⁽³⁾ On the other hand, certain chemical carcinogens may interact with cellular DNA and cause mutations. If the genes which are involved in growth control are mutated, the appropriate regulatory circuit becomes ineffective, and autonomous growth might begin. Furthermore, mutations of genes not directly involved in growth control could cause deletions of various enzymes, and directly affect growth regulation. The non-DNA-containing interactions are generally considered to involve proteins, resulting in loss of growth control as well as deletion of enzymes.

Malignant tumor cells have the additional features that they show invasive growth and often metastasize, i. e., they can be

transferred via the blood of lymphatic circulation to other organs and form secondary tumors. Much of the biochemical investigation of cancerous cells^(4, 5) has been directed toward the discovery of metabolic and compositional differences between normal and tumor tissues, with the hope that these differences might explain the phenomenon of carcinogenesis and provide a rational basis for therapy. Very few experiments, however, were concerned with the metastatic aspect of malignant tumor cells.

Let us first assume that the cancerous cell is due to an alternation in the DNA by mutation or other mechanisms. This would in turn produce faulty RNA. The concept proposed here is to conceive metastasis as a result of RNA transport from a cell with a pre-existing malignant condition to a normal cell, in which abnormal proteins are then synthesized, causing further malignant proliferation of the cell. There are several experimental evidences in support of this proposal. Johnson et al.⁽⁶⁾ have shown that acridine orange-stained lymphocytes from diseased humans showed a wide variety of stainable RNA. Schwarz and Rieke⁽⁷⁾ have demonstrated that high molecular weight RNA can be incorporated by mammalian cells and may eventually have some metabolic effects. Weisberger has shown that with immature erythrocytes from patients with sickle cell anemia, the formation of normal hemoglobin could be induced in vitro by RNA from normal red blood corpuscles, whereas DNA was found to be inactive.⁽⁸⁾ The added RNA was apparently functioning as a messenger in this case. Furthermore, some other metabolic changes initiated by RNA in mammalian cells have been known to persist through many generations.^(9, 10) This

may suggest that the incorporated RNA has a permanent effect on the genome. Experiments with Rous sarcoma virus, an RNA tumor virus, have shown that replication and release of new virus particles can continue along with the survival and multiplication of transformed cells.⁽¹¹⁾ These experiments suggest that the faulty RNA could migrate out of the cancer cell and into neighboring cells. It could also circulate through the blood or lymphatic stream to another tissue, inducing cancer by incorporating itself into the cell at a distant site. Transport of proteins or other cytoplasmic compound as the invading mechanism is unlikely due to concentration problems, and consequently the number of cells successfully invaded are limited. Transport of a faulty RNA, on the other hand, is consistent with the fact that cancer grows in a facultative manner. In addition, when the faulty RNA is transported to a new cell, this cell can immediately be in a "latent" state, and the initiation of a latent cell may be spontaneous or triggered by environmental factors. This is consistent with many clinical cases.

To provide evidence for the metastatic mechanism proposed above, an experiment is proposed here to determine if some RNA materials can be transported from a culture of cancerous cells to a colony of normal cells. Ascite tumor cells of mice offer a suitable model for this study. Uracil-1-¹⁴C will be inoculated with the cancerous cells for seven to eight hours so that it will be utilized and incorporated into the RNA molecules.⁽¹²⁾ Extracellular radioactivities are then removed by repeated, quick washings. The ¹⁴C-RNA-containing cancerous cells are then inoculated for twelve hours in a chamber with normal cells in the other, and the chambers are

separated by a membrane, which is permeable to macromolecules but not cells. At the end of this period, both radioactivity and the appearance of cancerous cells would be looked for in the normal cell compartment. Radioactivity in the culture medium after the cells are sedimented should also be looked for to detect extracellular RNA. Using this procedure, if metastasis is indeed a result of transport of faulty RNA, both initiation and promotion processes could be detected. Initiation here refers to the establishment of a small number of scattered latent or dormant tumor cells and promotion stimulates those latent tumor cells to multiply and form a visible tumor. Inoculation for a longer period of time and variation of environmental conditions may be necessary to observe both initiation and promotion processes.

REFERENCES

1. H. Busch, "An Introduction to the Biochemistry of the Cancer Cell", Academic Press, New York, 1962.
2. E. Harbers, G. F. Domagk, and W. Müller, "Introduction to Nucleic Acids", Reinhold, New York, 1968.
3. M. Vogt and R. Dulbecco, Virology, 16, 41 (1962).
4. P. Emmelot and O. Mühlbock, editors, "Cellular Control Mechanisms and Cancer", Elsevier, New York, 1964.
5. H. Rubin and M. Locke, editors, "Major Problems in Developmental Biology", Academic Press, New York, 1966.
6. D. M. Johnson, P. T. Pratt, and P. G. Rigby, Blood, 29, 800 (1967).
7. M. R. Schwarz and W. O. Rieke, Science, 136, 152 (1962).
8. A. S. Weisberger, Proc. Nat. Acad. Sci., U.S., 48, 68 (1963).
9. M. C. Niu, C. C. Cordova, L. C. Niu, and C. L. Radbill, Proc. Nat. Acad. Sci., U.S., 48, 1964 (1962).
10. M. C. Niu, Federation Proc., 22, 354 (1963).
11. W. S. Robinson, A. Pitkanen, and H. Rubin, Proc. Nat. Acad. Sci., U.S., 54, 137 (1965).
12. H. Busch, editor, "Methods in Cancer Research", Vol. 2, Academic Press, New York, 1967.

PROPOSITION V

FLUORESCENCE STUDY OF THE POSSIBLE
INTERACTION OF LYSERGIC ACID DIETHYLAMIDE
WITH DEOXYRIBONUCLEIC ACID

Abstract: In view of some recent reports on the possible LSD-induced chromosomal aberration in individuals who have used the drug, it is proposed to study the possible complexation of LSD with DNA using fluorescence measurements and fluorescence polarization technique.

It is well known that lysergic acid diethylamide (LSD), perhaps the most notorious psychedelic drug today, can produce various adverse effects when taken by individuals. ⁽¹⁾ Aside from its after-effects, which are generally psychological, physiological and sociological in nature, results of several studies have indicated that LSD can produce changes in the chromosomes of blood cells both in vitro and in individuals who have used the drug, but the results have not been unanimous. ^(2, 3) At the present time, the implications and potential significance of such chromosomal aberrations are still unknown. However, chromosomal abnormalities similar to those induced by LSD have been noted to occur spontaneously in three diseases inherited in an autosomal recessive pattern: Bloom's syndrome, ⁽⁴⁾ Fanconi's anemia ⁽⁵⁾ and ataxia telangectasia. ⁽⁶⁾ Patients with these syndromes show a high tendency towards developing leukemia or other types of neoplasms. The association of chromosomal abnormalities in cancer is also well documented. Moreover, the production of congenital

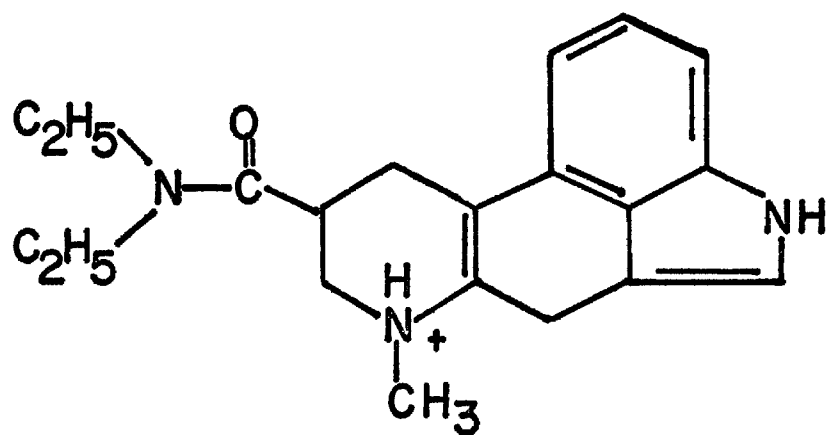
abnormalities and increased abortions in experimental animals studied suggest the teratogenic potential of chromosome breaking agents. (7-11) Perhaps the greatest danger of such agents lies in the potential chromosome damage to the gametes, (12, 13) in which case the effect of such agents may be truly a genetic one.

Although there has been some speculations on the mode of action of LSD, no specific studies on the mechanism of LSD-induced chromosomal damage have appeared in the literature. Recently, the circular dichroism spectra of calf thymus DNA solutions in the presence and absence of LSD were reported by T. E. Wagner. (14) The changes in the ultraviolet circular dichroism spectrum of DNA in the presence of LSD suggested that the drug may intercalate within the DNA helix in a manner similar to that of ethidium bromide, thereby causing changes in the conformation of the DNA. LSD is a planar, cationic, aromatic molecule (Fig. 1) and displays the molecular characteristics necessary to stack between the bases of the DNA helix and can also interact ionically with the anionic phosphate groups.

It is proposed to study the possible complexation of LSD with DNA using fluorescence measurements and fluorescence polarization techniques. Fluorescence studies have been very successful in recent years in the study of protein conformation (15) and model membrane systems. (16) A detailed investigation of the complex between ethidium bromide and nucleic acids has been carried out using these techniques. (17) Formation of the complex has been found to be specific for base-paired regions since ethidium bromide intercalates between base pairs. At low salt concentrations, however, a second mode of binding was

FIGURE 1

Lysergic acid diethylamide.



determined which involves electrostatic binding of the ethidium cation to negatively charged phosphate groups. The interaction of LSD with DNA can be conveniently studied by fluorescence methods since LSD at neutral pH is known to be highly fluorescent at $445\text{ m}\mu$ after excitation at $325\text{ m}\mu$.⁽¹⁸⁾ This study will be carried out using an Aminco Bowman spectrophotofluorometer with a Glan-prism polarization assembly for the measurement of polarization coefficients and fluorescence spectra of LSD in the presence and absence of DNA.

In general, the concentration of LSD bound can be determined by measuring the change in fluorescence intensities of LSD in the presence of DNA. Alternatively, binding can be determined by equilibrium dialysis or ultrafiltration technique. The binding data can be analyzed by Scatchard's method.⁽¹⁷⁾ When small molecules bind independently to a set of equivalent sites on a polymer, the equilibrium between free and bound molecules is given by:

$$r/c = Kn - Kr \quad (1)$$

where r is the ratio of bound LSD per nucleic acid phosphate, n is the number of binding sites per nucleic acid phosphate, K is the intrinsic association constant to a site and c is the free LSD concentration.

Both K and n are usually obtained using graphical methods. A study of the dependence of the binding on pH and salt concentration, as well as the secondary structure of the DNA would provide information on the nature of the binding involved.

It is also proposed to study the polarization characteristics of the emitted fluorescence to obtain some information on the relaxation

time of the molecule involved in the complexation. The partial polarization p is defined by the following equation:⁽¹⁵⁾

$$p = \frac{I_{\parallel} - I_{\perp}}{I_{\parallel} + I_{\perp}} \quad (2)$$

where I_{\parallel} is the fluorescence intensity measured with excitation and emission polarizing prisms oriented with their electric vectors parallel, and I_{\perp} is the fluorescence intensity measured with the electric vectors of the two prisms crossed. According to the theory developed by Perrin,⁽¹⁹⁾ the partial polarization of the fluorescent light emitted by molecules in solution depends upon the relation of their rotational relaxation time to the lifetime of the excited state of the fluorescence. The value of p for a collection of small fluorescent units attached with random orientation to macromolecules which are flat ellipsoids or prolate ellipsoids of small elongation has been shown to be.^(20, 21)

$$\left(\frac{1}{p} - \frac{1}{3} \right) \approx \left(\frac{1}{p_0} - \frac{1}{3} \right) \left(1 + \frac{3\tau_0}{\rho_h} \right) \quad (3)$$

Here, τ_0 is the lifetime of the excited state of the fluorescence, ρ_h the harmonic mean of the two principal relaxation times of the rotation of the ellipsoidal molecule, and p_0 is an empirical constant when no depolarization by molecular rotation takes place. When a molecule is involved in complex formation, the changes in rotational relaxation times are reflected in the partial polarization.

The genetic effect of LSD is undoubtedly more striking than

its immediate adverse manifestations. A direct study of the possible interactions of LSD and DNA as proposed herein are basic to the understanding of the teratogenic effects observed.

REFERENCES

1. R. G. Smart and K. Bateman, Canad. Med. Ass. J., 97, 1214 (1967).
2. M. Cohen, Can. J. of Genet. and Cyt., 11, 1 (1969).
3. R. G. Smart and K. Bateman, Canad. Med. Ass. J., 99, 805 (1968).
4. J. German, R. Archibald and D. Bloom, Science, 148, 506 (1965).
5. G. E. Bloom, S. Warner, P. S. Gerald and L. K. Diamond, New England J. Med., 274, 8 (1966).
6. F. Hecht, R. D. Koler, D. A. Rigas, G. S. Dahnke, M. P. Case, V. Tisdale and R. W. Miller, Lancet, 2, 1193 (1966).
7. G. J. Alexander, B. E. Miles, G. M. Gold and R. B. Alexander, Science, 157, 459 (1967).
8. W. F. Geber, Science, 158, 265 (1967).
9. R. Auerbach and J. A. Rugowski, Science, 155, 1325 (1967).
10. G. J. Alexander, S. Machiz and R. B. Alexander, Fed. Proc., 27, 220 (1968).
11. D. H. Carr, Am. J. Obstet. Gynecol., 99, 283 (1967).
12. N. E. Skakkeback, J. Phillip and O. J. Rafaelsen, Science, 160, 1246 (1968).
13. M. M. Cohen and A. B. Mukherjee, Nature, 219, 489 (1968).
14. T. E. Wagner, Nature, 222, 1170 (1969).
15. S. Udenfriend, "Fluorescence Assay in Biology and Medicine", Academic Press, New York, 1962.
16. R. A. Badley, H. Schneider and W. G. Martin, Biochem. Biophys.

- Res. Commun., 45, 174 (1971).
17. J. B. LePecq and C. Paoletti, J. Mol. Biol., 27, 87 (1967).
 18. J. Axelrod, R. O. Brady, B. Witkop and E. V. Evarts, Ann. N. Y. Acad. Sci., 66, 435 (1957).
 19. F. Perrin, J. Phys. Radium, 7, 390 (1926).
 20. G. Weber, Biochem. J., 51, 145 (1952).
 21. G. Weber, Biochem. J., 51, 155 (1952).